

Spring 1988

# Determination of the deterioration mechanisms caused by seawater corrosion and freeze-thaw action of portland cement solidified and stabilized heavy metal wastes

Tahar El-Korchi

*University of New Hampshire, Durham*

Follow this and additional works at: <https://scholars.unh.edu/dissertation>

---

## Recommended Citation

El-Korchi, Tahar, "Determination of the deterioration mechanisms caused by seawater corrosion and freeze-thaw action of portland cement solidified and stabilized heavy metal wastes" (1988). *Doctoral Dissertations*. 1531.  
<https://scholars.unh.edu/dissertation/1531>

This Dissertation is brought to you for free and open access by the Student Scholarship at University of New Hampshire Scholars' Repository. It has been accepted for inclusion in Doctoral Dissertations by an authorized administrator of University of New Hampshire Scholars' Repository. For more information, please contact [nicole.hentz@unh.edu](mailto:nicole.hentz@unh.edu).

## INFORMATION TO USERS

The most advanced technology has been used to photograph and reproduce this manuscript from the microfilm master. UMI films the original text directly from the copy submitted. Thus, some dissertation copies are in typewriter face, while others may be from a computer printer.

In the unlikely event that the author did not send UMI a complete manuscript and there are missing pages, these will be noted. Also, if unauthorized copyrighted material had to be removed, a note will indicate the deletion.

Oversize materials (e.g., maps, drawings, charts) are reproduced by sectioning the original, beginning at the upper left-hand corner and continuing from left to right in equal sections with small overlaps. Each oversize page is available as one exposure on a standard 35 mm slide or as a 17" x 23" black and white photographic print for an additional charge.

Photographs included in the original manuscript have been reproduced xerographically in this copy. 35 mm slides or 6" x 9" black and white photographic prints are available for any photographs or illustrations appearing in this copy for an additional charge. Contact UMI directly to order.



300 North Zeeb Road, Ann Arbor, MI 48106-1346 USA

**Order Number 8816686**

**Determination of the deterioration mechanisms caused by  
seawater corrosion and freeze-thaw action of portland cement  
solidified and stabilized heavy metal wastes**

**El-Korchi, Tahar, Ph.D.**

**University of New Hampshire, 1988**

**U·M·I**

**300 N. Zeeb Rd.  
Ann Arbor, MI 48106**

**PLEASE NOTE:**

In all cases this material has been filmed in the best possible way from the available copy. Problems encountered with this document have been identified here with a check mark .

1. Glossy photographs or pages
  2. Colored illustrations, paper or print \_\_\_\_\_
  3. Photographs with dark background
  4. Illustrations are poor copy \_\_\_\_\_
  5. Pages with black marks, not original copy \_\_\_\_\_
  6. Print shows through as there is text on both sides of page \_\_\_\_\_
  7. Indistinct, broken or small print on several pages
  8. Print exceeds margin requirements \_\_\_\_\_
  9. Tightly bound copy with print lost in spine \_\_\_\_\_
  10. Computer printout pages with indistinct print \_\_\_\_\_
  11. Page(s) \_\_\_\_\_ lacking when material received, and not available from school or author.
  12. Page(s) 144 seem to be missing in numbering only as text follows.
  13. Two pages numbered \*. Text follows.
  14. Curling and wrinkled pages \_\_\_\_\_
  15. Dissertation contains pages with print at a slant, filmed as received
  16. Other \* pages 81 and 165 are misnumbered--OK as is.
- 
- 
- 

U·M·I

**DETERMINATION OF THE DETERIORATION MECHANISMS  
CAUSED BY SEAWATER CORROSION AND FREEZE-THAW  
ACTION OF PORTLAND CEMENT SOLIDIFIED AND  
STABILIZED HEAVY METAL WASTES**

By

Tahar El-Korchi  
B.S., University of New Hampshire, 1980

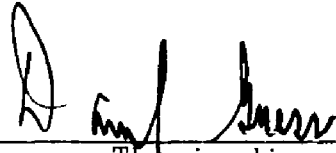
DISSERTATION

Submitted to the University of New Hampshire  
in Partial Fulfillment of  
the Requirements for the Degree of

Doctor of Philosophy  
in  
Engineering

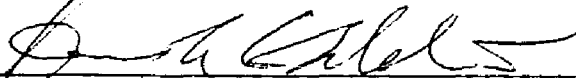
May, 1988

This dissertation has been examined and approved.



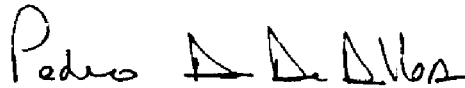
---

Thesis director, David Gress  
Associate Professor of Civil Engineering



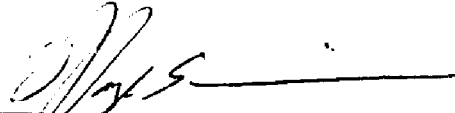
---

Kenneth Baldwin, Assistant Professor  
of Mechanical Engineering



---

Pedro DeAlba, Associate Professor  
of Civil Engineering



---

Nancy Kinner, Assistant Professor  
of Civil Engineering



---

David Meeker, Professor  
of Mathematics

December 16, 1987  
Date

## ACKNOWLEDGEMENT

I wish to thank my advisor David L. Gress for his support and guidance throughout this research program and my graduate studies at UNH.

Special thanks to Kenneth Baldwin for his invaluable guidance and help with the acoustic setup; Tim Kenney and Fred Hochgraff for their help and generous use of their laboratory facility especially the X-ray diffractometer; Nancy Churim for her assistance with the electron microscope facilities; Jim Greason with his dedication during the acoustic testing program even during ungodly hours of the night; Bob Ducette and Bob Blake with their creative assistance in the machine shop.

Special thanks to professors De Alba, Kinner and Meeker for being an integral part of this thesis committee.

The financial support of the Sea Grant Program and the National Oceanic and Atmospheric Administration is acknowledged.

Finally, I wish to thank my family and friends with special thanks and gratitude to my wife Marya for their continued support, encouragement and patience throughout this lengthy and at times, what appeared to be, an endless task.

## TABLE OF CONTENTS

ACKNOWLEDGEMENTS.....	ii
LIST OF TABLES.....	iii
LIST OF FIGURES.....	x
ABSTRACT.....	xii

CHAPTER	PAGE
INTRODUCTION.....	1
I.     FIXATION MECHANISMS OF SOLIDIFIED/STABILIZED WASTE.....	7
Introduction.....	7
Production and Hydration of Portland Cement...	8
Mechanisms of Fixation in Cement Based S/S Metal Wastes.....	12
Physical Encapsulation and Chemical Stabilization.....	12
Micro and Macro Encapsulation.....	13
Silica Gel Encapsulation.....	17
Crystal Capture.....	18
Effect of Heavy Metals on the Hydration of Portland Cement and Cement Compounds.....	19
Protective Membrane.....	19
Adsorption and Substitution.....	22
Discussion.....	26
II.    SEAWATER CORROSION OF PORTLAND CEMENT BASED SOLIDIFIED STABILIZED WASTE.....	29
Introduction.....	29
Chloride Attack.....	30
Sulfate Attack.....	33



	Mobility of Chlorides into Portland Cement Paste Matrix.....	35
	Chloride Reactions During Portland Cement Hydration.....	37
	Effect of Chlorides on Porosity.....	39
	Discussion.....	40
III.	EXPANSION MECHANISMS ASSOCIATED WITH CHEMICAL CORROSION OF HYDRATED PORTLAND CEMENT.....	42
	Introduction.....	42
	The Crystal Growth Theory.....	42
	The Swelling Theory.....	44
	Discussion.....	50
IV.	MICROSTRUCTURAL CHARACTERIZATION OF PORTLAND CEMENT SOLIDIFIED HEAVY METAL WASTE.....	51
	Introduction.....	51
	Objective.....	51
	Portland Cement Based Waste Preparation.....	52
	X-ray Diffraction Analysis.....	54
	Instrumentation.....	55
	Sample Preparation.....	55
	Results	
	Phase Identification in Metal Sludges.....	56
	Phase Identification of Heavy Metals in Hardened Paste Matrix.....	57
	Scanning Electron Microscopy and Energy Dispersive Spectrometry.....	61
	Instrumentation.....	62
	Sample Preparation.....	62
	Results.....	63
	Discussion.....	70
	Conclusion.....	71
	Proposed Future Work.....	72

V.	PHYSICAL AND MECHANICAL CHARACTERISTICS OF SOLIDIFIED AND STABILIZED WASTE.....	73
	Introduction.....	73
	Objective.....	73
	Mercury Intrusion Porosimetry.....	73
	Helium Displacement Porosimetry.....	76
	Experimental.....	77
	Results	
	Mercury Intrusion Porosimetry.....	78
	Helium Displacement Porosimetry.....	87
	Unconfined Compressive Strength.....	87
	Discussion.....	91
	Conclusion.....	95
	Proposed Future Work.....	95
VI.	SEAWATER AND CHEMICAL CORROSION OF SOLIDIFIED STABILIZED WASTE.....	96
	Introduction.....	96
	Objective.....	96
	Seawater Corrosion.....	97
	Sample Preparation.....	97
	Seawater Leaching.....	97
	Scanning Electron Microscopy.....	98
	X-ray Diffraction Analysis.....	98
	Linear Expansion Testing.....	99
	Results.....	101
	Linear Expansion.....	101
	SEM/EDAX.....	103
	X-ray Diffraction Analysis.....	107
	Discussion.....	109
	Chemical Corrosion.....	117
	Experimental.....	117
	Results.....	118
	Discussion.....	128

	Conclusion.....	130
	Proposed Future Work.....	130
VII.	ASSESSING THE FREEZE THAW RESISTANCE OF SOLIDIFIED STABILIZED WASTE.....	132
	Introduction.....	132
	Postulated Distress Mechanisms During Frost Action in Porous Materials and Portland Cement Paste and Concrete.....	133
	Hydraulic Pressure Theory.....	133
	Osmotic Pressure Theory.....	134
	Capillary Effect Theory.....	135
	The Effect of Salt and Air-Entrainment on the Freeze-Thaw Durability of Portland Cement Paste and Concrete.....	137
	Effect of Dissolved Salts.....	137
	Effect of Air Entrainment.....	137
	Objective.....	139
	Derivation of Acoustic Parameters.....	139
	Experimental.....	145
	Sample Preparation.....	145
	Freeze Thaw Cycling.....	146
	Acoustic Testing.....	147
	Results - First Run.....	149
	Discussion - First Run.....	151
	Results - Second Run.....	151
	Discussion - Second Run.....	156
	Results - Third Run.....	159
	Discussion - Third Run.....	159
	Conclusion.....	162
	Proposed Future Work.....	162
	SUMMARY.....	163

REFERENCES.....	164
APPENDIX.....	177

## LIST OF TABLES

TABLE NO.		PAGE
1.1	Nomenclature for Cement Chemistry.....	9
1.2	Bogue Equations for Cement Compounds.....	10
1.3	Stoichiometric Reactions for Fully Hydrated Clinker Phases.....	12
4.1	Composition of Portland Cement.....	52
4.2	Concentration of Metal in Sludge.....	53
4.3	Major Phases Detected in Portland Cement by XRD.....	58
4.4	Probable Hydration Products Detected in Partially Hydrated Portland Cement.....	59
4.5	XRD Phase Identification: Effect of Heavy Metal on Peak Intensity.....	60
4.6	QXRD Relative Intensities: Sludge/Cement vs CH/CdH ratios.....	62
4.7	Summary of EDAX Results for Different S/S Wastes.....	68
5.1	Helium Displacement Porosimetry.....	88
5.2	Unconfined Compressive Strength: 14 days and 3 years.....	89
5.3	Summary of Strength and Porosity Data.....	90
6.1	Synthetic Seawater Composition.....	98
6.2	Quantitative Phase Analysis of CH and AFT Before and After Leaching in Seawater.....	110
7.1	Specimen Identification and Quantity of Each Speciment Tested in the First Run.....	150
7.2	Number of Specimens Tested During Second Run.....	152

7.3	Freeze-Thaw Sample Composition Third Run.....	160
7.4	Test Parameters for Freeze-Thaw Cycling Third Run.....	161

## LIST OF FIGURES

FIGURE NO.		PAGE
4.1	SEM Photomicrograph of S/S Wastes (Control, Cd,Pb) at 3 and 7 Days and 3 Years With EDAX.....	64
4.2	SEM Photomicrograph of S/S Wastes (As, Cr, Mixed Metal) at 3 and 7 Days and 3 Years With EDAX.....	66
4.3	SEM Photomicrograph of Secondary Image and X-ray Dot Map of Cd Waste.....	69
5.1	Cumulative Pore Size Distribution Using Mercury Intrusion Porosimetry: Effect of Heavy Metals.....	79
5.2	Cumulative Pore Size Distribution Using Mercury Intrusion Porosimetry: Effect of Water-Cement Ratio.....	80
5.3	Cumulative Pore Size Distribution Using Mercury Intrusion Porosimetry: Effect of Seawater Curing and W/C ratio.....	81
5.4	Cumulative Pore Size Distribution Using Mercury Intrusion Porosimetry: Effect of Seawater Curing.....	82
5.5	Derivative Pore Size Distribution Using MIP: Effect of Heavy Metal Addition.....	83
5.6	Derivative Pore Size Distribution Using MIP: Effect of W/C ratio.....	84
5.7	Derivative Pore Size Distribution Using MIP: Effect of W/C ration and Seawater Curing.....	85
5.8	Derivative Pore Size Distribution Using MIP: Effect of Seawater Curing.....	86
6.1	Photograph of Linear Expansion Specimens After Being Stored in Seawater for Over 50 Days.....	100

6.2	Linear Expansion of Blank, Lead and Cadmium Waste Stored in Seawater.....	102
6.3	SEM Photomicrograph of the Surface Layer of S/S Waste During Seawater Leaching.....	104
6.4	SEM Photomicrograph of S/S Waste Before and After Seawater Leaching.....	105
6.5	XRD Pattern of S/S Waste Before and After Leaching in Seawater.....	108
6.6	pH and Alkalinity in Seawater Leachate.....	112
6.7	Metal Release in Seawater Leachate.....	113
6.8	SEM Photomicrograph of Cadmium Waste Leached in Seawater and Sulfate-Chloride Solutions for 12 Days.....	119
6.9	SEM Photomicrograph of Cadmium Waste Leached in Seawater and Sulfate-Chloride Solutions for 18 Days.....	120
6.10	SEM Photomicrograph of Cadmium Waste Leached in Seawater and Sulfate-Chloride Solutions for 33 Days.....	122
6.11	SEM Photomicrograph of Cadmium Waste Leached in Seawater for Over 70 Days.....	125
6.12	SEM Photomicrograph of Cadmium Waste Leached in Seawater and Sulfate-Chloride Solutions for Over 200 Days.....	125
6.13	SEM Photomicrograph of Surficial Layer of Cadmium Waste Leached in Seawater for 12, 50 and 200 Days.....	127
7.1	Generic Spectrum Level vs Frequency Indicating the Q Factor Parameters.....	144
7.2	Schematic of Measurement System Used to Obtain Acoustic Parameters.....	148
7.3	Freeze-Thaw Resistance as Monitored by Q Factor.....	153
7.4	Freeze-Thaw Resistance as Monitored by NNF Values.....	154



## ABSTRACT

### DETERMINATION OF THE DETERIORATION MECHANISMS CAUSED BY SEAWATER CORROSION AND FREEZE-THAW ACTION OF PORTLAND CEMENT SOLIDIFIED AND STABILIZED HEAVY METAL WASTES

by

TAHAR EL-KORCHI

University of New Hampshire, May, 1988

The use of cement based processes for stabilization-solidification of heavy metal wastes has been extensively studied and characterized. Microstructural characterization of the waste matrix was conducted using X-ray diffraction analysis, scanning electron microscope, energy dispersive spectroscopy, mercury intrusion and helium displacement porosimetry. The physio-chemical characteristics of the solidified waste are affected by the metal type, cement binder, additives, solution to cementitious ratio, and curing regime. All the heavy metals (Cd, Pb, As, Cr) analyzed were detected in the CSH structure; Cr, Cd and As were detected in ettringite, and only Cd was detected in CH. Cd was the only metal detected in the crystalline form as cadmium hydroxide determined by XRD.

All metals increased the total porosity and shifted the pore size distribution to the larger pores within the solidified matrix. Porosity and pore size distribution was not the only parameter affecting the unconfined compressive strength and leaching potential of the solidified waste. Different metal solidified wastes having similar pore characterization exhibited different strength and leaching characteristics.

The seawater leachability of the solidified waste appears to be a function of the metal complex formed and the microstructural changes that occur. Magnesium hydroxide and carbonation of the surface layer affects the apparent surface porosity and permeability and the heavy metal release.

Excessive expansion of the cadmium solidified waste leached in seawater was attributed to a combination of expansive ettringite formation and matrix weakening induced by softening of the CSH phase and gypsum formation. The combined presence of sulfate and chloride solutions is essential for a rapid cadmium waste deterioration as determined by the corrosion in sulfate and chloride solutions.

The sonic method proved very successful as a non-destructive technique for evaluating the freeze-thaw durability of cement solidified heavy metal wastes. These cement solidified wastes have very poor resistance to repeated cycles of freezing and thawing. Destructive forces are created during freezing of water and are a combination of expansive, hydraulic and salt crystallization pressures. Air-entrainment improves freeze-thaw characteristics of the cement solidified waste as expected.

## INTRODUCTION

American industry produced 255 million metric tons of hazardous waste in 1985 according to the Congressional Office of Technology Assessment (OTA). The OTA contends there may be at least 10,000 hazardous waste sites in the US that pose a serious threat to public health and should be given priority in any national cleanup effort. The estimated cost could easily reach 100 billion dollars or more than 1000 dollars per household. So far the EPA has only put 850 dumps on its priority list (Time 10-14-85).

The USEPA defines hazardous wastes as substances that are toxic, corrosive, ignitable or chemically reactive. These wastes are broadly divided into six basic categories (Bishop, 1982).

- 1) solvents and related organics such as trichloroethylene, chloroform and toluene
- 2) polychlorinated biphenyls (PCBs) and polybrominated biphenyls (PBBs)
- 3) pesticides
- 4) inorganic chemicals such as ammonia, cyanide, acids, and bases
- 5) heavy metals such as mercury, chromium, lead and cadmium
- 6) waste oils and greases

Liquid wastes are banned from landfills, and the options remaining for disposal are underground injection or waste treatment. Biological treatment is viable as long as the waste is not toxic enough to inhibit the microorganisms. Alternatively, if the waste is too toxic for direct biological treatment then treatments such as wet oxidation may be employed. For low organic wastes, activated carbon may be used to concentrate the organics for further treatment. Incineration may be used successfully on wastes with high organic content. Incineration will only reduce the volume and toxicity of the waste prior to ultimate land disposal, however, the high cost of the process limits its application to low volume organic wastes.

Historically, disposal to land has been the major technology used to manage the country's waste materials. However, the **Resource Conservation and Recovery Act** (RCRA) and the more recent **Hazardous and Solid Waste Amendments** (HSWA) have provided incentives and controls to reduce the use of land for managing hazardous waste and encourage other alternatives for waste management. Other technologies used and being considered for treating hazardous waste may produce residues still requiring management. In general for these residues, which may be concentrated with toxic contaminants, land disposal will be the only remaining option. In addition, these wastes banned from land

disposal, must be managed by an alternative technology. If not, land disposal may still be the only option available for these wastes (Wiles, 1987).

Solidification/Stabilization (S/S) is being considered as a technology available for treating selected banned waste prior to land disposal. This technology is also being considered for treating residues from other treatment technologies. S/S processes employ select materials to alter the physical and chemical characteristics of the waste stream prior to land disposal. Solidification refers to physical alteration of the waste to improve its handling characteristics. Stabilization refers to the process or technology that transforms the waste to a chemically stable, detoxified waste with a reduced solubility. Fixation on the other hand has been used synonymously with both processes, and is commonly used to incorporate both processes. Reviews of S/S technology for hazardous industrial wastes have been recently published (Landreth, 1979; Pojasek, 1979; Poon et al. 1983 and Wiles 1987). These earlier publications have been reviewed extensively by Ransom (1983), Brown (1984) and Shively (1984).

S/S processes have been broadly categorized into two subdivisions based on their binder type; organic and inorganic. Organic processes that have been commercially or experimentally used include epoxy, polysters, asphalt, bitumen, polyolefins (primarily polyethylene and

polyethylene-polybutadiene) and urea-formaldehyde (Wiles, 1987). Leachability of these wastes as assessed experimentally, are typically low depending on the permeability of the matrix. Usually organic binders do not react with the waste and hence the waste is not detoxified, destroyed or converted to an insoluble form. Therefore the long term stability of the waste is a function of the physical integrity of the binder matrix. Organic-based processes are highly specialized, requiring high cost additives and blending equipment, their use has practically been limited to high hazard, low volume wastes such as radioactive wastes. This topic will not be considered further in this study.

Most inorganic fixation processes use some type of hydraulic cement, pozzolanas, lime, gypsum and soluble silicates. Portland cement is most common however other types have also been used such as aluminous cement, natural cement, slag cement etc. Cement-based S/S processes are well suited for treatment of aqueous waste since portland cement and pozzolonic materials require water for their hydration. The leachability of the contaminant thus depends on whether it remains in solution in the pore system or is immobilized through chemical reaction.

Cement-based processes create an alkaline environment suitable to the containment of heavy metals. The interaction between the heavy metals and portland cement based S/S

system is not well understood. A better understanding of the fixation mechanism is necessary for improved design processes that would ultimately reduce pollutant mobilization in S/S wastes placed in landfill environments.

Even if S/S processes were shown to be effective in immobilizing inorganic hazardous wastes so that they pose no threat to the environment, location of disposal sites for S/S wastes is met with great public opposition (Bishop and Gress, 1983). This is due in part to the general public's fear of such possible mishaps as groundwater contamination and air and land pollution problems. One way to overcome this strong local opposition is to dispose of S/S wastes in the ocean rather than on land, if the material can be shown to be environmentally safe.

The purpose of this thesis is to characterize the fixation mechanisms involved in cement S/S heavy metal wastes, characterize the interactions involved when disposing of selected S/S wastes in the ocean, and develop a non-destructive test to assess the physical durability of S/S wastes subject to environmental stresses.

The scope of work conducted includes the following (each subject is included as a chapter of this thesis):

- o Review of the literature and discussion of the mechanisms of fixation involved in fixing heavy metal wastes with cement based S/S process.
- o Review of the literature and discussion of the chemical and physical processes involved during the interaction of hydrated portland cement and seawater constituents.

- o Review of the literature and discussion of the expansion mechanism potentially involved with seawater corrosion of cement based S/S wastes.
- o Microstructural characterization of S/S wastes using SEM/EDS analysis and XRD.
- o Physical characteristics of S/S wastes using helium intrusion porosity and mercury intrusion porosimetry.
- o Assessment of seawater corrosion of S/S wastes and determination of the deterioration mechanisms.
- o Assessment of the freeze-thaw durability of S/S wastes using acoustical non-destructive testing and determination of the failure mechanism.



## CHAPTER I

### FIXATION MECHANISMS IN SOLIDIFIED/STABILIZED WASTES

#### Introduction

The goal of S/S technology is to transform potentially toxic contaminants into a non-toxic form with improved handling characteristics. The physical characteristic required is enough shear strength for ultimate land disposal. The chemical characteristics required are decreased leachability and pollutant immobilization. This physio-chemical transformation of the waste requires a reduced final surface area to minimize potential leaching sites and to control the aqueous environment to achieve minimal solubility. The resulting physio-chemical transformation will govern the fixation mechanism in a particular S/S process and influence the potential for leaching under a given environmental condition. A better understanding of the interaction between pollutants in heavy metal sludges and cement based matrices will help improve the design process to successfully use S/S technology to manage hazardous waste.

Currently, technology is not available for such idealistic results. However, Malone and Larson (1983) have proposed systems to potentially obtain more efficient and

improved containment of toxic materials if simple chemical concepts are considered. These include adsorption, chemisorption, passivation, diaadochy and reprecipitation of newly insoluble compounds.

Adsorption involves loose bonding of ions to the particle surface. Chemisorption is the loose bonding of ions not necessarily related to particle surface. Passivation is the chemical coating of a substance preventing further chemical attack. Diaadochy is a process that removes elements from the environment by substitution during precipitation of commonly occurring compounds.

#### Production and Hydration of Portland Cement

Portland cement is widely used in most S/S processes. A brief introduction to the material and its hydration mechanisms will aid in understanding its interactions with other metal contaminants.

Portland cement is a finely ground hydraulic cement consisting mainly of calcium silicates, calcium aluminates and ferrites and gypsum. The manufacturing process of portland cement consists of sintering natural calcarous deposits (such as limestone, chalk, marl, and seashells) as a source of lime and natural argellaceous deposits (such as clay, shale and slate) as a source of silica. Clays also contain alumina ( $Al_2O_3$ ), iron oxide ( $Fe_2O_3$ ), magnesium carbonate ( $MgCO_3$ ) and alkalies.

The desired proportions of the homogenized mixture is fed through a kiln with temperatures up to 1900 °C. Under these conditions, chemical reactions occur to form the product called "clinker" which consists of the major phases tricalcium silicate ( $3 \text{ CaO} \cdot \text{SiO}_2$ ), dicalcium silicate ( $2 \text{ CaO} \cdot \text{SiO}_2$ ), tricalcium aluminate ( $3 \text{ CaO} \cdot \text{Al}_2\text{O}_3$ ), and tetracalcium aluminoferrite ( $4 \text{ CaO} \cdot \text{Al}_2\text{O}_3 \cdot \text{Fe}_2\text{O}_3$ ). Minor impurity phases such as free lime ( $\text{CaO}$ ), periclase ( $\text{MgO}$ ), and alkalis are usually present.

The chemical composition of portland cement is commonly expressed in the oxide form of the elements. This is because direct determination of the compound composition requires specialized techniques and facilities. In addition, cement chemists use a specialized abbreviation to present oxide composition as shown in Table 1.1.

Table 1.1 - Nomenclature for Cement Chemistry  
(Adapted From Mehta, 1986.)

Oxide	Abbreviation	Compound	Abbreviation
$\text{CaO}$	C	$3\text{CaO} \cdot \text{SiO}_2$	$\text{C}_3\text{S}$
$\text{SiO}_2$	S	$2\text{CaO} \cdot \text{SiO}_2$	$\text{C}_2\text{S}$
$\text{Al}_2\text{O}_3$	A	$3\text{CaO} \cdot \text{Al}_2\text{O}_3$	$\text{C}_3\text{A}$
$\text{Fe}_2\text{O}_3$	F	$4\text{CaO} \cdot \text{Al}_2\text{O}_3 \cdot \text{Fe}_2\text{O}_3$	$\text{C}_4\text{AF}$
$\text{MgO}$	M	$4\text{CaO} \cdot 3\text{Al}_2\text{O}_3 \cdot \text{SO}_3$	$\text{C}_4\text{A}_3\text{S}$
$\text{SO}_3$	S	$3\text{CaO} \cdot 2\text{SiO}_2 \cdot 3 \cdot \text{H}_2\text{O}$	$\text{C}_3\text{S}_2\text{H}_3$
$\text{H}_2\text{O}$	H	$\text{CaSO}_4 \cdot 2\text{H}_2\text{O}$	$\text{CSH}_2$

The properties of portland cement are related more to the compound composition than the oxide analyses. The compound composition for portland cement is commonly computed in the cement industry using oxide composition by a set of equations originally developed by R. H. Bogue (Mehta, 1986). The Bogue Equations for estimating the potential compound composition for portland cement are presented in Table 1.2. The computed potential compound composition as determined by the Bogue method is very sensitive to minor changes in the chemical analyses (Mehta, 1986); however, the method is very quick and inexpensive for its capabilities.

Table 1.2 - Bogue Equations

---

% C <sub>3</sub> S	= 4.071C - 7.600S - 6.718A - 1.430F - 2.850S
% C <sub>2</sub> S	= 2.867S - 0.7544C <sub>3</sub> S
% C <sub>3</sub> A	= 2.650A - 1.692F
% C <sub>4</sub> AF	= 3.043F

---

Adapted from (Mehta, 1986)

The hydration of portland cement is a "very complex sequence of chemical reactions between clinker components, calcium sulphate and water, leading to continuous cement paste stiffening and hardening. The stiffening process is the consequence of a change 'from a system of flocs in concentrated suspension to a viscoelastic skeletal solid capable of supporting applied stresses, at least for the

short time without significant deformation'" (Jawed, Skalny and Young, 1983).

The hydration of the clinker phases may be represented by the following simplified stoichiometric equations as shown in Table 1.3. However, the hydration of portland cement is a much more chemically complex dissolution-precipitation process where the hydration reactions proceed simultaneously at various reaction rates and degrees of compound influence. The addition of pozzolonic binders react with the bi-product CH to form CSH although at slow rate. A vast amount of information is available on this topic and will not be discussed further.

Two hydration mechanisms of portland cement have been proposed, through solution hydration and topochemical or solid-state hydration (Mehta, 1986). As described by Mehta the **through-solution** hydration involves dissolution of the anhydrous compounds to their ionic constituents, formation of hydrates in solution, and precipitation of the hydrates from the supersaturated solution. **Topochemical** hydration on the other hand, involves the reaction process to take place at the surface of the anhydrous particles without complete dissolution as suggested in the latter mechanism. More information is available on this topic elsewhere.

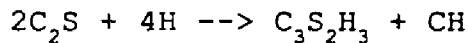
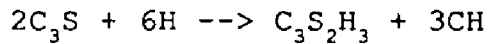
Mechanisms of Fixation in Cement Based  
S/S Metal Wastes

Physical Encapsulation and Chemical Stabilization

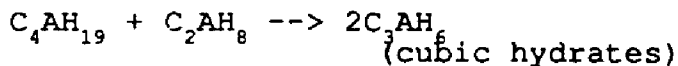
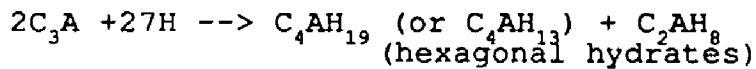
The mechanism of fixation was broadly categorized by Poon et al. (1985a, 1985b) as chemical fixation or physical encapsulation. The authors assessed the leachability and

Table 1.3 - Stoichiometric reactions for fully hydrated clinker phases

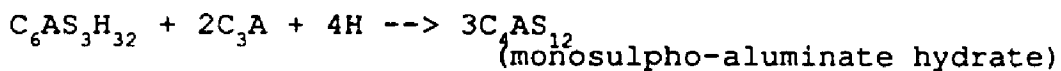
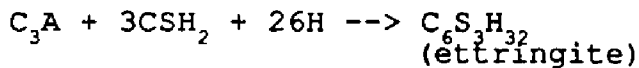
-----  
Hydration of calcium silicates



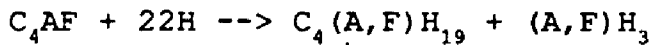
Hydration of calcium aluminates in absence of sulfate



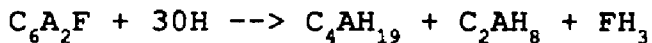
Hydration of calcium aluminates in the presence of sulfates



Hydration of the Ferrite Phase



|  
V  
(usually detected as  $C_4(A,F)H_{13}$ )



investigated the microstructure by scanning electron microscopy and X-ray diffraction of a cement-silicate solidified zinc and mercury waste. They proposed zinc to be chemically stabilized and mercury to be physically encapsulated or at the most, loosely bound to the hydration products through sorption. Furthermore, they claim calcium hydroxide plays an important role in the fixation of zinc ions and ettringite is considered to be related to the structural integrity responsible for fixation of metals in the cementitious system. However, the CSH phase, the major hydration product of portland cement, is not considered to be involved in fixation.

#### **Micro and Macro Encapsulation**

The postulated fixation mechanisms as employed in current technology are presented by Lubowitz et al.(1984). The authors presented data based on a literature survey to describe and evaluate elements of toxic waste fixation. They concluded the fixation mechanisms currently used to be primarily microencapsulation and not chemical fixation and that only minimal amounts of contaminants are actually fixed in molecular or colloidal dispersion. They note that fixing agents (i.e. portland cement, fly-ash, lime) react with the heavy metal contaminants to form precipitation of microscopic and macroscopic particles that were microencapsulated within the solidified matrix.

The views of Lubowitz et al. are shared by Malone and Larson. They state that current technology uses or proposes to use the following: coating grains of material with inert, non-reactive impermeable material (plastic incorporation or microencapsulation), embedding the waste particles in organic or silicated polymer matrices to reduce effective surface area, and coating blocks of waste material with inert, nonreactive impermeable material (macroencapsulation).

Poon et al. (1986b) disagree with Lubowitz et al. and Malone and Larson in reference to the fixation mechanisms being not being chemical in nature. The authors used extended X-ray analysis of fine structure (EXAFS) to investigate the atomic interaction of zinc and mercury in the PC. They observed that Hg is incapable of forming a definite local environment in the cementitious matrix resulting in poorly defined EXAFS spectra. However, Zn shows a defined spectra with 4 coordinated oxygen shell around the zinc atom. The second shell is postulated to consist of O-H and Si atoms. They further claim that their results support the proposed mechanism of a colloidal membrane around cement grains. Furthermore, another interesting observation in their study was that sodium silicate and fly ash did not contribute to the reaction with the metal.

The authors conclude that strong chemical bonding with high dissociation energy can be realized by simple



precipitation reaction although crystal substitution claimed by some vendors is unlikely to take place in normal S/S processes. Their study disclaims the general statement that microencapsulation is the primary fixation mechanism involved in current S/S technology.

The fixation mechanisms claimed by Tashiro et al. (1977) may be categorized as both physical and chemical. The authors suggest a broad generalization for fixation of heavy metals involving adsorption by cement hydrates, substitution and solid solution in the hydrate structure, and formation of chemical complexes. These fixation mechanisms are based on their experiments of Cr, Cu, Zn, As, Cd, Hg and Pb in the hydroxide (oxide) and sulfide pulverized solid forms on the hardening properties of portland cement mortar mixtures and subsequent leaching in distilled water and synthetic seawater. They observed Zn, Pb and Cu inhibited the hardening and Cr, Cd and Hg showed a negligible effect on hardening. Leaching of the heavy metals from the cement mixtures showed  $\text{CrO}_3$ ,  $\text{As}_2\text{O}_3$  and  $\text{HgO}$  exhibited the largest concentrations in the leachate possibly due to the higher solubilities of the complexes formed with hydration products.

Leach testing with weak organic solutions of portland cement solidified metal sludges were performed by Shively et al. (1986). The extractions were kinetically limited and equilibrium was not attained. Concentrations of the metals

were found to be below the solubility of stable hydroxides indicating the probable formation of a more stable compound. Cadmium was the first cationic metal detected in the leachate as compared to chromium and lead. This behavior agrees well with adsorption/desorption characteristics of the metals (Benjamin et al. 1979 and Tipping et al. 1986). Arsenite was detected even earlier than cadmium however as an anion it is expected to be involved in different fixation mechanisms.

Two types of leaching mechanisms are proposed by Shively and coworkers, at pH values greater than 10 sorption-precipitation, and limited dissolution of the cement matrix restricts metal leaching. Peak releases for the more soluble metals occurs as the pH drops to less than 6. Metal leaching at pH less than 6 is suggested to have been limited by diffusion through the solid matrix or slow dissolution of the silicate matrix. Both Shively et al. and Poon et al. observed a substantial increase in metal release as the pH of the leachate dropped below 7.

Long term leach testing of cement, fly ash, lime and silicated S/S wastes was also conducted by Cote (1986). Leach tests on a cement S/S cadmium waste showed a leaching efficiency of 50 percent (half of the original cadmium in the S/S waste was leached out). Furthermore, leaching was a function of the acid neutralizing capacity and metal concentration of the binder matrix. Cote proposes two

binding mechanisms, contaminants that precipitate in the pores of the matrix and those that become incorporated within the cement hydrates are considered to immobilized. Contaminant which are not immobilized (i.e. physically entrapped in the pore solution) are leached readily, and the rate of leaching is a function of available leaching sites (i.e. exposed surface area to acidic leachant).

### **Silica Gel Encapsulation**

Falcone et. al. (1984) observed that the addition of alkaline silicates influenced the solubility of metal ions (Zn and Cr) and reduced the acid leachability of the silica gelled sludge. The effect is much more dramatic when the sludge is treated with a gelled silicate/cement/fly ash composite. They proposed at least three mechanisms that may be involved in reducing the solubility of chromium and zinc ions in the waste:

- o The formation of insoluble chromium and zinc hydroxide silicates
- o Encapsulation of chromium and zinc that involves the formation of insoluble calcium and magnesium (hydroxide), oxide silicates on the sludge particle surface, and
- o Encapsulation of chromium and zinc that involves the formation of a gelled silicate sheath over the sludge particles, which is then rendered insoluble by the addition of calcium ions, supplied by cement.

However it is not possible to distinguish which of the three mechanisms apply to a particular waste treatment, since calcium and magnesium are present in the sludge and also in

the cement. The authors could not determine whether the reduced leachability is the result of encapsulation by a calcium-magnesium (hydrous) silicate species or by formation of chromium-zinc (hydrous) silicated species which are less soluble than the corresponding metal (hydrous) oxides.

The effect of added silicates to a waste sludge was also studied by Ghosh and Johannesmeyer (1985). The authors investigated the effectiveness of fixing chromium and cadmium in an electroplating waste sludge with a silicate-cement mixture and a fly ash-lime mixture. The silicate-cement method is more effective in immobilizing the heavy metals due to the higher silicate content of the mixture.

### Crystal Capture

The Chemfix<sup>R</sup> process is claimed to be based on three phases of reaction. The initial rapid reaction occurs between the soluble silicate and polyvalent metal ions to form insoluble metal silicates, followed by a slower reaction between the silicate and reagent to form a gel and lastly hydration of the cement. The final product is thought to be built on tetrahedrally coordinated silicon atoms alternating with oxygen atoms along the backbone of a linear chain. The pollutant metal ions are ionically bonded between adjacent chains to form a cross-linked, three dimensional, polymer matrix. (Pojasek, 1981)

The Sealosafe<sup>R</sup> process uses cement and fly ash and is claimed to be based on "crystal capture" which is a combination of two interdependent reaction mechanisms. The pollutants present in solution form as ions or complexes react with portland cement and fly ash to form a strong bond within the matrix. Pollutants present in insoluble form are homogeneously dispersed and trapped within the solidified matrix (Pojasek, 1981).

**Effect of Heavy Metals on Hydration of  
Portland Cement and Cement Compounds**

**Protective Membrane**

The formation of a protective membrane around cement grains was suggested by Thomas et al. (1981) while investigating the effect of lead nitrate on the hydration of portland cement. The authors concluded that the hydration process is retarded by the very rapid formation of a protective mixed lead salt gelatinous and colloidal coating of variable stoichiometry involving hydroxide, nitrate and sulfate. A similar type of binding (interactive) mechanism was suggested to occur with other metal cations which yields highly insoluble hydroxy compounds in alkaline solutions (vis -a- vis Cu, Zn, Sn, Cd). It was postulated that similar colloidal membrane formation is typical of precipitation processes occurring within a narrow zone between two solutions with a high degree of supersaturation.

Based on literature cited by Thomas et al. (1981), the authors categorized the retarding capacity of inorganic salt admixtures to occur with metal cations grouped in the middle of the periodic table (groups I<sup>F</sup> - V<sup>B</sup>) with some having amphoteric properties. These metals produce insoluble hydroxides in alkaline solutions, with solubilities considerably less than that of  $\text{Ca}(\text{OH})_2$ . This would support the theory that these insoluble hydroxides suppress cement hydration through the precipitation of protective coatings around cement grains. It is suggested that a protective layer induces retardation by preventing the contact solution from becoming supersaturated with respect to calcium hydroxide (Young, 1972).

A protective membrane was also observed by Arligue et al. (1982) when adding zinc to  $\text{C}_3\text{S}$  and  $\text{C}_3\text{A}$ . The authors observed the hydration mechanism to be disrupted by the rapid formation of a thin layer of amorphous zinc hydroxide around the anhydrous grains. The retardation of  $\text{C}_3\text{A}$  was not as pronounced compared to  $\text{C}_3\text{S}$  due to the crystallization of the envelope rendering it heterogeneous and permeable. In contrast, the hydration of  $\text{C}_3\text{S}$  is reduced or at times completely arrested due to the more homogeneous and impermeable zinc hydroxide envelope surrounding the grain. When the pore solution was enriched with  $\text{Ca}^{2+}$  and  $\text{OH}^-$  ions the authors observed that zinc hydroxide converted to crystalline calcium zinc hydroxide. This crystallization

destroyed the "impermeability" of the envelope and hydration resumed. Similarly, zinc crystallization was observed by Tashiro and Tatibana (1983) and Lieber (1968), however, this phenomenon was not observed by Poon et. al. (1985).

A protective coating was also suggested by Lieber (1968) to explain the retardation of  $C_3S$  by the addition of  $ZnO$  and  $PbO$ . The addition of heavy metals retarded the hydration of  $C_3S$ , while the other clinker phases  $C_2S$ ,  $C_3A$  and  $C_4AF$  were not influenced. Reaction of aluminate and ferrite phases with gypsum proceeded normally and no crystalline lead complexes were detected by XRD. However, a calcium - trihydroxo - aquo - zincate ( $Ca[Zn(OH)_3 \cdot H_2O]_2$ ) was formed during the retardation period. The retardation effect of  $ZnO$  was suggested to be due to a "blocking-up" of the surface of  $C_3S$  particles. In Lieber's closure, he suggests that zinc may enter the lattice of the CSH phase as  $Zn(OH)_2$  interlayer material. When calcium zincate was substituted for  $ZnO$  retardation was found to be less effective and early strength was even enhanced.

Stepanova et al. (1982) are also supporters of the protective membrane for retardation of portland cement hydration due to the addition of heavy metals. The effectiveness of the additives in affecting the strength of cement paste is in the sequence  $Mn < Co < Ni > Cu > Zn$ . The effectiveness of retardation and contribution to strength was attributed to variations of the enthalpies of complex

formation and of the stability constants of complexes of the metals with various ligands. Sychev et al. (1984) attribute their observed acceleration of paste hydration to the 3d metals having incomplete d-orbitals ( $d^{2-8}$ ) and retardation to  $d^{10}$  metals having complete d-orbitals. The authors concluded that 3d metals with acceptor properties are activators while metals with donor properties are inhibitors.

### Adsorption and Substitution

Retardation of  $C_3A$  by  $Cu(OH)_2$  has been suggested by Tashiro (1980). The author observed that  $Cu(OH)_2$  strongly retards the early hydration of  $C_3A$ , and hinders the formation of  $C_3AH_6$ , however hexagonal hydrates  $C_4AH_{13}$  eventually grow with temporal hydration. It appears that the mechanism of retardation is a result of coating or adsorption of  $Cu^{2+}$  onto  $C_3A$  grains. The similarity in ionic potential and crystal structure between  $Ca^{2+}$  and  $Cu^{2+}$  is claimed to be responsible for the retarding mechanism.

Tashiro and Tatibana (1983) analyzed the interface between zinc, iron, and copper wire and  $C_3S$  and  $C_3A$  paste. Crystalline  $Ca[Zn(OH)_3 \cdot H_2O]$  was observed in the interfacial zone between zinc wire and  $C_3S$  paste and it inhibited the bond strength which decreased as follows:  $Fe > Cu > Zn$ . The microstructure of the interface in the case of copper wire showed non-crystalline CSH and that of iron wire was



comparable to the  $C_3S$  paste. These characteristics are believed to be a function of solubility and reactivity of ions under strong alkaline conditions. The bond strength of  $C_3A$  and metal wire was in order of  $Zn > Cu > Fe$ .

The effect of different metals on  $C_3A$  paste was also investigated by Tashiro and Oba (1979). Oxides that retard the hydration of  $C_3A$  (e.g.  $Cu(OH)_2$  and  $ZnO$ ) stabilized the hexagonal hydrates with respect to  $C_3AH_6$ , while those that accelerated hydration (e.g.  $PbO$ ) increased the rate of conversion. Retardation was also noticed when  $Cr_2O_3$  and  $CaCrO_4$  were added to  $C_3A$  paste. The effect of  $CaCrO_4$  is attributed to the initial formation of the chromate analog of ettringite which later transforms to the hexagonal  $C_3A.CaCrO_4.nH_2O$  (Skalney and Young, 1980).

The effect of different metals on the formation and stability of ettringite have been studied by Bensted and Varma (1970, 1971, 1972). These studies have shown the substitution of  $Al(III)$  in ettringite by  $Ti(III)$ ,  $Cr(III)$ ,  $Mn(III)$  and  $Fe(III)$  leads to the formation of similar compounds of the type  $Ca_6[Al(OH)_6]_2.(SO_4)_3.26.H_2O$  which undergo extensive solid solution reactions. Replacement of the  $SO_4^{2-}$  by  $CrO_4^{2-}$  ions results in the compound chromate-ettringite  $Ca_6[Al(OH)_6]_2.(CrO_4)_3.26 H_2O$ . Furthermore, the authors indicate that chromate-ettringite is isomorphous with ettringite, however, unlike the latter, does not undergo substitution of its  $Al(III)$  readily by the larger

Metal(III) ions like Ti(III), Cr(III), Mn(III) and Fe(III) under comparable conditions. Apparently for steric reasons as stated by the authors.

In another study Bensted and Varma (1972) investigated the potential for substitution of SrO and BaO for CaO. A strontium sulfo-aluminate hydrate was formed which bore a close structural relationship to ettringite, however barium oxide did not form a comparable type of compound under similar conditions.

The mechanism of portland cement hydration has been reviewed by Skalney and Young (1980) and Jawed et al. (1983). The authors state that most inorganic electrolytes accelerate the hydration of  $C_3S$ , with soluble calcium salts being the most effective due to their greater effect on the crystallization of  $Ca(OH)_2$ . The exceptions are fluorides, phosphates and cations that form insoluble hydroxides.

Kondo et. al. (1977) are in agreement with Skalney and Young who suggest that salts forming the least soluble hydroxides have the greatest retarding effect and those forming hydroxides of high solubility exhibit only a slight degree of retardation. The authors also considered the effectiveness of ion diffusion to be an important property characteristic in hydration. For example, the high mobility of the  $Cl^-$  ion permits it to penetrate the protective membrane around the  $C_3S$  grain forcing diffusion of other ionic species vis a vis  $Ca^{2+}$  to maintain electro-neutrality

and accelerating hydration. The formation of an impermeable layer of insoluble calcium salts around the  $C_3S$  grain would prevent the pore solution from becoming supersaturated with respect to calcium hydroxide (Young, 1972).

Ranking inorganic salts according to their accelerating and retarding ability using conduction calorimetry was conducted by Wilding et al. (1984). Results in the ranking according to ionic constituents was in agreement with others mentioned above. Based on the "osmotic membrane" theory by Double et al. (1980), it is proposed that the heavy metals that retard or accelerate the hydration of portland cement affect the physiochemical properties of the membrane. The additives could modify this gelatinous colloidal membrane to either a more flocculated and open structure resulting in an accelerated hydration or a more dense and dispersed envelope contributing to retardation.

Kantro (1975) provides the following comments on the acceleration of portland cement paste due to cations:

Although ion size and valence may have some relationship to the accelerations observed, they do not seem to be the only factors involved. Some of these other factors may include influence on the lime solubility, silica solubility, nucleation and precipitation of calcium hydroxide, and the nature of the hydration product, that is, do the ionic components of the salt added enter into the calcium silicate hydrate?

### Discussion

The literature consists of numerous postulated mechanisms on the fixation of heavy metals in S/S systems and of inorganic additives on portland cement hydration. These mechanisms range from simple physical encapsulation to complex chemical reactions. However it can be seen that no one single mechanism can explain all the interactions observed by different heavy metals and inorganic admixtures. Metals have been shown to precipitate out of solution and form colloidal membranes or crystallize in the alkaline solution. The question still remains, how do these heavy metals interact with the hydrating cement and the hydration products. Do these metals actually combine within the major hydration products such as CSH, CH, Aft and Afm? It is possible that these ions or complexes would enter the structure of hydration products since it is known that they accomodate extrenuous ions and their stoichiometry is not exact. Or do these metals reside as ions or complexes within the pore solution? A wide range of pore sizes exists within the hydrated matrix, ranging from a few millimeters to a couple Angstroms in cross section. Those heavy metals that are physically entrapped may exist as complexes in the pore solution or strongly adsorbed by hydration product or as interlayer material within the CSH lattice.

The release of heavy metals from the solidified matrix is usually assessed using empirical leaching studies

involving different solutions and procedures (i.e. water, acids, extraction procedure, toxicity characteristic leaching procedure etc.). The prediction of pollutant mobility requires characterization of the precipitation-dissolution and adsorption/desorption reactions involved. In the case of redox-sensitive elements, the kinetics of redox transformation are also essential to determine the redox species and their precipitation-dissolution and adsorption-desorption reactions. Other waste characteristics such as pH, Eh, solid phase composition, complexing ligands, competing ions, and gaseous phases, influence both precipitation-dissolution and adsorption-desorption reactions which in turn influence the final pore solution. The solid phase composition controls the final aqueous concentration as well as precipitation of secondary phases.

Neutralizing capacity and buffering capacity during acid leaching is an important parameter which affects adsorption-desorption characteristics. The hydration product, calcium hydroxide provides such a buffering capacity against the acidic environment during leach testing and therefore should not be considered as responsible during the initial fixation as suggested by Poon et al (1986). Also the fact that ettringite was not observed during their microstructural analysis of leached samples is a result of the reduced alkaline environment due to the acidic leachant. It is therefore not the loss or instability of ettringite

that causes the metals to be leached out but it is the reduced alkaline environment that causes ettringite to become unstable. Hampson and Bailey (1983) have observed ettringite to be unstable as the pH of the pore solution drops below 11.8 and dissolves at an increased rate below a pH of 10. The release of metals is a function of the local environment which affects the adsorption/desorption and solubility characteristics of the individual metals and metal complexes.

The addition of pozzolonic material and soluble silicates to portland cement based matrices, involves the consumption of calcium hydroxide. This result of the pozzolanic reaction significantly increases durability to acidic environments. The newly formed reaction products in the form of CSH effectively fill up available capillary porosity, increasing strength and impermeability. Which in turn decreases, the availability of leaching sites.

In the case of Gosh and Johannesmeyer (1985) the addition of soluble silicates to their cement solidified metal sludge altered the hydration process of portland cement to create more calcium silicates (i.e. CSH at the expense of CH). This would create a matrix which would be less prone to dissolution by a corrosive environment. The new matrix would be less porous with limited permeability and hence less metals released due to more limited availability of leaching sites.

## CHAPTER II

### SEAWATER CORROSION OF PORTLAND CEMENT BASED SOLIDIFIED STABILIZED WASTES

#### Introduction

Disposal of S/S wastes in the ocean would avoid the socio-political problem resulting from location of landfill sites (Bishop and Gress, 1983). The general public is reluctant to allow landfills to be located in their communities. Marine disposal would also minimize corrosive effects on the cement based S/S waste associated with acidic waters encountered at landfill sites. However, there are physical and chemical interactions between the seawater and the hydrated cement paste that may be detrimental to the solidified matrix. The ions present in seawater that are most corrosive to hydrated cement paste include chlorides, sulfates, carbonates and magnesium.

Additional factors that are known to affect the deterioration potential of the hydrated paste matrix include the porosity and permeability of the hardened material, the uncombined calcium hydroxide of the hydrated paste, and the  $C_3A$  content of the unhydrated cement. The chemical reactions occurring between the corrosive ions and cement paste could manifest into physical deterioration. Formation

of highly soluble compounds and subsequent dissolution would increase the porosity and permeability of the matrix and result in decreased strength.

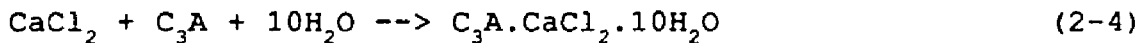
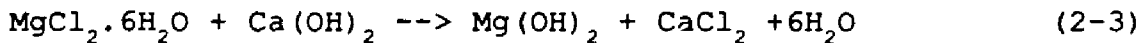
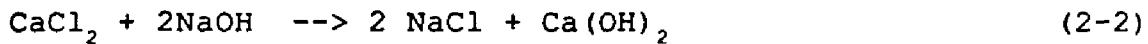
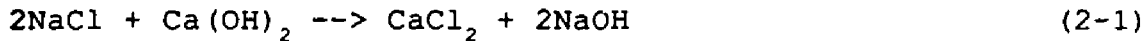
The mechanism of seawater corrosion is very complex due to the numerous corrosive ions and simultaneous chemical reactions involved. Researchers warn against oversimplifying, generalizing and extrapolating the complex situation involved during seawater attack of hydrated cement paste. Never-the-less to understand this complex phenomenon, researchers have conducted corrosion studies on samples immersed in single or combined solutions of the corrosive ions.

#### **Chloride Attack**

The chloride ion as supplied by NaCl and  $MgCl_2$  in seawater could potentially react with hydrated cement paste and result in the formation of monochloro-aluminate hydrate ( $C_3A \cdot CaCl_2 \cdot 10H_2O$  or Friedal's salt), sodium chloride or calcium chloride as shown in Equations 2-1 to 2-4. The higher solubility of calcium and sodium chloride would contribute to increased porosity resulting in increased permeability and subsequent strength loss. The increased permeability could allow further access of the more corrosive ions deeper into the cementitious matrix. The crystallization of chloro-aluminates is accompanied by an increase in volume which may be beneficially accommodated by



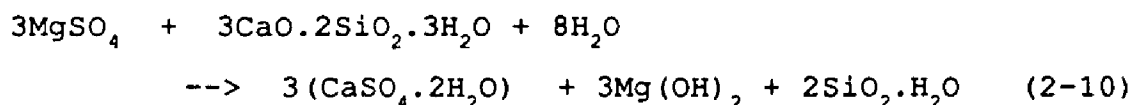
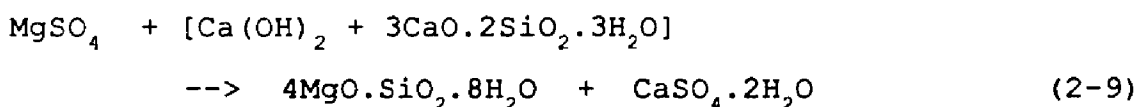
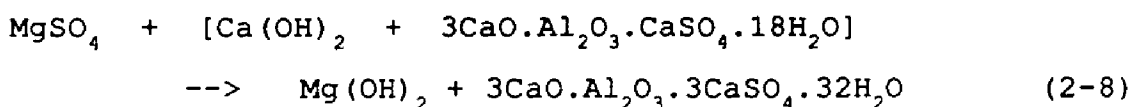
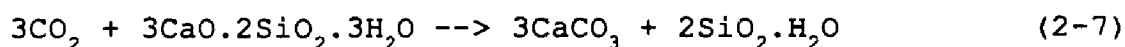
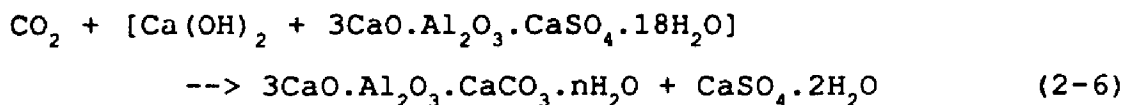
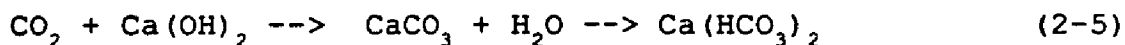
the pores as observed by Conjeaud (1980). This would lower the apparent porosity and may even increase strength.



In the presence of a sulfate environment, monochloroaluminate hydrate becomes unstable and may convert to ettringite (Ftikos and Parissakis, 1985). The  $\text{Cl}^-$  ion is highly mobile and is usually found at much greater depths within the paste matrix than the other ions (i.e.  $\text{SO}_4^{2-}$ ,  $\text{CO}_3^{2-}$  and  $\text{Mg}^{2+}$ ) (Kalousek and Benton, 1970). The chlorides may be removed from solution by reaction with the calcium aluminates, however, if they do not react as such, they could form calcium chloro-silicate hydrate as observed by Conjeaud (1980).

Magnesium and carbonate ion corrosion is commonly surficial at early ages of seawater attack. Formation of potential compounds are shown in Equations 2-5 through 2-10. The  $\text{Mg}^{2+}$  and  $\text{CO}_3^{2-}$  ions will be restricted to the surface layer as long as  $\text{Ca}^{2+}$  and  $(\text{OH})^-$  ions diffuse to the surface (Kalousek and Benton, 1970). Brucite and aragonite precipitation in the pores will decrease the porosity and may limit the permeability (Harvey and Haynes, 1980). This

will result in decreased diffusion of corrosive ions into the paste.



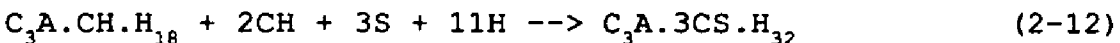
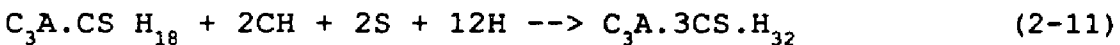
Calcite is unstable with respect to aragonite in seawater due to the  $\text{Mg}^{2+}$  ion (Regourd, 1980). Brucite, however, is very insoluble in seawater and according to Conjeaud its formation is simultaneous to calcite dissolution and aragonite formation.

Chemical reactions involving magnesium and carbonate ions are not restricted to the surface of the paste. When a supply of  $\text{OH}^-$  and  $\text{Ca}^{2+}$  ions to the surface has ceased the  $\text{Mg}^{2+}$  and  $\text{CO}_3^{2-}$  ions find their way into deeper zones of the hydrated matrix.  $\text{Mg}^{2+}$  cations can enter into cation exchange with  $\text{Ca(OH)}_2$  forming  $\text{Mg(OH)}_2$  or with CSH forming

non hydraulic calcium magnesium silicate hydrate (CMSH). The deeper penetration of  $\text{CO}_3^{2-}$  ions may react with soluble calcium silicates and ettringite to form fibrous thaumite ( $\text{CaCO}_3 \cdot \text{CaSO}_4 \cdot \text{CaSiO}_3 \cdot 15\text{H}_2\text{O}$ ). Thaumite weakens the matrix due to low binding characteristics (Regourd, 1980). Occasionally, hydrotalcite ( $\text{Mg}_6\text{Al}_2\text{CO}_3(\text{OH})_{16} \cdot 4\text{H}_2\text{O}$ ) has been observed at the surface of deteriorated concrete samples exposed to excessive seawater attack.

### Sulfate Attack

The alumina-bearing hydrates  $\text{C}_3\text{A} \cdot \text{CaSO}_4 \cdot 18\text{H}_2\text{O}$  and  $\text{C}_3\text{A} \cdot \text{Ca}(\text{OH})_2 \cdot 18\text{H}_2\text{O}$  form as a product of portland cement hydration depending on  $\text{C}_3\text{A}$  content. These alumina containing hydrates both convert to the high-sulfate form ettringite ( $\text{C}_3 \cdot 3\text{CS} \cdot \text{H}_{32}$ ) as shown in Equations 2-11 and 2-12 (Mehta, 1986).



Sulfate related expansion in hydrated cement is agreed upon by most researchers to be associated with ettringite formation, however, the mechanism by which ettringite causes expansion is still a subject of controversy. Induced pressure due to ettringite crystal growth, and swelling due to adsorption of water in an alkaline environment by poorly

crystalline ettringite, are two of the several hypotheses that are supported in most of the literature. The subject of expansion mechanisms by ettringite formation will be reviewed and discussed in detail in Chapter III.

The formation of gypsum as a result of cation exchange is also capable of causing expansion in accordance to the following Equations 2-6, 2-8 and 2-10. Formation of gypsum may also contribute to deterioration of hydrated portland cement paste by causing a reduction in stiffness and strength (Mehta, 1983). Subsequent formation of ettringite will eventually lead to loss of dimensional stability. Excess sulfates may also attack CSH and reduce its stability through the formation of CSSH.

Exposure to seawater generally results in a reduction in volume of the larger pores accompanied by a corresponding increase in the volume of the smaller pores. (Buenfeld, 1986). A low  $C_3A$  content in cement reduces the corrosion associated with seawater, however, a low uncombined CH content in hydrated paste is considered more critical (Ftikos and Parissakis, 1985). The addition of pozzolanic admixtures to portland cement pastes reduces the CH in hydrated paste which is generally more durable to seawater attack (Mehta, 1986).

The breakdown of portland cement concrete placed in concentrated  $CaCl_2$  solution is attributed to crystal growth pressure. However this crystal growth pressure is not

always attributed to Friedal's salt and CH dissolution, but is also associated with the formation of complex salts (Chatterji, 1978)

Dissolution of CH is considered an integral part of chemical corrosion and has been observed by other researchers while investigating the effect of chloride solution on hydrated cement pastes and mortars (Richartz, 1968; Regourd, 1980; Hoffman, 1984; Ben Yair, 1971; and Heller and Ben Yair, 1966). It was also observed that NaCl was more effective in CH dissolution than  $MgSO_4$ ,  $CaCl_2$  or distilled water. Effective dissolution of CH from the hardened cement paste changes the microstructure and increases porosity and permeability and permits further intrusion of other corrosive ions.

#### **Mobility of Chlorides into Portland Cement Paste Matrix**

The chloride ion is highly mobile and is usually found at greater depth from the surface within a hardened paste matrix. The mechanism by which the  $Cl^-$  penetrates the hydrated paste is still a subject of controversy. Collepardi et al. (1969) suggests that the  $Cl^-$  diffuses into the hardened cement paste following Fick's diffusion law and it is independent of the chloride concentration. Gjorv and Vennesland (1979), showed that time was the governing factor in chloride penetration although the w/c ratio also influenced the surface layer penetration. Page et al.

(1981) have observed that activation energies for diffusion of the  $\text{Cl}^-$  ion in OPC differed as a function of water-cement ratio. This was attributed to different pore structures of these materials as availability of large unrestricted capillary pores was absent in the low water-cement ratios. Page et al. (1981) also state:

The rate limiting process governing the diffusion of chloride ions in mature portland cement paste involves some form of surface interaction as others have suggested. The precise nature of this interaction is uncertain as desorption of the diffusing ions from binding sites on the pore walls and structural rearrangements necessary to accommodate ion migration through surface bound water may be involved. Interaction between diffusing chloride ions and the pore surface/bound water layer might therefore be different in character and more easily overcome, implying a lower activation energy in pastes with high w/c ratio.

Chloride diffusion is also influenced by the cement composition. Blended cements containing pfa and bfs sustained lower diffusion while SRPC sustained more. This phenomenon is supposedly attributed to coarser pore size, and not to the  $\text{C}_3\text{A}$  content (Page et al., 1981). Gjorv and Vennesland (1979) observed that the rate of penetration of chloride ions into concrete immersed in seawater shows little dependence on the  $\text{C}_3\text{A}$  content of the cement used, hence the effect of chloro-aluminate formation is termed secondary as compared to factors determined by pore structure.

In their chloride intrusion studies Goto and Roy

(1981) stated that cement paste behaved as an electro-negative semi-permeable membrane so that anions may diffuse faster than cations. They also found that the effect of the w/c ratio on the diffusion coefficients of  $\text{Na}^+$  and  $\text{Cl}^-$  ions is relatively small. This is proposed to be due to the probability that the ions diffuse on the surface of hydrates or that strong interaction of the ions with the surface of hydrates occurs during diffusion.

The formation of Friedal's salt has been observed by numerous researchers conducting chloride solution corrosion studies (Ben-Yair, 1971; Hoffman, 1984; Regourd, 1980; Congeaud, 1980; and Chatterji, 1978). The sequence of formation and stability of Friedal's salt varies depending on the environmental conditions and other constituents in solution. Ben Yair (1974) claims that  $\text{NaCl}$  reacts with  $\text{CH}$  forming  $\text{CaCl}_2$  before the precipitation of Friedal's salt. The instability of Friedal's salt in  $\text{SO}_4^{2-}$  ion solutions gives rise to ettringite formation (Regourd, 1980).

#### **Chloride Reactions During Portland Cement Hydration**

The chloride ions react differently during the course of cement hydration as compared to the corrosion process. The formation of ettringite always occurs first during the hydration of portland cement in the presence of  $\text{Cl}^-$  ions until all gypsum is consumed, then monochloroaluminate is formed, indicating ettringite is more stable (Richartz,

1968). Midgley and Illston (1984) support Richartz's observation and state that the  $\text{Cl}^-$  ion reacts with anhydrous  $\text{C}_3\text{A}$  in hydrated cement paste but not with the calcium aluminates already formed (i.e. ettringite). They maintain that monochloro-aluminate is formed but not all chlorides react as such. The quantity of monochloro-aluminate formed is a function of  $\text{C}_3\text{A}$  present.

Tenoutasse (1968) concludes that  $\text{CaCl}_2$  accelerates the reaction between gypsum and  $\text{C}_3\text{A}$ . The  $\text{SO}_4^{2-}$  ions react first to form ettringite, and formation of monochloro-aluminate begins only after all  $\text{SO}_4^{2-}$  ions have been used up. The trisulpho-aluminate formed in the presence of  $\text{CaCl}_2$  is converted into monosulpho-aluminate only after all the  $\text{CaCl}_2$  has been used up.

In his discussion of Chatterji's paper, Bensted (1979) maintains that calcium monochloro-aluminate hydrate is stable in a cementitious environment and can enter into the solid solution with monosulfate and  $\text{C}_4\text{AH}_{19}$ . He also states that calcium trichloro-aluminate hydrate is much less stable than ettringite, particularly at ordinary temperatures and in the presence of calcium chloride solutions of lower concentration. Bensted adds that monosulfate is formed by the reaction of ettringite with  $\text{C}_4\text{AH}_{13}$ . The compound  $\text{C}_4\text{AH}_{13}$  is produced in significant quantities after insufficient gypsum remains in the partially hydrated paste for reaction with  $\text{C}_3\text{A}$  (and ferrite in the presence of calcium hydroxide)



to form ettringite.

Berntsson and Chandra (1982) and literature cited by them state that a strong calcium chloride solution could cause severe damage to cement mortar. This is attributed to a complex salt formation when  $C_3A$  reacts with  $CaCl_2$  and expansion occurs. According to Richartz and the literature cited by him, Friedal's salt forms on the surface of concrete, however it is not stable during carbonation and forms hydroargillite and restablized vaterite, a calcium carbonate. It appears that the presence of chloride ions influences the formation of vaterite.

#### **Effect of Chlorides on Porosity**

It has been observed that chloride ions alter the porosity of hardened cement paste and change its microstructure morphologically. Regourd, (1980) and others observed that the fibrous CSH changes to a reticulated morphology. Efes (1980) observed that the  $Cl^-$  ion decreased the total and gel pore volume and increased the amount of capillary pores. Hoffman (1984) suggested that changes in the content of gel pores was attributed to the formation of new mineral phases such as the relatively stable Friedal's salt, monosulfate crystalline complex minerals containing chloride. Coarsening of the pores is attributed to calcium hydroxide dissolution.

Similarly, Midgley and Illston (1984) observed a

reduction in small pores and they attributed this reduction in gel pore volume to the formation of "extra material" such as  $\text{CaCl}_2$ . The surface binding of chloride ions on to the CSH surface would fill the pores, however the  $\text{Cl}^-$  ion could possibly be affecting the rate of formation of CSH or its morphology to reduce the inter solid pores. Since no changes in the mineralogical data could be detected it was conclusively suggested that the reduction in pore size is due to the formation of calcium chloride on the surface of the CSH.

Hoffmann (1984), observed a decrease in the finest porosity (less than 30nm) in the superficial layer, but an increase of the microporosity (30 nm - 5 um) as well as the median porosity which corresponds to the pore radius at a pore volume of 50 percent. The modification of the pore structure as suggested by Regourd (1983) may be attributed to changes in the cement paste such as leaching of CH and soluble products as  $\text{CaCl}_2$  or expansion compounds such as monochloro-aluminate.

### Discussion

Seawater corrosion is a very complex phenomenon due to the numerous chemical reactions occurring simultaneously. The extent of corrosion is dependent on the physio-chemical characteristics of the hydrated cement paste. If the permeability allows intrusion of corrosive ions, then the necessary ingredients for the formation of expansive

crystals must be available. If the necessary ingredients are available then the corrosive ions must diffuse through the matrix. The formation of soluble and insoluble products would affect the physical characteristic of this matrix and in turn the corrosion potential.

The physio-chemical interactions presented in this chapter would apply to cement based S/S wastes subject to seawater corrosion. Part of this thesis deals with investigating the effect of seawater on S/S waste as will be presented in Chapter VI.

## CHAPTER III

### EXPANSIVE MECHANISMS ASSOCIATED WITH CHEMICAL CORROSION OF HYDRATED PORTLAND CEMENT

#### Introduction

Sulfate-related expansion in portland cement concrete is generally agreed upon to be caused by ettringite formation, however, the mechanism of expansion caused by ettringite is still a subject of controversy. Cohen (1983) discussed two theories of expansion associated with sulfoaluminate type expansive cements; the crystal growth theory and the swelling theory. According to the crystal growth theory expansion occurs when ettringite crystals grow topochemically on the surface of expansive particles or from solution inducing crystallization pressures and eventually expansive forces. In the swelling theory expansion is caused by water adsorption on to colloidal size ettringite.

#### The Crystal Growth Theory

In the crystal growth theory one scenario that appeals to numerous researchers involves a coating of ettringite crystals surrounding an expansive cement particle. When coating layers exceed the solution thickness, contact pressures develop and expansion occurs (Cohen, 1983).

Kalousek and Benton (1970) studied the effect of seawater attack on cement pastes and attributed the expansion observed to the growth of effective ettringite crystals that grow in confined pores and exert expansive forces against the surrounding walls. The authors subdivided the ettringite crystals into "F-rich" (iron rich) ettringite and aluminum-rich ettringite which they termed "F-poor". The "F-rich" ettringite is a product of the ferrite phases and these crystals do not grow significantly in size and therefore do not induce expansive forces. The "F-poor" ettringite is a product of the aluminate phases formed through-solution. These crystals grow in size and when confined by pore walls, their restrained energy would become the expansive forces leading to expansion.

Brown (1970) challenged Kalousek and Benton's hypothesis that crystal growth is the cause of expansive pressure. Brown stated that crystal growth from solution is not a source of significant energy release and the thermodynamic property associated with pressure of crystal growth is only the heat of solution. He added, that crystals can grow in solution as long as the necessary ingredients are provided, however when crystals become confined and the surrounding "feeding solution" in that particular direction will cease to be available, then growth in that direction will stop. In their rebuttal Kalousek and Benton used a thermodynamic analysis to state that the

free energy of the reaction would convert to work. They added that products such as CH,  $Mg(OH)_2$  and ettringite would cause expansion simply because the product formed had a larger volume as compared to the original anhydrous material.

Nakamura et al. (1968) studied the expansibility of the  $C_4A_3S - CH - CaSO_4 - H_2O$  system, they reported the formation of ettringite to be dependent on the saturation level of the  $SO_4^{2-}$  ion contiguous to the expansive particles regardless of the concentration of CH. In the presence of CH, ettringite crystallizes as fine grains and the magnitude of expansion is a function of the amount of CH. When CH was not present, expansion is not produced even though ettringite formed. Ettringite crystals grow to a larger size in this case. Expansion appears to be a function of crystal size produced, being larger with the smaller crystal.

Kurdowski and Thiel (1981) investigated the role of CaO in expansive cements. They attributed the expansion to ettringite formation and the presence of free CaO in solution. However, it was concluded that the concentration of CaO in the liquid phase seemed to influence the rate of ettringite formation more than the size of its crystals.

#### The Swelling Theory

Expansion according to the swelling theory was proposed by P.K. Mehta (1973). In the presence of a lime saturated

solution, Mehta suggests that the rate of hydration of the aluminate phases decreases substantially and causes the ettringite crystals to be gel-like and colloidal in size. Due to the large specific surface area characteristic of this gel, significant amounts of water adsorb onto the ettringite crystals and generate strong swelling pressures. This leads to expansion of the matrix without any change in the crystal lattice of ettringite. In the absence of lime, the aluminate phases will hydrate rapidly and this forms large, long-lathed ettringite crystals. According to Mehta these crystals will not produce expansion due to their low specific surface area and their adsorbing lesser amounts of water.

Chen and Mehta (1982) reported the zeta potential of synthetic ettringite to be -13.4 mV in a CH solution would promote adsorption of water molecules onto the ettringite surface and increase inter-particle repulsion. The specific surface area as determined by small angle X-ray scattering was 153 m<sup>2</sup>/g, however, this is less than the value of surface area reported to be in the millions by Mather. Cohen (private communication, 1986) stated that Mehta's reported area is insufficient for expansion by water adsorption.

Mehta and Wang (1982) observed in their expansion experiments that finer grained ettringite expanded more than the coarser grained crystals. The expansion was again

attributed to the finer grained ettringite crystals having the larger surface area and hence adsorbing a large amount of water. Negro and Bachiorrini (1982) also reported their expansion to be due to the formation of colloidal ettringite in agreement with Mehta. They also observed that temperature facilitated the formation of colloidal ettringite and hence expansion. Monosulfate hydrate was detected to be formed only after most of the expansion had ceased.

Mehta (1983) proposed another hypothesis regarding sulfate attack. He stated that in the case where sulfate ions are being continuously replenished by an outside source, calcium is removed from the pore solution by means of gypsum precipitation. This eventually depletes all solid CH, removes hydroxyl ions from solution and hence lower the pH. When CSH and ettringite are surrounded with crystalline gypsum instead of crystalline CH, the hydroxyl ion concentration of the contact solution becomes low and the sulfate ions concentration becomes high. The author proposes that under these circumstances CSH begins to lose strength and stiffness and colloidal ettringite crystals become expansive.

In the case of sulfate attack, where the sulfate ions are being continually replenished by an outside source, precipitation of gypsum will eventually deplete  $\text{Ca}^{2+}$  and  $\text{OH}^-$  at the expense of CH dissolution, thus lowering the pH.



Mehta proposes that a drop in the hydroxyl ion concentration and an increase in the sulfate ion concentration of the environment lowers the stiffness of the cement paste and increases the water adsorption capacity of the colloidal ettringite.

Odler (1984) challenged Mehta's proposed theory and stated that:

simultaneous calcium sulfate precipitation and decrease of hydroxyl ion concentration may not occur in cement pastes, unless they are exposed to sulfuric acid solutions. In pastes exposed to calcium sulfate solutions no change of the pH value takes place upon gypsum crystallization, while in those exposed to alkali metal sulfate solutions an eventual precipitation of gypsum is accompanied even with an increase of the hydroxyl ion concentration in the pore liquid due to a simultaneous formation of alkali metal hydroxide.

In his rebuttal, Mehta (1984) states:

... the precipitation of gypsum and its presence in the deteriorated cement paste is not central to the proposed theory; it is only a symptom of the environment which has become supersaturated with respect to sulfate ions. It is speculated that the adhesive strength and stability of cement pastes, which derive their cementing property mainly from CSH, would be reduced when the hydroxyl ion concentration of the pure solution drops with simultaneous increase of the sulfate ion concentration. Thus, the presence of gypsum and depletion of calcium hydroxide need not be directly associated with the sulfate-related expansions. These are only indicative of the environmental change where the attractive forces normally present at the surface of CSH and ettringite particles would no longer be operative.

Rossetti et al. (1982) observed a 77% volume increase when monosulfo-aluminate converts to ettringite. Their zeta potential values of +30 mV in saturated CH solution were not

in agreement with those measured by Chen and Mehta (1982). Expansion due to water adsorption and inter-particle repulsion was not considered significant. The authors' proposed mechanism of expansion was due to crystallization pressure generated by ettringite formation. This crystallization pressure increased the internal porosity of the matrix and consequently a suction of the outside fluid by capillarity occurred. Total expansion is a combined result of crystallization pressure, water adsorption as related to the specific surface area and inter-particle repulsion as quantified by zeta potential. These mechanisms are said to be more effective when the contact solution maintains a high concentration of CH resulting in larger final expansions.

Mehta (1983) discussed Rossetti's paper and stated that the authors should have observed a shrinkage in their samples as the transformation of smaller crystals into bigger ones should lead to densification or shrinkage rather than expansion. Mehta adds that the dissimilarities in stiffness were the probable cause of the observed differences in expansion. Furthermore, the removal of the adsorbed water layers is known to cause an increase in the London van der Waals' forces of attraction, thus increasing strength and stiffness (i.e. elastic modulus).

According to literature cited by Regourd (1983) expansion is not always proportional to the amount of

ettringite formed and the supersaturation of the solution in lime, alumina and sulfate is a major factor in expansion phenomenon. In expansive cements, the  $Al_2O_3$  concentration in solution is low due to ettringite formation at the surface of expansive particles resulting in a localized increase in volume. In non-expansive cements,  $CaO$ ,  $Al_2O_3$  and  $SO_3$  are present in the liquid phase and ettringite precipitates from solution as well formed fibers. In the case of topochemically formed ettringite, a localized supersaturation of the solution and an absence of mass transfer is emphasized.

Buil (1983) calculated the crystal pressure of ettringite as a function of degree of supersaturation of the solution. The degree of supersaturation of solution was higher in the expansive cement paste which lead to higher crystal pressure and subsequently larger expansion.

Cohen (1983) summerizes the similarities and dissimilarities between the crystal growth and swelling theories:

The crystal growth theory and the swelling theory are in agreement about the size and the presence of lime affecting expansion. In the presence of lime, sulfate ions, water and expansive alumina-bearing hydrates, ettringite is formed as small crystals contributing to expansion. In the absence of lime, sulfates, water and alumina bearing hydrates form large ettringite crystals that do not conttribute to expansion.

In disagreement, the crystal growth theory advocates the mode of formation of ettringite crystals as topochemical in the presence of lime and hydration being more favorable and quicker. According to the swelling theory, ettringite always forms in a through-solution mechanism, regardless of the presence or absence of lime. The rate of hydration is believed to be smaller in the presence of lime in disagreement with the crystal growth theory.

### Discussion

The expansion mechanisms just presented are applicable to cement based S/S wastes. It is not certain how the addition of heavy metals will influence these proposed mechanisms. Possible ion substitution in the crystal structure and changes in the pore solution will influence ettringite formation. These concepts will be applied in Chapter VI to identify the expansion mechanisms associated with seawater corrosion of cadmium waste.

**CHAPTER IV**

**MICROSTRUCTURAL CHARACTERIZATION OF**

**SOLIDIFIED STABILIZED WASTE**

**Introduction**

The use of S/S technology is becoming popular among the waste disposal industry to reduce the toxicity of the waste prior to ultimate land disposal. However, there is little knowledge or understanding of the mechanism of containment in cementitious matrices. Leaching studies characterize the mechanism by which contaminants are released from the solidified matrix. However, they do not shed any light on how these contaminants combine within the cementitious matrix and their interactions with other phases of the host matrix. Numerous fixation mechanisms have been claimed by patented processes and researchers and the degree of containment is markedly affected by the particular binding mechanism. A better understanding of the binding mechanisms for particular wastes will aid in improving S/S processes to better serve our waste disposal needs.

**Objective**

The objective of this study is to characterize selected S/S wastes using microstructural techniques. X-ray diffrac-

tion (XRD) analysis is used to identify crystalline forms in the S/S waste. And scanning electron microscopy (SEM) is used with energy dispersive spectrometry to observe the microstructure of the solidified matrix and the distribution of contaminants within the binder matrix.

**Portland Cement Based Waste Preparation**

The contaminants cadmium, lead, chromium and arsenic were selected for their common occurrence in industrial wastes and their high toxicity characteristics. The solidified wastes were prepared with synthesized heavy metal sludges and a Type II portland cement in accordance with Shively (1984) and Brown (1984). The oxide composition of the cement used and the computed Bogue compound composition is shown in Table 4.1.

Table 4.1 - Composition of Portland Cement

---

<u>Oxide</u>	<u>Percent</u>
CaO	62.8
SiO <sub>2</sub>	21.1
Al <sub>2</sub> O <sub>3</sub>	4.6
Fe <sub>2</sub> O <sub>3</sub>	3.3
MgO	3.7
SO <sub>3</sub>	2.8
Na <sub>2</sub> O	0.6
<u>Calculated Bogue</u>	
<u>Compound Composition</u>	
C <sub>3</sub> S	51.7
C <sub>2</sub> S	21.5
C <sub>3</sub> A	6.6
C <sub>4</sub> AF	10.1

---

The heavy metal sludges were prepared from cadmium nitrate, chromium nitrate, lead nitrate and sodium arsenite. The solution pH was adjusted to 8.5 with 6.0 M sodium hydroxide. Partial precipitation of the cationic metals occurred at this pH, however arsenic was added as the anion, sodium arsenite, and did not precipitate at pH of 8.5. The metal concentrations after pH adjustment are shown in Table 4.2.

These heavy metal sludges were mixed with Type II portland cement in accordance to ASTM Standard Method for "Mixing Pastes and Mortars of a Plastic Consistency" (C305-65). The sludges compensated for solids content with distilled water were used as mix water at a water-cement ratio of 1.0. Sample cylinders measuring 1.5 by 3.0 inches were molded and left to set overnight before stripping and curing in a humidity room with a relative humidity of approximately 100 percent.

Table 4.2 - Concentration of Metal in Sludge

---

<u>Metal</u>	<u>Concentration</u>	
	<u>(ppm)</u>	<u>(M)</u>
arsenic	24,000	0.32
cadmium	23,000	0.20
chromium	24,000	0.46
lead	23,000	0.11
mixed-metals:		
arsenic	3,000	0.04
cadmium	4,500	0.04
chromium	2,080	0.04
lead	8,290	0.04

---

### X-ray Diffraction Analysis

X-ray diffraction analysis has been used extensively in the study of portland cement and clinker. This technique is primarily used for phase analysis by cement chemists and researchers (Copeland et al., 1959; Berger et al., 1966; Yamaguchi and Takagi, 1966).

X-ray diffraction as used in this study, identifies crystal structures. The method is blind to amorphous materials and only weakly sensitive to atomic species. The method very accurately measures the spacing between the crystal planes and obtains a rough measurement of X-ray scattering. The resulting spectrum is characteristic of each crystalline phase. Complications arise when a crystal is stressed or unevenly hydrated so as to possess a range of interplanar spacings. High concentrations of one phase frequently interferes with the detection of minor phases.

In the powder method, the crystals to be examined are placed in a beam of monochromatic X-rays. Some of the particles are correctly oriented to satisfy the Bragg Law and reflect the incident beam (Culity, 1978). Every set of lattice planes is capable of reflection, provided that the crystals in the powder specimens are rotated under the X-ray beam. The primary beam is diffracted through an angle of two theta ( $2\theta$ ) and enters the counter tube provided that diffraction conditions of the Bragg Law are satisfied. A recorder automatically plots the intensity of the diffracted



beam as the counter moves on the goniometer circle in synchronization with the specimen over a range of (20) values. The interplanar spacing "d", corresponding to a given value of theta can be calculated by the Bragg Equation (reproduced in Equation 4-1 below) since the wavelength lamda ( $\lambda$ ) is known.

$$\lambda = 2d \sin \theta \quad (4-1)$$

### Instrumentation

A General Electric XRD-3 X-ray diffraction machine with an SPG-1 goniometer and Harshaw detector components was used for this study. A copper X-ray tube was oriented for a line focus at 40,000 volts and 15 ma. Sollar slits were used in both primary and secondary beams as well as a nickel filter for the secondary beam. The detector tube was a sealed Argon-methane proportional counter operated at 1800 volts. The pulse height analyzer settings were chosen to give a 2.6 volt window above a 2.6 volt background level. The integration time constant was 2 seconds and the recorder operated at  $2 \times 10^3$  counts per second full scale for phase identification. The time constant and recorder scale were 40 seconds and  $1 \times 10^2$  counts per second, respectively for semi-quantitative analysis.

### Sample Preparation

XRD analysis was conducted on waste samples cured for 7 and 28 days and 3 years. The cast cylinders were crushed with a mortar and pestle and approximately 10 grams of the hardened waste was hand picked from the core fragments. This selective sampling was employed purposely to avoid fragments that had experienced atmospheric carbonation. Sample pieces were washed with acetone to stop hydration at 7 and 28 days. The fragments were pulverized to pass the No. 200 sieve. The material fraction passing the No. 200 mesh sieve was gently placed in a 2mm deep plexiglass holder and the surface was smoothed with an aluminum spatula to avoid preferred orientation.

## **Results**

Crystalline Phase Identification in Metal Sludges - The precipitates in the metal sludges were analyzed to determine their crystalline compound forms in an effort to possibly locate them in the cement waste matrix. The metal hydroxide precipitated should be a stable form in the alkaline environment of the paste. The lead sludge was identified as lead oxide nitrate hydroxide  $[\text{Pb}_6\text{O}_3(\text{NO}_3)_2(\text{OH})_4]$ . The cadmium sludge precipitated as cadmium hydroxide  $[\text{Cd}(\text{OH})_2]$ . Chromium did not exhibit any strong diffraction peaks, however, there were broad peaks between 37.5 - 39.8 degrees two theta. The arsenite solution did not precipitate at pH of 8.5 and X-ray diffraction was not possible, however, the

solution was oven dried and as expected sodium arsenite crystallized [NaAsO<sub>2</sub>].

Phase Identification of Heavy Metals in the Hardened Paste Matrix - The major anhydrous phases in a Type II portland cement detected by XRD is shown in Table 4.3. A compilation of the probable hydration products in partially hydrated portland cement is shown in Table 4.4.

XRD analysis was conducted on all wastes after 7 and 28 days and 3 years of hydration (3 year samples were originally mixed by Shively, 1984 and Brown, 1984). Cadmium hydroxide was the only crystalline metal hydroxide detected in all the metal wastes. The effect of different metal sludges on the peak intensity of major crystalline compounds in partially hydrated portland cement waste is shown in Table 4.5. The major compounds qualitatively analyzed were calcium hydroxide, ettringite and residual alite and belite from unhydrated cement. It is apparent that cadmium, lead and chromium affect the normal hydration process at early ages. The calcium hydroxide peaks were weakly detected in these wastes after curing for 7 days, however, the peaks were strongly detected after continued curing at 28 days and subsequently at 3 years.

The effect of cadmium on the hydration of portland cement is investigated by quantitatively monitoring the calcium hydroxide formation as a function of the cadmium content added to the mix. The ratio of peak intensities is

Table 4.3 - Major Anhydrous Phases Detected in Portland Cement by XRD  
Adapted from El-Korchi (1982)

<u>2θ</u>	<u>PHASE</u>	<u>2θ</u>	<u>PHASE</u>	<u>2θ</u>	<u>PHASE</u>
22.7	C <sub>3</sub> S	34.2	C <sub>3</sub> S,β-C <sub>2</sub> S	47.1	C <sub>4</sub> AF,C <sub>3</sub> S,C <sub>3</sub> A
24.1	C <sub>4</sub> AF	34.8	C <sub>4</sub> AF	48.8	C <sub>4</sub> AF,C <sub>3</sub> S
25.3	C <sub>4</sub> AF	36.6	β-C <sub>2</sub> S	50.2	C <sub>4</sub> AF,C <sub>3</sub> S
26.2	C <sub>3</sub> S	37.2	C	50.5	C <sub>4</sub> AF
27.8	β-C <sub>2</sub> S	38.6	C <sub>3</sub> S	51.6	C <sub>3</sub> S
29.2	C <sub>3</sub> S,β-C <sub>2</sub> S,C $\bar{S}$ H <sub>2</sub>	39.3	β-C <sub>2</sub> S	53.2	C <sub>4</sub> AF
29.9	C <sub>3</sub> S,β-C <sub>2</sub> S	41.4	C <sub>3</sub> S,β-C <sub>2</sub> S	53.8	C
30.8	β-C <sub>2</sub> S	41.9	C <sub>4</sub> AF	56.3	C <sub>3</sub> S,C <sub>3</sub> A
		to 42.2			
32.1	C <sub>3</sub> S,β-C <sub>2</sub> S,C <sub>3</sub> A,C	42.8	M	58.3	C <sub>4</sub> AF
32.4	C <sub>3</sub> S,β-C <sub>2</sub> S	43.8	C <sub>4</sub> AF,β-C <sub>2</sub> S	59.8	C <sub>3</sub> S
33.0	C <sub>3</sub> A,β-C <sub>2</sub> S			60.2	C <sub>4</sub> AF
33.8	C <sub>4</sub> AF	45.6	C <sub>3</sub> S,β-C <sub>2</sub> S	62.2	C <sub>3</sub> S

Table 4.4 - Probable Hydration Products Detected in Partially Portland Cement by XRD

Adapted from El-Korchi (1982)

d	2θ	Probable Phase Contribution
8.2	10.78	$C_4ASH_{10}^{(22)}$ ; $C_4AC_{1/2}H_{12}^{(15)}$
7.95	11.12	$C_3AH_7^{(15)}$
5.61	15.78	Ettringite <sup>(15)</sup>
5.06	17.52	Hydrogarnet <sup>(23)</sup>
4.9	18.1	CH <sup>(15)</sup> ; $C_4ASH_{12}^{(15)}$
4.69	19.9	Ettringite
4.52	19.18	$C_4AC_{1/2}H_{12}^{(24)}$
4.38	20.25	Hydrogarnet
4.10	21.64	$C_2AC_{1/2}H_{12}$ ; $C_4AS_2H_{10}$
3.88	22.9	Ettringite; $C_3AC_{1/2}H_{12}$ ; $C_3AH_{13}$
3.11	28.66	CH
3.06	29.14	C-S-H <sup>(24)</sup>
3.04	29.34	Alite <sup>(15)</sup> , Belite <sup>(15)</sup>
2.97	30.06	Alite
2.88	31.02	$C_2ASH_{12}^{(24)}$ ; $C_4ASH_{10}$ ; $C_2AC_{1/2}H_{12}$ ; $C_3AH_{13}$ ; Belite
2.80	31.92	C-S-H
2.77	32.29	Alite; Belite; Hydrogarnet; Ettringite
2.74	32.54	Alite; Belite; $C_3AC_{1/2}H_{12}$ ; $C_4AC_{1/2}H_{12}$
2.70	33.14	$C_3A^{(15)}$ ; $C_3AH_{13}$
2.63	34.08	CH
2.56	34.96	Ettringite; $C_4AC_{1/2}H_{12}$
2.45	36.56	$C_3AH_{13}$ ; $C_4ASH_{12}$ ; $C_4AC_{1/2}H_{12}$
2.40	37.44	$CaO^{(15)}$
2.27	39.66	Hydrogarnet; $C_4ASH_{12}$
2.23	40.4	Ettringite; $C_2ASH_{12}$
2.21	40.82	Ettringite; $C_2ASH_{12}$
2.18	41.28	Alite; Belite
2.17	41.50	Alite; Belite
2.10	43.02	$MgO^{(15)}$
2.07	43.68	$C_4ASH_{12}$
2.00	45.28	Hydrogarnet
1.93	47.12	CH
1.81	50.6	CH
1.79	51.3	CH
1.69	54.32	CH; $C_3AH_{13}$

Table 4.5 - XRD: Phase Identification  
Effect of Heavy Metal on Peak Intensity

<u>Sample</u>	<u>Phase</u>	<u>7 days</u>	<u>28 days</u>	<u>3 years</u>
Control	CH	s	s	s
	Aft	s	s	s
	A + B	m	w	vw
Cadmium Waste	CH	w	s	s
	Aft	w	s	s
	A + B	m	w	vw
	CdH	s	s	s
Lead Waste	CH	w	s	s
	Aft	w	s	s
	A + B	s	w	vw
	Lead Complex	nd	nd	nd
Chromium Waste	CH	s	s	s
	Aft	s	s	s
	A + B	s	w	vw
	Chromium Complex	nd	nd	nd
Arsenite Waste	CH	w	s	s
	Aft	s	s	s
	A + B	m	w	vw
	Arsenite Complex	nd	nd	nd

vw = very weak; w = weak; m = medium; s = strong  
 CdH = Cadmium Hydroxide; A = Alite, impure C<sub>3</sub>S;  
 B = Belite, impure C<sub>2</sub>S; Aft = "aluminate-ferrite-trisubstitute" or ettringite

used since the ratio of peak intensities of two substances is directly proportional to their weight percentage ratio (Culity, 1978). Due to its crystallinity, only the cadmium waste will be investigated in this quantitative analysis. The peaks used for the relative quantitative analysis are

located at two theta (2 $\theta$ ) degrees (Cu, K $\alpha$ ) corresponding to interplanar "d" spacings of 34.08 deg and 2.63 A $^\circ$  for CH and 35.14 deg and 2.55 A $^\circ$  for cadmium hydroxide. The intensity ratios are obtained by measuring the area under the respective peaks. The goniometer was scanning at a rate of 0.2 degrees per minute while the strip chart recorder was operating at 2 feet per hour. This combination produced a diffraction pattern of 0.5 degree per inch. The average of four readings ( $\pm$  2 std deviations) is presented in Table 4.6.

The cadmium sludge to cement ratio increased from 1.0 to 5.0 while calcium to cadmium hydroxide ratios decreases significantly (determined using ANOVA). The binding properties of the cadmium waste are also affected as was visually and qualitatively noted during sample preparation. The cadmium waste with the sludge-cement ratio of 5.0 crumbled when handled during the course of curing even after 28 days. This indicates that cadmium hydroxide affects the normal course of hydration resulting in an increasingly non-cohesive or non-binding matrix.

#### **Scanning Electron Microscopy and Energy Dispersive Spectrometry**

Scanning electron microscopy was utilized to observe the microstructure of the different S/S wastes during the temporal hydration process. Energy dispersive spectrometry was used to locate the heavy metals within the hydrated

cement matrix and identify various microstructures by determining their elemental composition.

Table 4.6 - QXRD Analysis  
Relative Intensities

---

Sludge ----- Cement	1.0	3.0	5.0
CH ----- CdH	5.58 ± 1.10	3.67 ± 1.56	1.04 ± 0.22

---

#### Instrumentation

An American Research model 1000 SEM fitted with an EDAX model 711 energy dispersive X-ray detector was used. The exciting voltage was 20 KeV and all elemental analysis was conducted on selected sites for an accumulated count duration of 100 seconds.

#### Sample Preparation

Waste samples were manually fractured to expose the internal surface and then mounted on carbon stubs with conductive carbon-silver paint. This sampling technique will produce fractured faces along the weakest planes, however, this does not appear to be selective along heavy metal or non-heavy metal bearing sites as compared to



samples frozen in liquid nitrogen prior to fracturing. The fractured samples were coated with a thin layer of approximately 200 Å of chromium, copper or gold-palladium. Chromium and copper were used to avoid interferences with the sulfur and cadmium lines in elemental analysis.

### Results

The microstructure of the waste as observed under the SEM is shown in Figures 4.1 and 4.2. These SEM photomicrographs show typical microstructures at 3, 7 and 28 days and 3 years of hydration accompanied by a typical EDAX spectrum at 3 years. The 3 and 7 day specimens were oven dried at the end of their curing period while those at 28 days and 3 years were vacuum desiccated to stop the hydration and out gas the specimen.

Microstructure of the control paste specimen is shown in Figure 4.1 A-C. The microstructure of 3 day hydration is typified by anhydrous cement grains coated with hydrated CSH gel layer with initial fibrous morphology. Ettringite crystals appear prismatic and deposit in the voids or on the surface of hydration material. Calcium hydroxide crystals initiate as thin hexagonal plates and then develop into larger striated ones induced by fracture during sample preparation. Continued hydration as observed in the specimens cured for 3 years, results in continued CSH

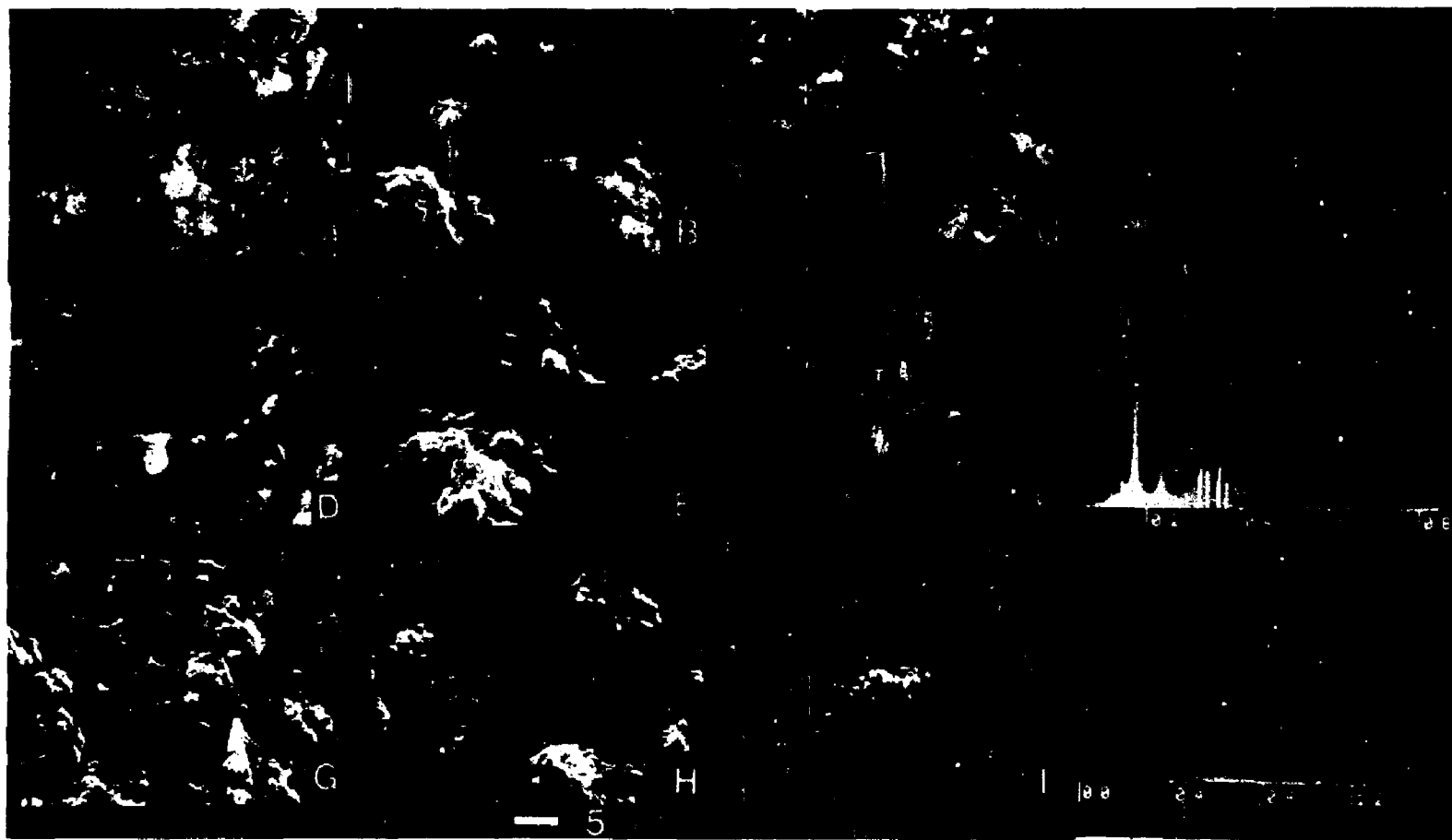


Figure 4.1 - SEM photomicrograph of S/S wastes: Control A) 3 days B) 7 days C) 3 years + EDAX  
Cadmium waste D) 3 days E) 7 days F) 3 years + EDAX; Lead waste G) 3 days  
H) 7 days I) 3 years + EDAX.

development, and interconnecting cement particles. CH and Aft crystal grow larger as well.

Micrstructural differnces are observed upon addition of the heavy metals. The cadmium waste (Figure 4.1 D-F) exhibits a more reticulated and fibrous hydration layer at 3 days and with lesser ettringite crystals as compared to the control. The growth of CH crystals appears normal. Continued hydration for 3 years exhibits typical microstructures. The lead waste (Figure 4.1 G-I) exhibits the most dramatic difference in early hydration characteristics. The 3 day specimens showed only anhydrous cement grains with thin gelatinous surfaces at 7 days. After continued hydration into 28 days and longer, typical hydration microstructure appears.

Figure 4.2 consists of representative SEM photomicrographs for arsenic (Figure 4.2 A-C), chromium (Figure 4.2 D-F) and mixed metals (Figure 4.2 G-I) wastes. The addition of sodium arsenite creates a highly reticulated surface at early ages and well developed ettringite crystals. Continued hydration inter-contacts the cement grains with the fibrous hydrates and well developed Aft. Calcium hydroxide is not apparent at 3 days but is well developped at 28 days and 3 years.

The chromium waste exhibits well developped CH hexagonal plateletts, however it was not possible to determine if the smaller thin plates are Aft crystals. The

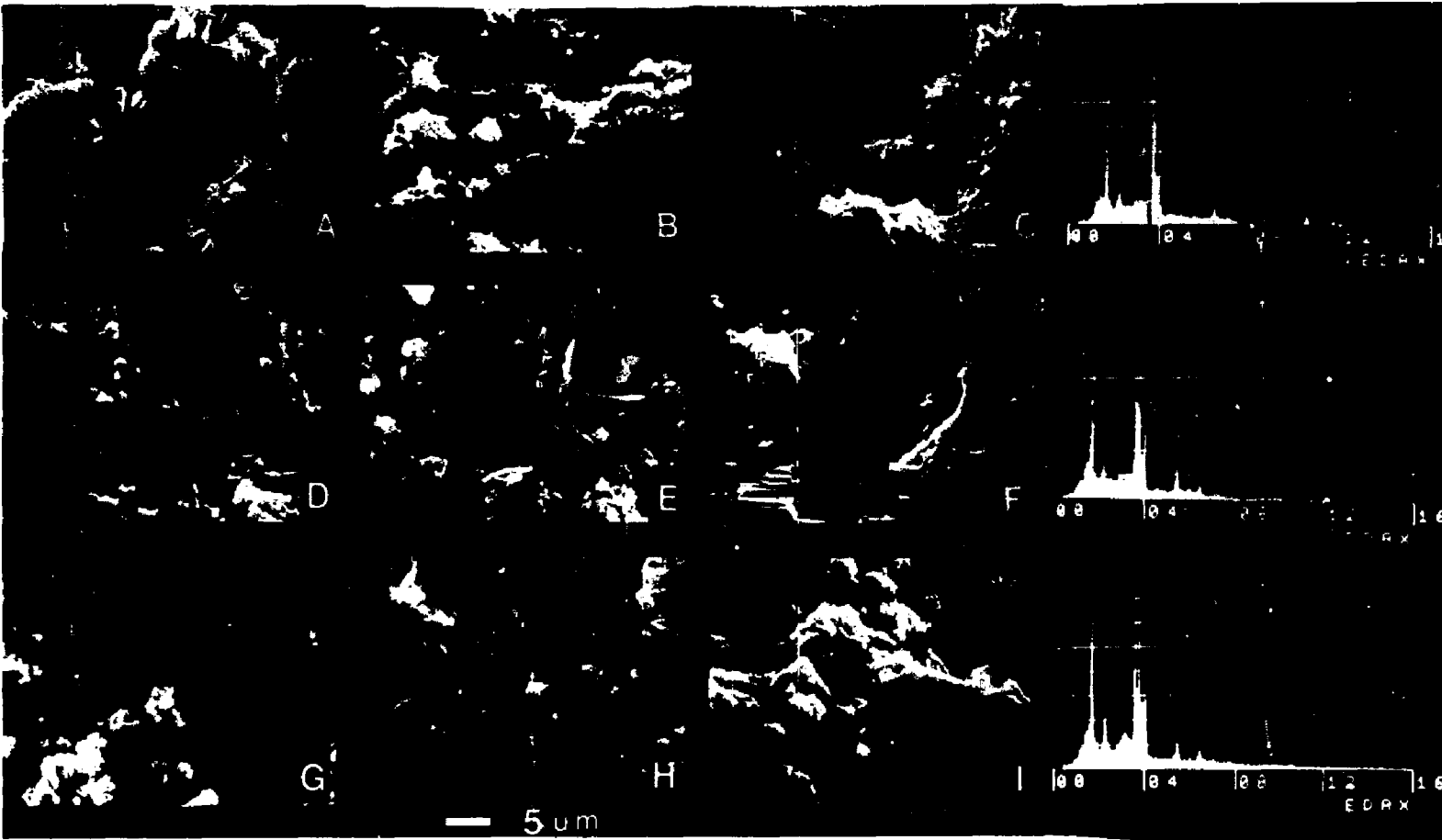


Figure 4.2 - SEM photomicrograph of S/S wastes: Arsenic A) 3 days B) 7 days C) 3 years + EDAX  
 Chromium waste D) 3 days E) 7 days F) 3 years + EDAX ; Mixed Metal waste G) 3 days  
 H) 7 days I) 3 years + EDAX

hydration product covering the cement grains appears equant grain and not as fibrous as observed previously. Continued hydration shows well developed CH plates and visibly denser material.

The mixed metal waste has a microstructure similar to anhydrous cement grains with a thin layer of hydration product. After 7 days of hydration, hexagonal platelets appear with minute fibers. The mature paste at 3 years shows a visibly dense structure with equant grain CSH and CH plates.

Chemical analysis using EDAX was performed on various microstructures as observed by SEM to qualitatively determine their association with different metals. Results of the EDAX analysis is summarized in Table 4.7. These chemical compositions should be interpreted with caution due to the limitations associated with sample roughness and beam spread (Diamond, 1972; Diamond et al. 1974).

X-ray dot maps were made of the desired elements of interest on fractured and polished wastes as shown in Figure 4.3 were also attempted. All waste samples appear to be homogeneously distributed within the waste matrix. However, it is difficult to associate a particular metal with a known morphology using X-ray dot mapping due to limitations as mentioned above.

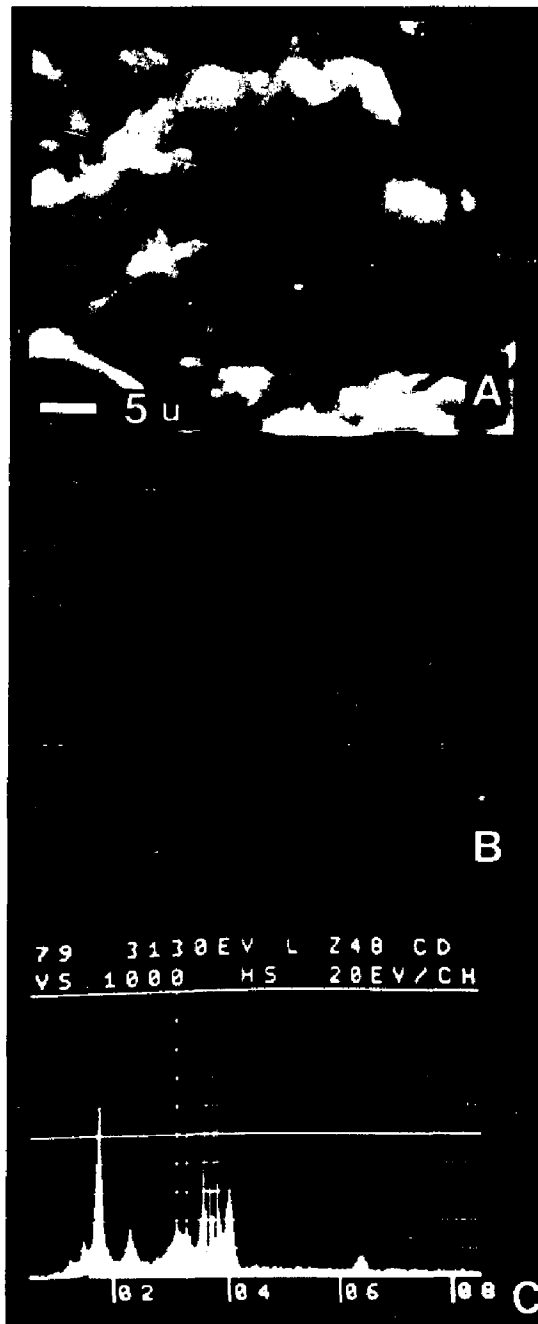


Figure 4.3 - SEM photomicrograph of cadmium waste cured 28 days  
A) secondary image B) X-ray dot map C) EDAX  
spectrum showing detectio of cadmium

Table 4.7 Chemical Composition of Different Solidified Wastes  
using SEM/EDAX (w/c = 1.0 and cured 28 days)

Element	Cr	Pb	As	Cd	Mixed Metal
Na	2.26*	0.82	1.03	0.71	0.3
Mg	1.48	1.12	1.32	1.09	1.07
Al	2.69	2.52	1.99	3.29	2.3
Si	16	16.43	13.24	16.17	14.9
S	1.67	2.69	2.07	1.77	2.3
Cl	0.99	0.63	-	-	0.51
K	0.36	-	-	0.31	0.22
Ca	69.75	72.97	72.7	71.43	68.7
Fe	2.05	1.97	1.41	2.15	1.82
Cd	-	-	-	2.32	0.3
Cr	2.65	-	-	-	0.7
As	-	-	0.46	-	-
Pb	-	0.84	-	-	-

\* all values in g/g of solidified waste  
- element not detected

### Discussion

The microstructure as determined by both techniques, XRD and SEM/EDAX had a good correlation in identifying the different microstructures during the course of temporal hydration. XRD was successful in identifying the crystalline phases in the hydrated cement waste. Cadmium hydroxide was identified as the crystalline metal phase, however, lead, chromium and arsenic did not exhibit similar crystalline behavior. It is not clear why the other metals did not develop a crystalline phase in the highly alkaline environment of hydrating cement. A possible explanation for this observation could be related to the nature of the precipitate forming from two supersaturated solutions (Birchall et al., 1980). These heavy metals have to form into some amorphous phase with or without other cement constituents because they do not crystallize upon drying the sample.

The retarding effect of lead is well documented and was observed in this study. A gelatinous coating was observed around cement grains during the early periods of hydration and CH peaks were not detected in XRD analysis. This retarding or gelatinous membrane effect was not observed with chromium sludge or arsenite solution but slightly with cadmium. However, the loss in binding characteristic of the cadmium waste with the addition of cadmium sludge is attributed, in my opinion, to the hinderence of calcium



hydroxide formation by the cadmium hydroxide.

I personally believe that the  $\text{Cd}^{2+}$  ions compete with  $\text{Ca}^{2+}$  for  $\text{OH}^-$  ions. The formation of cadmium hydroxide would limit or poison the formation of calcium hydroxide. This would maintain a solution supersaturated with  $\text{Ca}^{2+}$  ions and prevent further dissolution of calcium silicates which in turn limits the formation of CSH. Calcium hydroxide crystals are considered to be nucleation sites for CSH formation (Birchall, 1986). The limited formation of CSH in the waste will result in a low binding matrix.

Detection of all heavy metals was made possible by EDAX analysis. The heavy metals appear to be homogeneously distributed within the hydrated paste matrix as observed by X-ray dot maps. Spot analysis was able to detect different metals within morphologically recognized microstructure, however, it is difficult to associate a single metal with a particular hydration product due to the resolution of the SEM and contributions from other phases due to beam spread. It is stated qualitatively that all heavy metals (Cd, Pb, As, Cr) were detected in the CSH structure; chromium, cadmium and arsenic in ettringite, and cadmium in CH.

### Conclusions

o XRD analysis was successful in identifying the crystalline phases. Crystalline cadmium hydroxide was formed in the cement waste matrix. The other metals (Pb, As and Cr) formed amorphous phases and were not detected.

o The addition of heavy metal sludges affects the normal temporal hydration process and was followed by XRD and SEM.

o All metals were detected by EDAX and were homogeneously distributed within the waste matrix.

o Equipment limitations and beam spread difficulties precluded the definitive association of the heavy metals with particular hydration products. Qualitatively, all heavy metals were detected in the CSH, lead, cadmium and chromium in ettringite and cadmium in CH.

#### **Proposed Future Work**

o Use pure cement compounds (i.e.  $C_3S$ ,  $C_2S$ ,  $C_3A$ ,  $C_4AF$ ) to determine the possible association of these metals with cement hydrate phases.

o The use of high voltage TEM with EDAX capabilities should be used to determine the extent of microstructural inclusion of the metals within some hydration products.

## **CHAPTER V**

### **PHYSICAL AND MECHANICAL CHARACTERISTICS OF SOLIDIFIED STABILIZED WASTE**

#### **Introduction**

The total porosity and pore size distribution of a solid affects its physio-mechanical properties and permeability characteristics. The correlation between porosity and permeability is dependent on total porosity, pore size distribution, tortuosity of the pores and the morphology and configuration of the pores. Total porosity and pore size distribution may be used as potential indicators of the physio-mechanical properties and leaching potential of S/S wastes.

#### **Objective**

The objective of this study is to determine the total porosity and pore size distribution of S/S wastes by helium displacement and mercury intrusion porosimetry (MIP) in an effort to relate the porosity data to mechanical strength and leaching potential.

#### **Mercury Intrusion Porosimetry**

Mercury intrusion porosimetry is extensively used in

cement and concrete research to determine pore size distribution. This is considered to be more important in determining physio-mechanical properties than total porosity. The pore size distribution rather than the total porosity is suggested to influence (or control) strength, permeability and volume changes in a hardened cement paste as well as other properties like freeze-thaw resistance.

Mercury intrusion porosimetry (MIP) is very informative in determining pore size distribution, density and specific surface area of porous materials. The pore size distribution is approximated by estimating the intruded volume of mercury under pressure. The Washburn Equation (Orr, 1969) relates the pore radius to the applied pressure by Equation (5-1).

$$r = \frac{2 \sigma \cos \theta}{P} \quad (5-1)$$

where:

r = pore radius

$\theta$  = contact angle

$\sigma$  = surface tension of mercury

P = pressure of intrusion

The pore size distribution is affected by water-cement ratio and degree of hydration. Strength and permeability

are governed by large pores while the small pores influence the drying shrinkage and creep (Mehta, 1987). Goto and Roy (1981) and Mehta (1987) suggest that pores larger than 50 to 100 nm may be detrimental to strength and permeability. Mehta and Manmohan (1980) found a positive correlation between the permeability coefficient and volume of pores greater than  $1320 \text{ \AA}$ . This condition was typical of paste samples made with water-cement ratios of 0.5 or less and cured for 28 days or more. An increase in volume of pores greater than  $1320 \text{ \AA}$  caused the permeability coefficient to increase exponentially. Also, the addition of chlorides to the mix reduced the volume of large pores significantly.

Although used extensively the MIP method is controversial due to the high pressures involved during the test and the method of moisture evacuation used for sample preparation. The effect of "ink well" pores which are pores with small neck openings and larger bodies also adds to the complexities of this technique. This tends to over estimate the volume of smaller pores and underestimates the larger ones, however, by monitoring mercury volume during extrusion this effect may be detected (Orr, 1969).

There are at least two other sources of error that exist in the test. The value of contact angle between mercury and hardened cement paste is generally not known with precision and may vary with pressure and the nature of hydrates in pastes. The Washburn equation is sensitive to

contact angle, hence the calculated pore size distribution can only be comparative rather than absolute (Hughes, 1982).

The technique strictly assigns a pore volume to the size of the pore entrance rather than giving a continuous representation of pore profile. It is also assumed that the preparation of the specimen and mercury intrusion do not damage the pore structure which may be particularly erroneous. In the absence of a better alternative, this technique provides useful information on pore size distribution.

#### Helium Displacement Porosimetry

Conventional tests using water for determining specific gravity/density measurements may not be suitable for S/S waste testing due to potential dissolution of waste and binder material. To measure true density of samples, full displacement of pore volume is required and alternative methods such as mercury intrusion and gas displacement may be used.

Total porosity was determined for this study by the gas volume displacement method using a helium pycnometer. Air pycnometer measurements are based on Boyle's Law. The volume of a sample can be obtained by changes in pressure as compared to a reference chamber pressure. The sample volume may be calculated from equations (5-2) (Hannak, 1986).

$$V_s = V_r \frac{(P_{eq} - P_{atm})}{P_1 - P_{eq}} \quad (5-2)$$

where:

- $V_s$  = sample volume
- $V_r$  = reference chamber volume
- $P_{eq}$  = equilibrium pressure at  $V_s = V_r$
- $P_{atm}$  = atmospheric pressure
- $P_1$  = evacuated sample chamber pressure

### Experimental

Porosity measurements were conducted on the 3 year old heavy metal samples prepared as described in Chapter IV and newly mixed samples cured in seawater for 6 months. MIP testing was done at the Energy, Mines and Resources Canada, Coal Research Centre, Devon, Alberta, Canada. Helium displacement testing was conducted at the Alberta Environmental Centre, Vegreville, Alberta, Canada.

Unconfined compressive strength tests were conducted on the cylindrical specimens as described in Chapter IV using ASTM Test for "Compression Strength of Cylindrical Concrete Specimens" (C39-836). The specimen ends were sulphur capped prior to testing using ASTM Method for "Capping Cylindrical Concrete Specimens" (C617-84).

## Results

### Mercury Intrusion Porosimetry

Results as presented in Figure 5.1 show the pore size distribution for heavy metal and control samples. Only one set of data is available for each metal waste with one duplicate, therefore a statistical analysis is not possible. All samples have the same characteristic distribution with the heavy metal waste specimens having the higher intruded volume compared to the control paste as shown in Figure 5.1. The threshold capillary ( $T_c$ ), defined as the diameter where significant mercury intrusion first occurs, is approximately the same for all specimens and is located between 4 and 7  $\mu\text{m}$ . The total intruded volume follows the trend Arsenic > Mixed Metal > Cadmium > Lead > Blank.

The effect of water-cement ratio (0.5 and 1.0) on cumulative MIP for the control sample is presented in Figure 5.2. The specimen with the higher water-cement ratio increases both the total intruded volume and the volume for  $T_c$ , however  $T_c$  is shifted to the pores with smaller entrance diameter. Similar behavior is observed with the cadmium waste specimens presented in Figure 5.3. (This behavior could then be attributed to the water-cement ratio rather than chemical interactions such as precipitation in pores or newly formed products depositing in the pores and resulting in a shift of pore entrance size). Seawater curing of the cadmium specimen shifts  $T_c$  to an even smaller pore entrance



### Cummulative Pore Size Distribution mercury intrusion

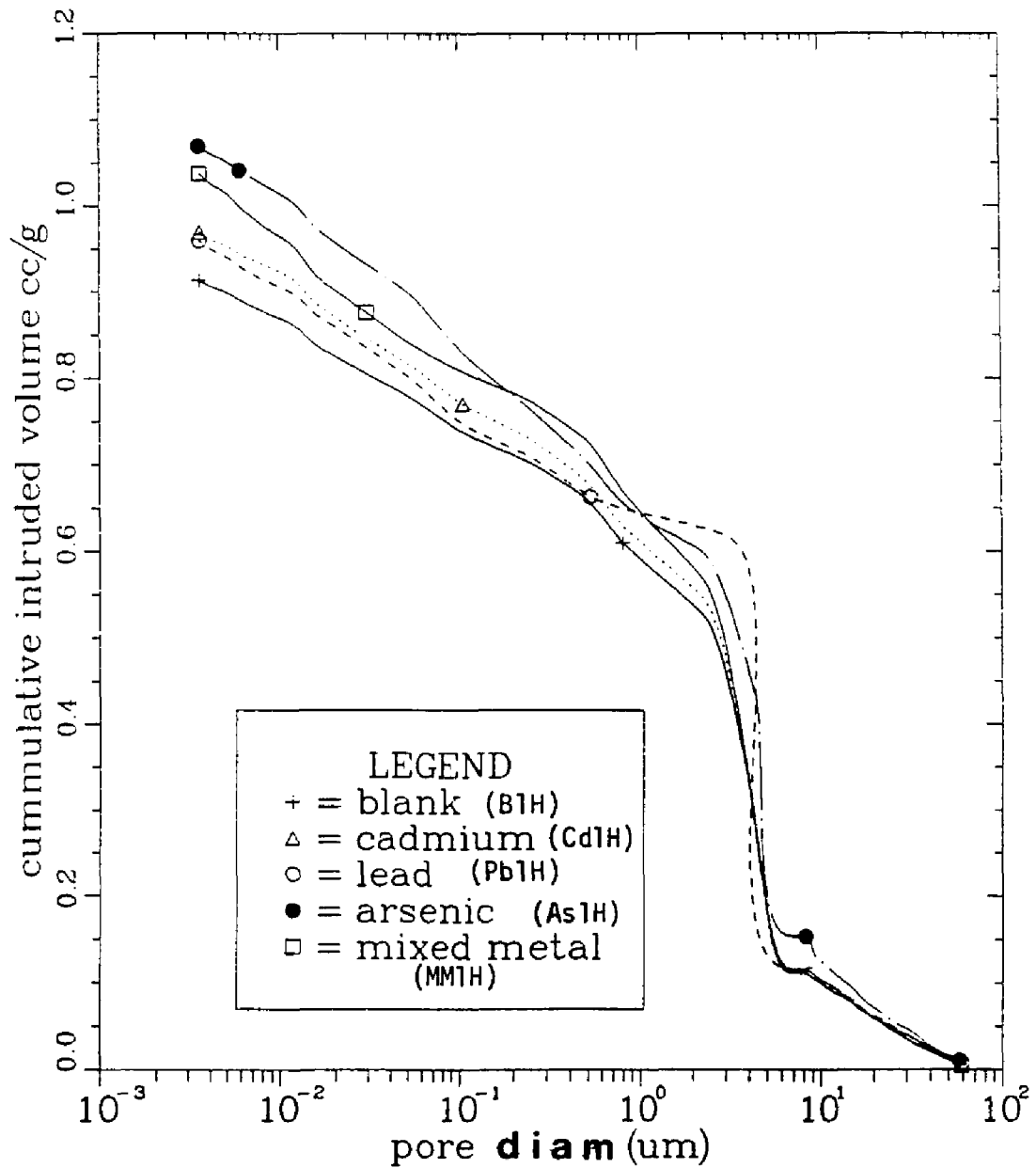


Figure 5.1 -

### Cummulative Pore Size Distribution mercury intrus ion

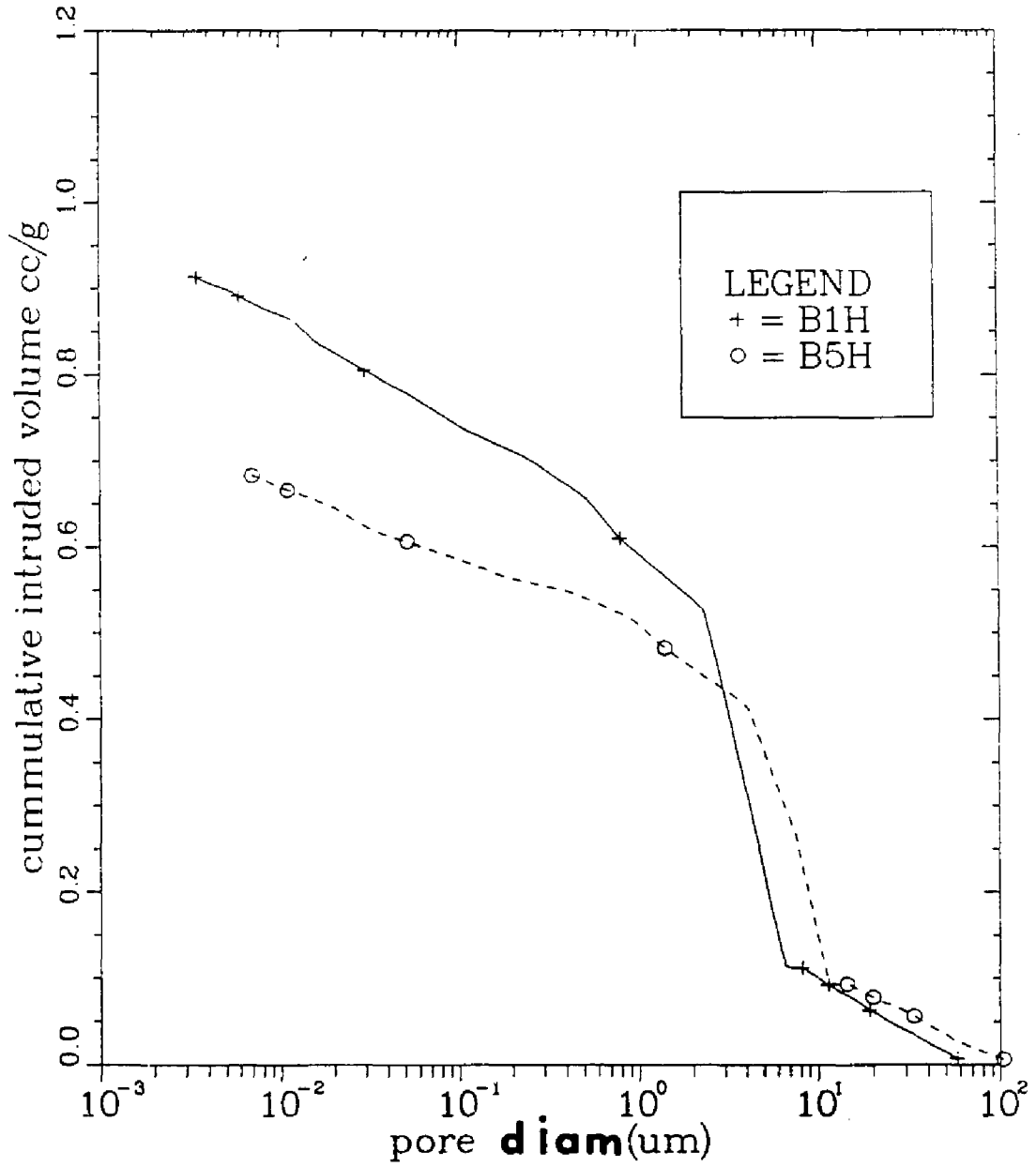


Figure 5.2 -

### Cummulative Pore Size Distribution mercury intrusion

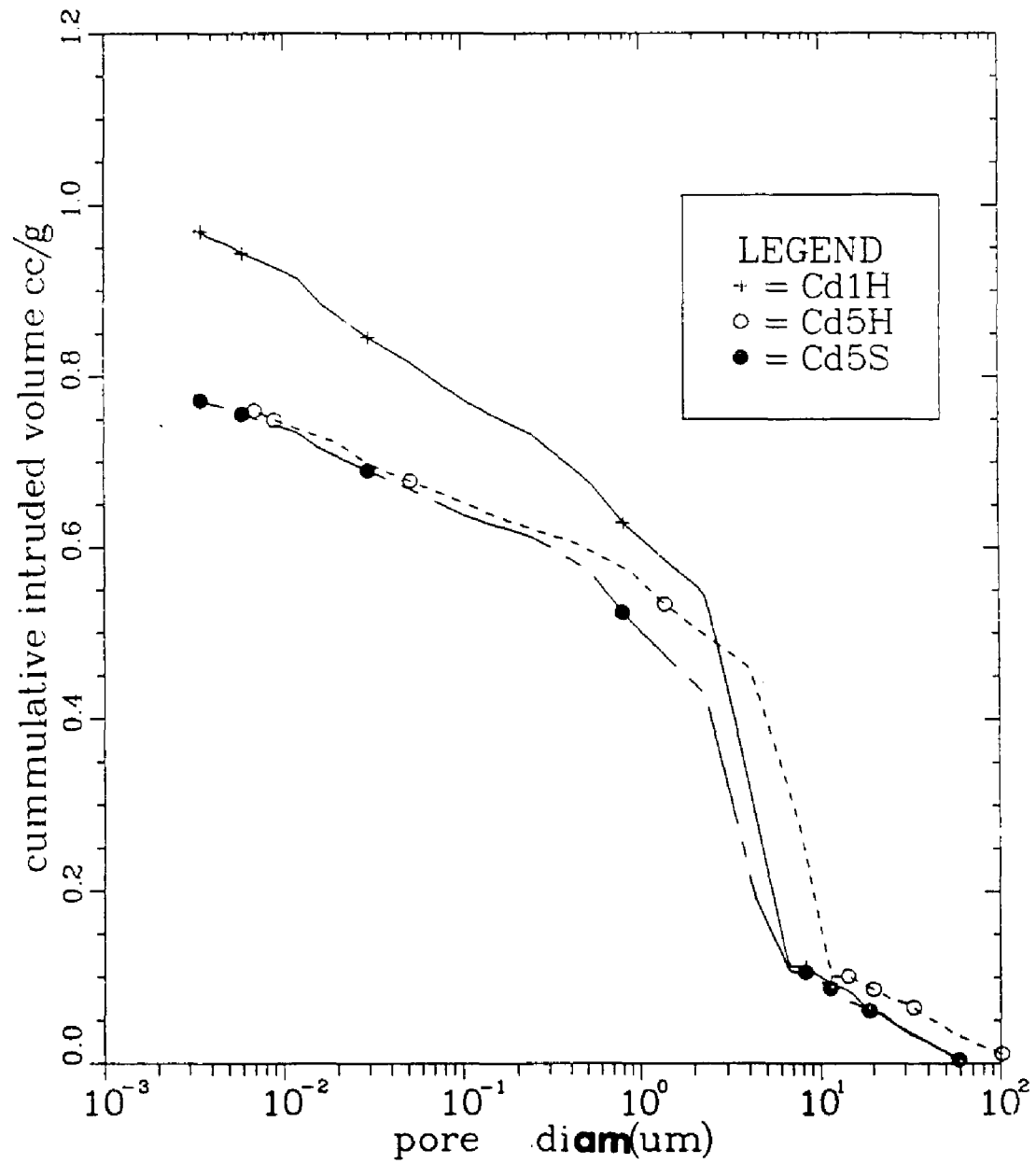


Figure 5.3 -

size, and decreases the volume of  $T_c$ . The total intruded volume, however, remains relatively unchanged. This indicates increased smaller pores. Figure 5.4 shows the cumulative intruded volume for the 0.5 water-cement ratio for the control and cadmium cured in 100 percent relative humidity and cadmium cured in seawater. Total cumulative intruded volume is increased with cadmium addition even at the lower cadmium concentration.

Hughes (1985) identified the derivative of the pore size as represented by the  $(dV/d \log r)$  distribution to be a sensitive indicator to pore refinement. This concept will be adopted in this study. The pore size distribution as characterized by  $(dV/d \log d)$  is presented in Figures 5.5 through 5.8. The curves have a characteristic modal distribution with four peaks. The peaks are located at approximately 500, 50, 15 and 5 nm.

The differential curve is markedly affected by heavy metal addition and changes in water-cement ratio. Figure 5.5 shows the differential curve for all heavy metal and control samples. Figure 5.6 and 5.7 show the effect of water-cement ratio on the differential curve for the control and cadmium samples respectively and the effect of seawater curing on cadmium. Figure 5.8 show the effect of cadmium on the lower water-cement ratio. The shape of the distribution curves are similar however the lower water-cement ratio shifts all peaks to the larger pore sizes and the area under

# Cummulative Pore Size Distribution mercury intrusion

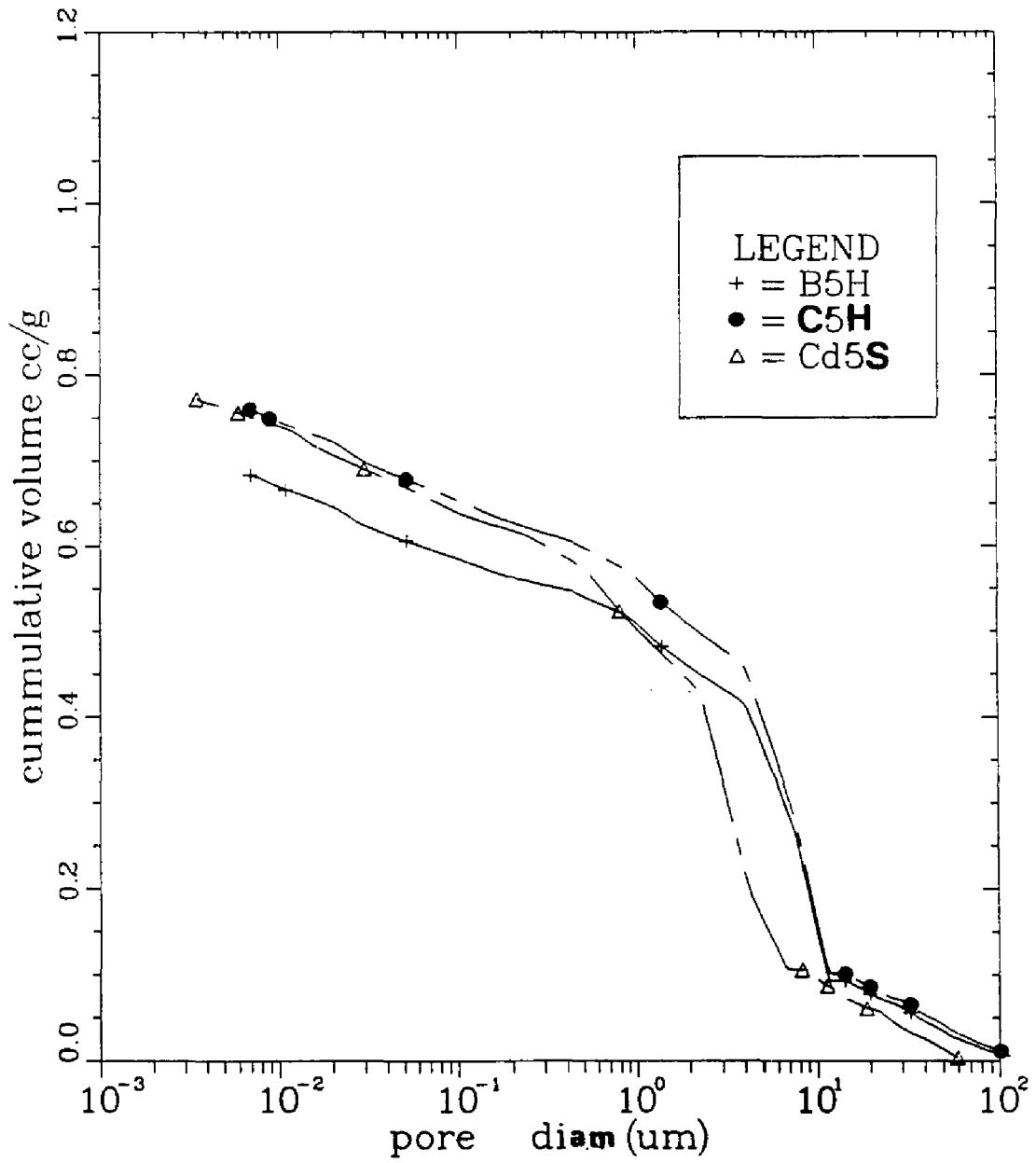


Figure 5.4 -

# Derivative Pore Size Distribution mercury intrusion

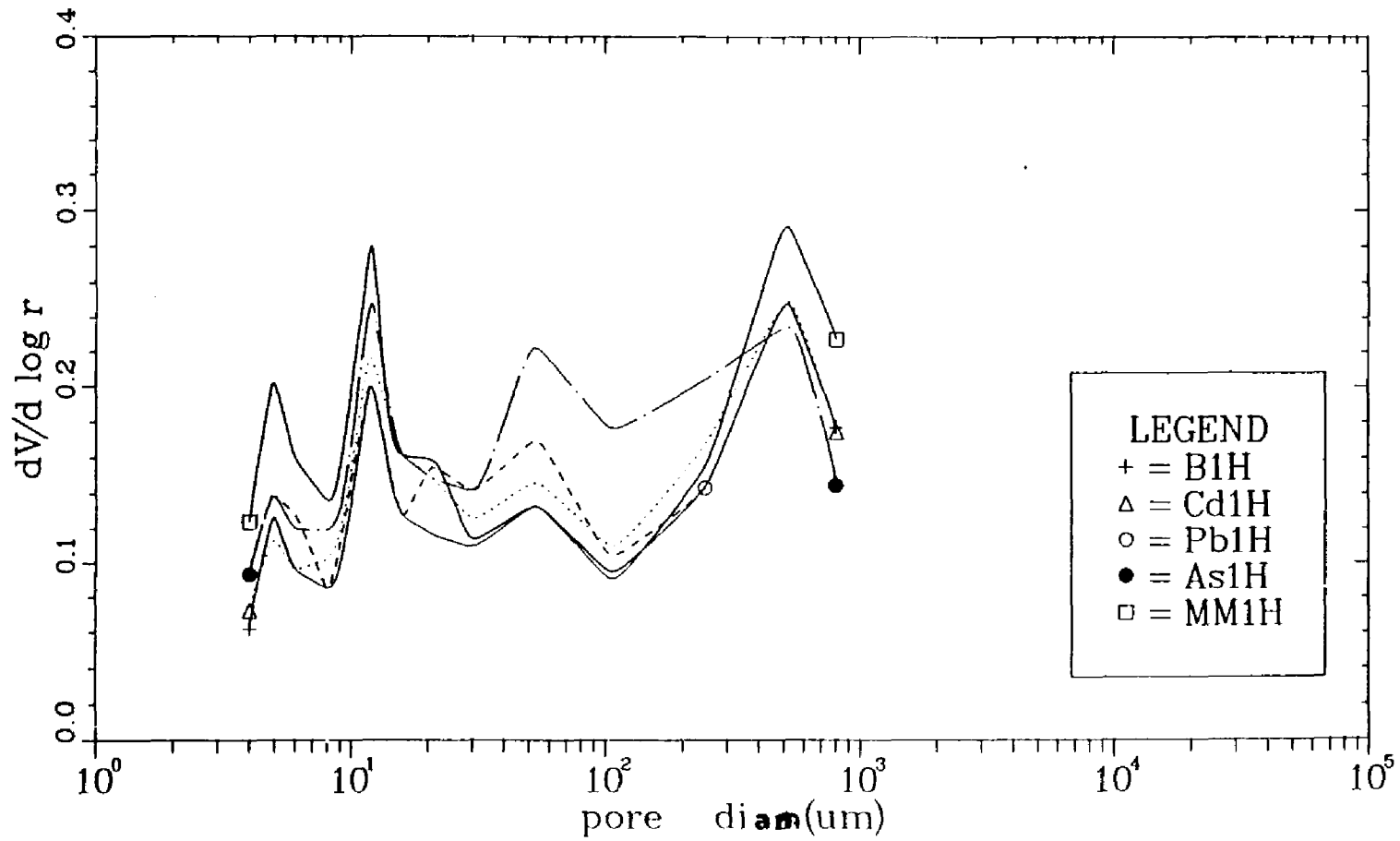


Figure 5.5 -

# Derivative Pore Size Distribution mercury intrusion

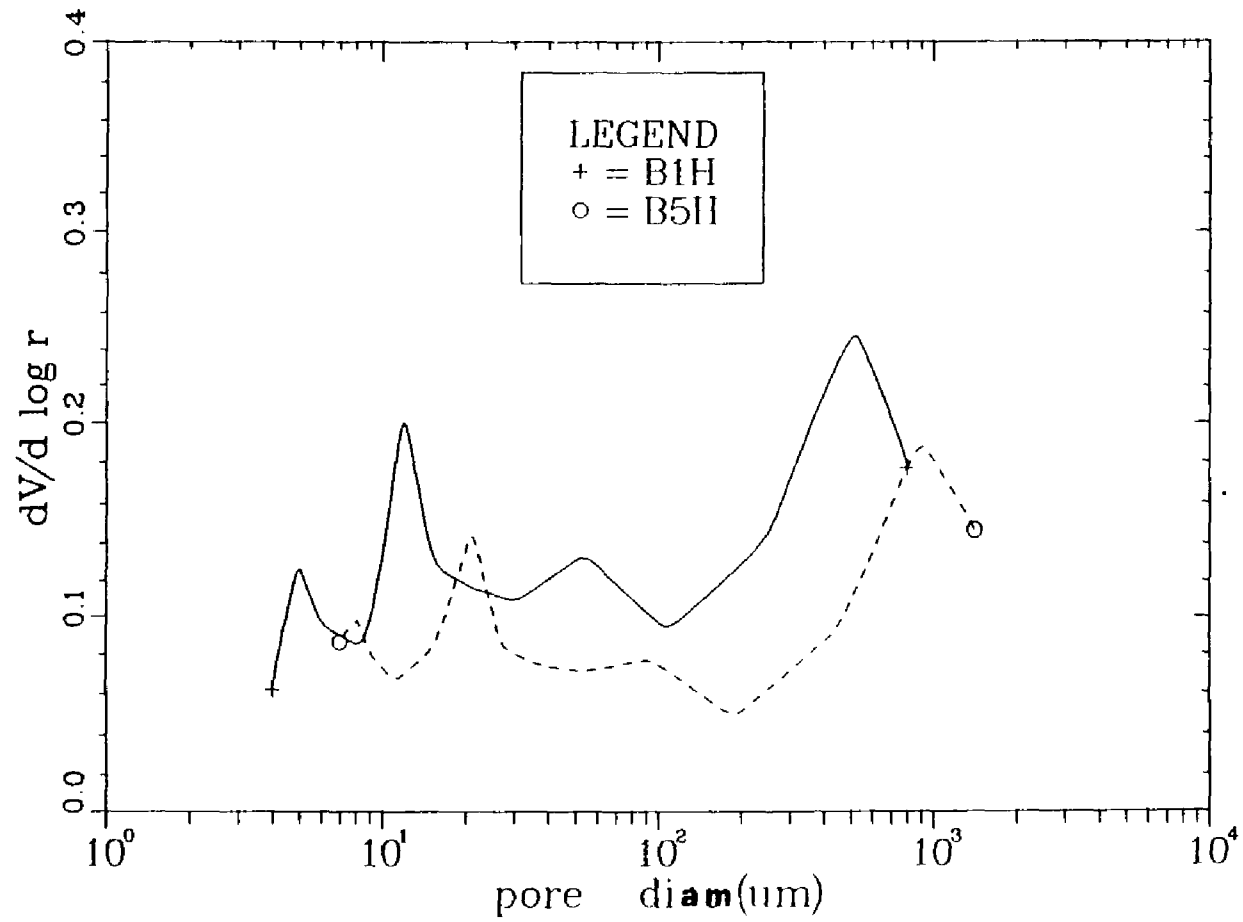


Figure 5.6 -

# Derivative Pore Size Distribution mercury intrusion

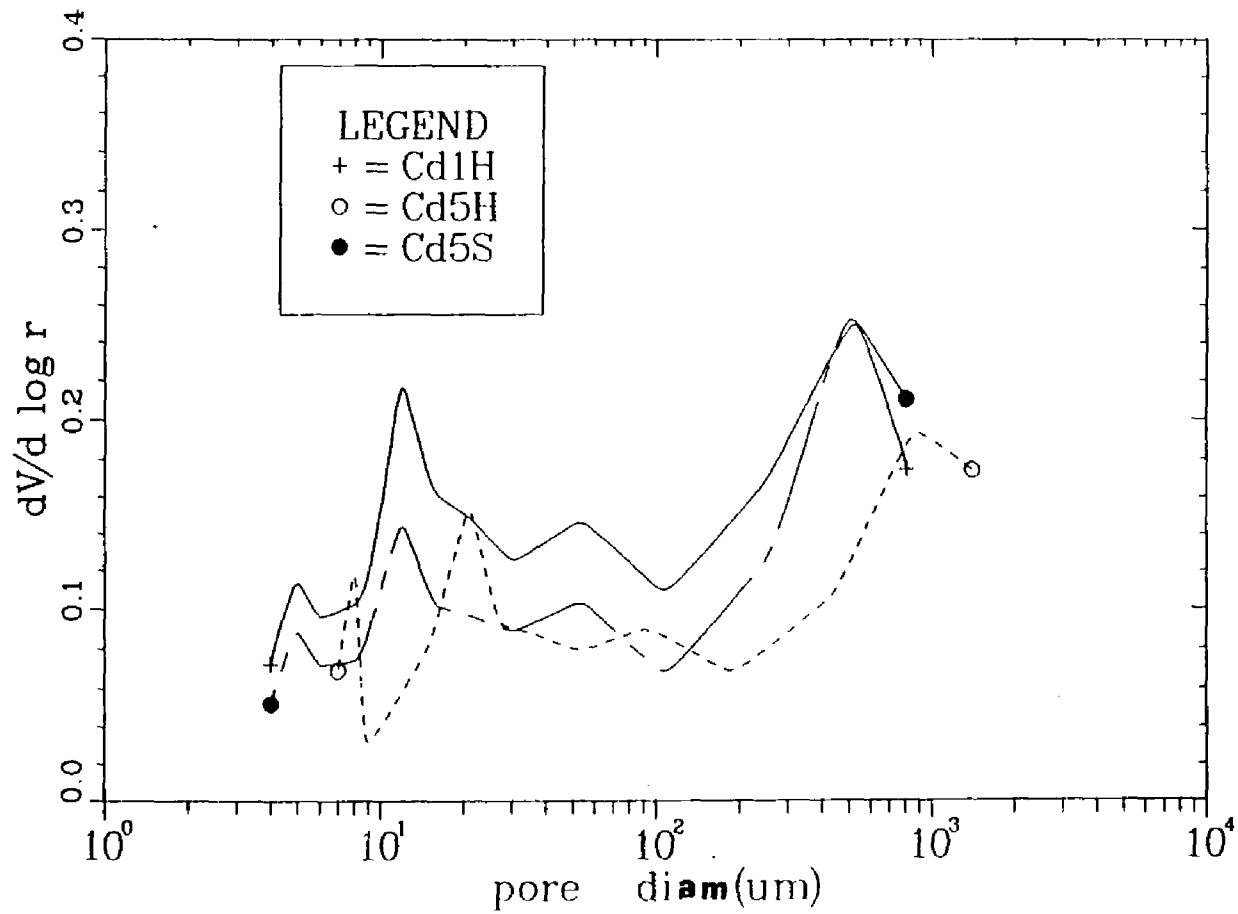


Figure 5.7 -



# Derivative Pore Size Distribution mercury intrusion

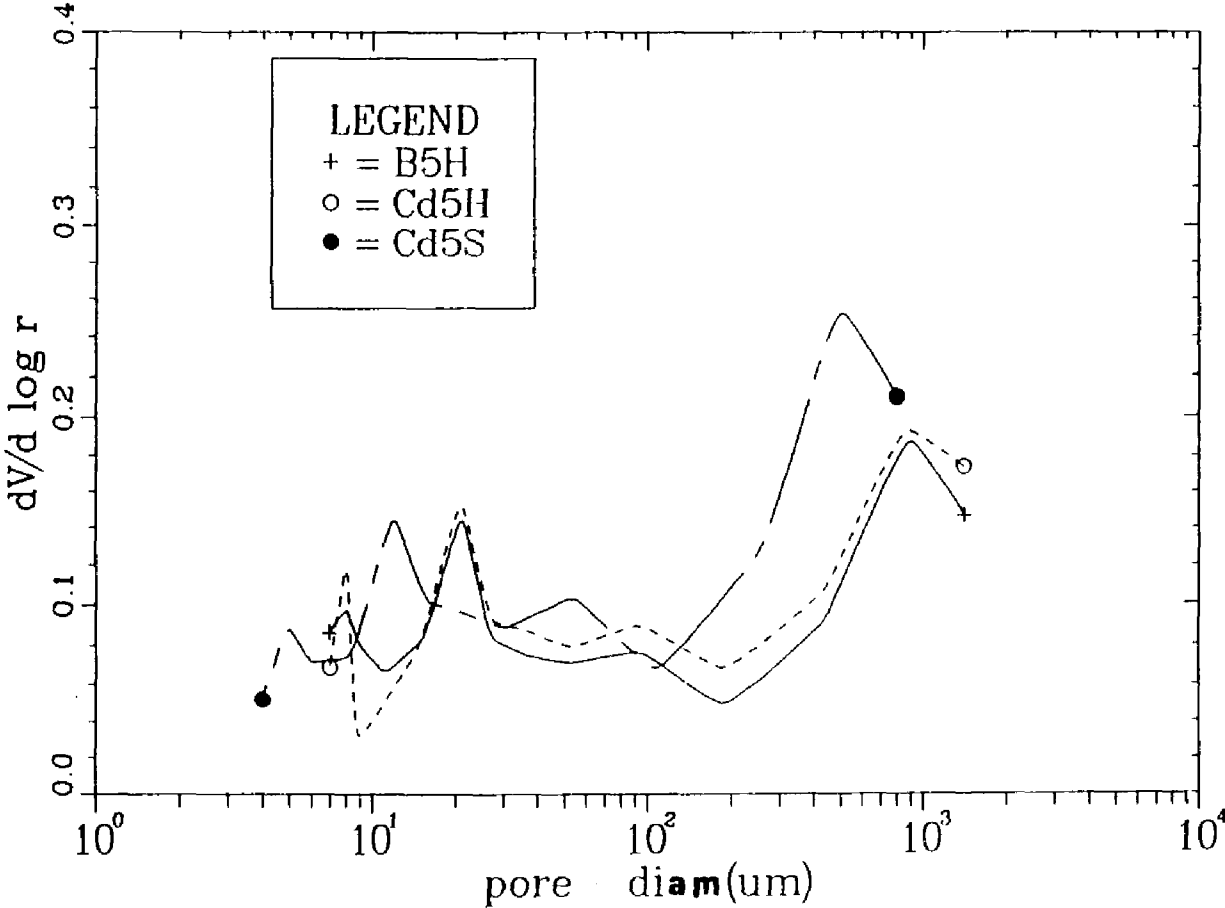


Figure 5.8 -

the curve is decreased. Seawater curing of the cadmium waste causes an increase in the first peak and shifts the distribution curves to the pores with smaller size openings.

#### Helium Displacement Porosimetry

The results for total porosity bulk and true density determined by the helium displacement technique are presented in Table 5.1. The addition of heavy metals to the cement paste increased the porosity. The extent of this increase depended on the individual metal sludge. The trend for total porosity for specimens originally mixed at a water-cement ratio of 1.0 is as follows:

Chromium > Arsenic > Mixed Metal > Cadmium > Lead > Blank. Obviously, the higher the water-cement ratio the higher the porosity as observed for the control and cadmium specimens. Seawater curing increased total porosity for both control and cadmium samples, however, the increase for cadmium is more than the control.

#### Unconfined Compressive Strength

The unconfined compressive strength results and statistical analysis of the S/S waste is presented in Table 5.2 and summarized with all cumulative and derivative porosity data in Table 5.3. After 3 years of curing in 100 percent relative humidity the samples containing chromium, lead, and mixed metals all had average compressive

Table 5.1 - Helium Displacement Porosimetry

Sample	Bulk Density (BD)	True Density (TD)	Moisture Content (MC)	1-MC	Porosity
B1H	1.78	2.40	0.250	0.750	0.444
Pb1H	1.71	2.66	0.283	0.717	0.539
Cd1H	1.64	2.48	0.313	0.687	0.546
As1H	1.61	2.70	0.375	0.625	0.627
Cr1H	1.59	2.90	0.356	0.644	0.647
MM1H	1.63	2.91	0.286	0.714	0.600
B5H	2.02	2.28	0.161	0.839	0.257
Cd5H	1.91	2.20	0.178	0.822	0.286
B5S	1.85	2.33	0.161	0.839	0.334
Cd5S	1.83	2.53	0.192	0.808	0.416

B - Blank  
 Pb - Lead  
 Cd - Cadmium  
 As - Arsenic  
 MM - Mixed Metals  
 1 - 1.0 water-cement ratio  
 5 - 0.5 water-cement ratio  
 H - 100 % RH cure  
 S - Seawater cure

$$\text{Porosity} = 1 - \frac{\text{BD}}{\text{TD}} [1-\text{MC}]$$

Table 5.2 - Unconfined Compressive Strength  
at 14 Days and 3 Years (psi)

Sample	Metal Conc. (mg/L)	14 Days <sup>e</sup>		3 Years		Conf. Interval for Expected Variation of True Mean <sup>**</sup>	
		Mean	Std. Dev.	Mean	Std. Dev.	95 %	99 %
BlH	----	1520	70.5	2197	380	1725 - 2670	1415 - 2980
Pb1H	23,000	1420	240	2310	266	1975 - 2640	1760 - 2850
Cd1H	23,000	870*	108	1080*	175	866 - 1300*	7240 - 1440*
As1H	24,000	370*	23	690*	185	460 - 920*	310 - 1070*
Cr1H	24,000	1560	63	1950	255	1634 - 2266	1426 - 2474
Mixed Metal: Pb	8290	2040	100	2247	338	1830 - 2670	1550 - 2940
	Cd	4500					
	As	3000					
	Cr	2080					

<sup>e</sup> 14 day compressive strength data adapted from Shively (1984)

\* Indicates a significant difference from the Blank

\*\* number of specimens = 5.

Table 5.3 - Summary of Strength and Porosity Data

	<u>Sample</u>					
	Cr1H	As1H	MM1H	Cd1H	Pb1H	B1H
			<u>Porosity</u>			
He (%)	64.7	62.7	60.0	54.6	53.9	44.4
MIP: (cc/g)	---	1.069	1.038	0.970	0.959	0.914
			<u>Porosity &gt; 100nm</u>			
(cc/g)	---	0.830	0.808	0.771	0.748	0.738
(%)	---	77.6	77.8	79.5	80.0	80.7
		<u>True Water-Cement Ratio</u>				
	0.97	0.99	0.95	0.78	0.66	0.56
		<u>Compressive Strength (psi)</u>				
14 days	1560	370	2040	870	1420	1520
3 years	1960	690	2250	1080	2300	2200
		<u>MIP dV/d log r (%)</u>				
520 nm	---	21.5	28.0	26.0	---	27.4
50 nm	---	20.8	10.2	14.9	17.9	14.6
12 nm	---	22.4	27.2	23.2	20.9	21.9
5 nm	---	13.9	19.4	13.1	14.5	12.4
<u>Compressive Str. Using Power's Relationship:</u>					$f_c^* = ax^3$	
	570	670	830	1210	1270	---

\*  $f_c = ax^3 = a(1-\text{porosity})^3$  where  $a = 13,000$  is calculated using the control data.

strengths that were not significantly different from the control specimens. However the arsenic and cadmium samples both had strengths significantly different from the control. Similar behavior was also observed at 14 days (Shively, 1984).

### Discussion

There is good agreement among total porosity determined by the helium displacement method, total pore volume by mercury intrusion and the true water-cement ratio as shown in Table 5.3. However unconfined compressive strength does not appear to correlate with porosity (cumulative or derivative) for all specimens also in Table 5.3. Chromium, arsenite and mixed metal S/S waste all have similar total porosities and mercury intruded volumes, however the compressive strength for chromium and mixed metals is approximately three times higher than for arsenite waste. Similar behavior is observed with cadmium and lead wastes.

The relatively high characteristic compressive strength of the chromium and mixed metal specimens is probably due to the chlorides present in the chromium sludge used for preparing the specimens. Chromium chloride was used to make chromium sludge. The presence of chlorides would explain the high initial strength at 14 days (Shively, 1984) and the resulting strength at 3 years albeit at a considerably

higher porosity. The higher compressive strength observed with the mixed metal samples at 14 days could be attributed to a more optimum chloride content and total porosity combination.

The arsenic sample shows considerably lower compressive strength and higher porosity. The addition of arsenite (as sodium arsenite) caused rapid set to occur within 20 minutes. It is not certain if this is a "quick set" resulting from insufficient soluble sulfates in pore solution. If so it is possible that the sodium would remove sulfate ions from solution by forming sodium sulfate and the arsenite could form a calcium-arsenite complex. Conversely, the arsenite could increase the reactivity of the  $C_3A$ . The results of a "quick set" are deleterious to the potential strength gain of portland cement paste (Neville, 1981; Mindess and Young, 1982; Mehta, 1986).

There exists a fundamental inverse relationship between strength and porosity for most homogeneous solids. This strength-porosity relationship is observed for various materials such as portland cement mortars (Powers, 1958), portland cement paste (Verbeck and Helmuth, 1968), iron, stainless steel, plaster of Paris, sintered alumina and Zirconia (Neville, 1981). This porosity-strength relationship does not appear to hold for all S/S waste specimens collectively. However the coefficients for Power's strength-gel/space ratio determined using the

control value appears to be in good agreement for the arsenic and cadmium specimens but not so for chromium, mixed metals and lead waste.

Since the compressive strength does not appear to correlate with porosity in all waste specimens, then the chemical composition of the binding material formed must contribute to strength properties. The chemical composition of the resulting binding material in S/S wastes is just as important for mechanical properties as are the physical characteristics. The low compressive strength observed with the cadmium sample could be a result of the cadmium hydroxide formation in the hydrated paste. As previously discussed it is possible that the cadmium and calcium cations compete for the hydroxide ions to form cadmium hydroxide and calcium hydroxide. This would deplete the pore solution of  $\text{OH}^-$  ions, lower the pH and weaken the CSH phase. This cadmium hydroxide formation results in reduction of calcium hydroxide formation which is proposed to be the nucleus for CSH formation (Birchal, 1986). Similarly the membrane formation associated with retardation and hydration of portland cement as discussed previously may form permanently with these cadmium samples as observed temporarily with lead.

The compressive strength of lead appears unaffected as compared to the control and may even be improved if total porosity is considered. It is possible that the increased



gel formation as observed in this study and by others and the altered chemical composition of hydrates contributes to the improved strength.

The change in porosity and pore size distribution with higher water-cement ratio is expected. The higher water-cement ratio will reach a higher degree of hydration accompanied by the inherent porosity. Seawater curing for the cadmium waste increases the first peak of the derivative curve which may be attributed to calcium hydroxide dissolution. The relative decrease and shift of the rest of the peaks may be attributed to precipitation of newly formed salts in the smaller pores.

Convective transport through a solid matrix increases with higher porosities. A matrix with a lower porosity will provide better resistance to water and solution infiltration which is a result of the reduced permeability. This general observation does not hold for these particular S/S wastes when leached in acidic solutions (Shively et al., 1986) and seawater (Melchinger et al., 1987). Both Shively and Melchinger and coworkers used similar specimens for their metal leaching studies as the ones used in this study and observed different leaching behaviors depending on the metal waste. The cadmium and lead wastes have similar porosities as observed in this study, however, their release behavior was different. Cadmium release occurred earlier and at a higher rate than lead. Similar observations were

made with arsenic and chromium wastes. Therefore the release of heavy metals from the solidified matrix is probably more dependent on the precipitation/ dissolution and adsorption/desorption characteristics than porosity and pore size distribution. In fact, the porosity of the matrix is continually changing during the leaching process and does not attain steady state conditions.

### Conclusion

- o There is a positive correlation between total porosity (determined by He and MIP) and true water-cement ratio.
- o Unconfined compressive strength does not appear to be totally dependent on total porosity or pore size distribution for all metal wastes. Binding characteristics of the matrix appear to be important in determining strength characteristics as well.

### Proposed Future Work

- o Investigate the actual porosity characteristics to the dynamic leaching front in the S/S waste.
- o Investigate strength-porosity-binding characteristic for different metals ( i.e. why does chromium and arsenic have similar porosities but different compressive strength?)

## **CHAPTER VI**

### **SEAWATER AND CHEMICAL CORROSION OF SOLIDIFIED STABILIZED WASTES**

#### **Introduction**

The disposal of S/S wastes in the ocean is a viable alternative to land disposal. This would alleviate the socio-political and economic problems associated with locating land fill sites, however, chemical reactions between hydrated cement waste and seawater may be detrimental to the structural integrity of the solidified waste. This has been extensively reviewed in Chapter II and III.

#### **Objective**

The suitability for disposal of portland cement based S/S waste in a marine environment was evaluated. A microstructural investigation using SEM/EDAX and XRD was conducted in parallel to metal leaching studies by Melchinger (1987). Cadmium and lead waste were chosen for this investigation due to their different metal release behavior in acid leaching tests (Shively et al., 1986 and Bishop et al., 1982). Expansion tests were also carried out

to evaluate the dimensional stability of the solidified matrix.

The study presented in this chapter was conducted as two parts. The first part was initially conducted to evaluate the corrosion associated with disposal of cadmium and lead waste in a seawater environment. The second part of this study was added to further investigate the excessive corrosive and expansive characteristics associated with the cadmium waste.

### Seawater Corrosion

#### Sample Preparation

The cadmium and lead waste samples used in this study were originally prepared by Shively (1984) and Brown (1984). The waste samples were mixed at a water-cement ratio of 1.0 and cured for approximately 3 years at the time they were used. In practice these wastes will not be stored for 3 years, however, the intent was to use the same samples used by Shively and Brown (1984) and Melchinger (1987) for the purpose of expanding the already existing data base.

#### Seawater Leaching

The corrosion test for microstructural investigation was conducted in parallel with metals leaching. A batch-type leaching method was utilized. The sample cylinders were crushed with a mortar and pestle to a particle size ranging

from 5 to 10 mm. Ten grams of waste particles by dry weight were placed in a glass beaker and 500 mls of synthetic seawater were added. The waste to leachant ratio was arbitrarily chosen but is large enough to maintain a dynamic influx of ions to the solidified waste. The composition of seawater used is shown in Table 6.1. The glass beakers were placed on a shaker table set at a frequency of 2 Hz. The seawater was decanted and renewed every three days and samples were removed periodically for microstructural analysis.

Table 6.1- Synthetic Seawater Composition

<u>Ion</u>	<u>% Total Weight</u>	<u>% Solids</u>	<u>PPM @ 34%</u>
Chloride	46.9	55.2	18,788
Sodium	26.0	30.6	10,424
Sulfate	6.4	7.5	2,577
Magnesium	3.1	3.7	1,265
Calcium	0.9	1.1	398
Potassium	0.9	1.0	371
Bicarbonate	0.3	0.4	145

#### Scanning Electron Microscopy

SEM/EDAX analysis was performed as previously described in Chapter IV.

#### X-ray Diffraction Analysis

Phase identification was conducted using X-ray diffraction analysis. Sample preparation and apparatus

used were previously described in Chapter IV. Quantitative analysis using  $\text{Al}_2\text{O}_3$  as an internal standard was used to determine relative ratios of CH and ettringite ("Aft"). The procedure consisted of grinding 20 percent by weight of  $\text{Al}_2\text{O}_3$  with the waste sample and sieved through a No. 200 sieve. The resulting powder was then placed in a sample holder for X-ray scanning.

The peaks used for semi-quantitative analysis are located at two theta degrees (Cu,Ka) corresponding to interplanar "d" spacings of 34.08 deg and  $2.63 \text{ \AA}^\circ$  for CH , 15.78 deg and  $5.61 \text{ \AA}^\circ$  for ettringite and 14.46 deg and  $6.12 \text{ \AA}^\circ$  for  $\text{Al}_2\text{O}_3$ . The ratios are determined by measuring the respective areas under the CH, and ettringite to alumina peaks. The background was subtracted manually from the XRD pattern.

### Linear Expansion Testing

Linear expansion tests were conducted on the heavy metal wastes cured for 3 years and subject to seawater leaching. Thin disks cut from cylinders were used for expansion testing. The disks were cut using a diamond saw with water used as a coolant. The disks were then polished to the specified thickness (approximately 0.1 inches) using silicon carbide as an abrasive powder. Expansion monitoring studs were mounted onto the sides of the disks as shown in Figure 6.1. The samples were not allowed to dry at any

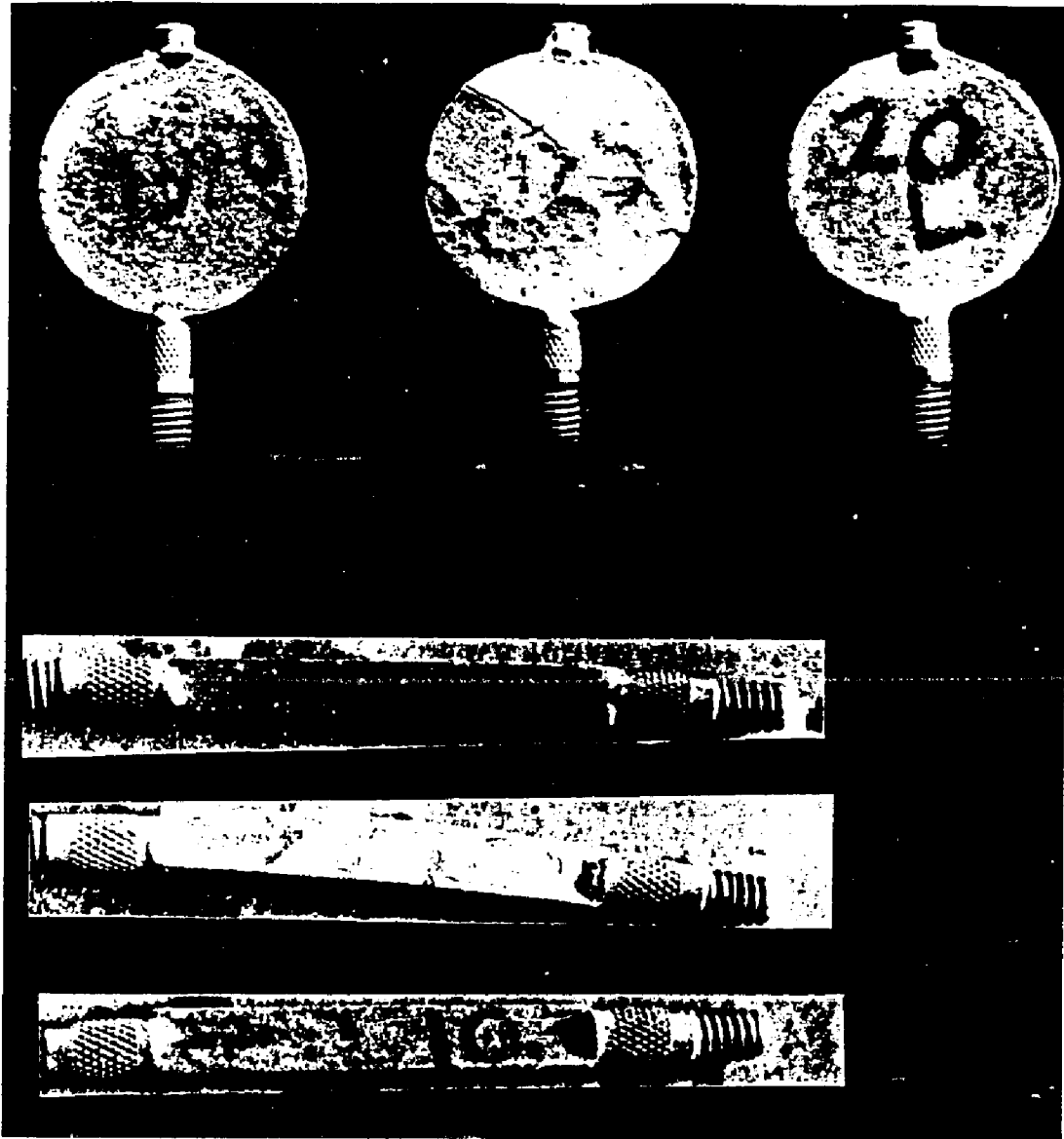


Figure 6.1 - Photograph of expansion monitoring specimens taken after seawater storage for over 50 days. Cadmium specimens show extensive cracking.

point of preparation and testing.

Initially, expansion prisms rather than disks were cut longitudinally from the cylinders and polished to the desired dimensions. However great difficulty was encountered in preparing reproducible prisms. Hence the decision was made to use the non-conventional disk specimens in an effort to control specimen dimensions.

Linear expansion was monitored periodically while the disks were subjected to seawater corrosion. The seawater solutions were renewed every five days. The expansion monitoring apparatus was custom made to accommodate the relatively small specimens measuring approximately 1.5 inches in diameter. The sensitivity of the dial gauge was 2.5 microns.

### **Results**

Linear Expansion - The linear expansion results of the cadmium, lead and control specimens leached in seawater are presented in Figure 6.2. The data show cadmium waste exhibits the most dramatic expansion as compared to the control and lead specimens. The expansion in the cadmium waste specimens was of large enough magnitude that it could be observed in a photograph (Figure 6.1) of the expansion specimens after seawater corrosion for 50 days. The cadmium sample particles used for microstructural investigation



### Linear Expansion in seawater

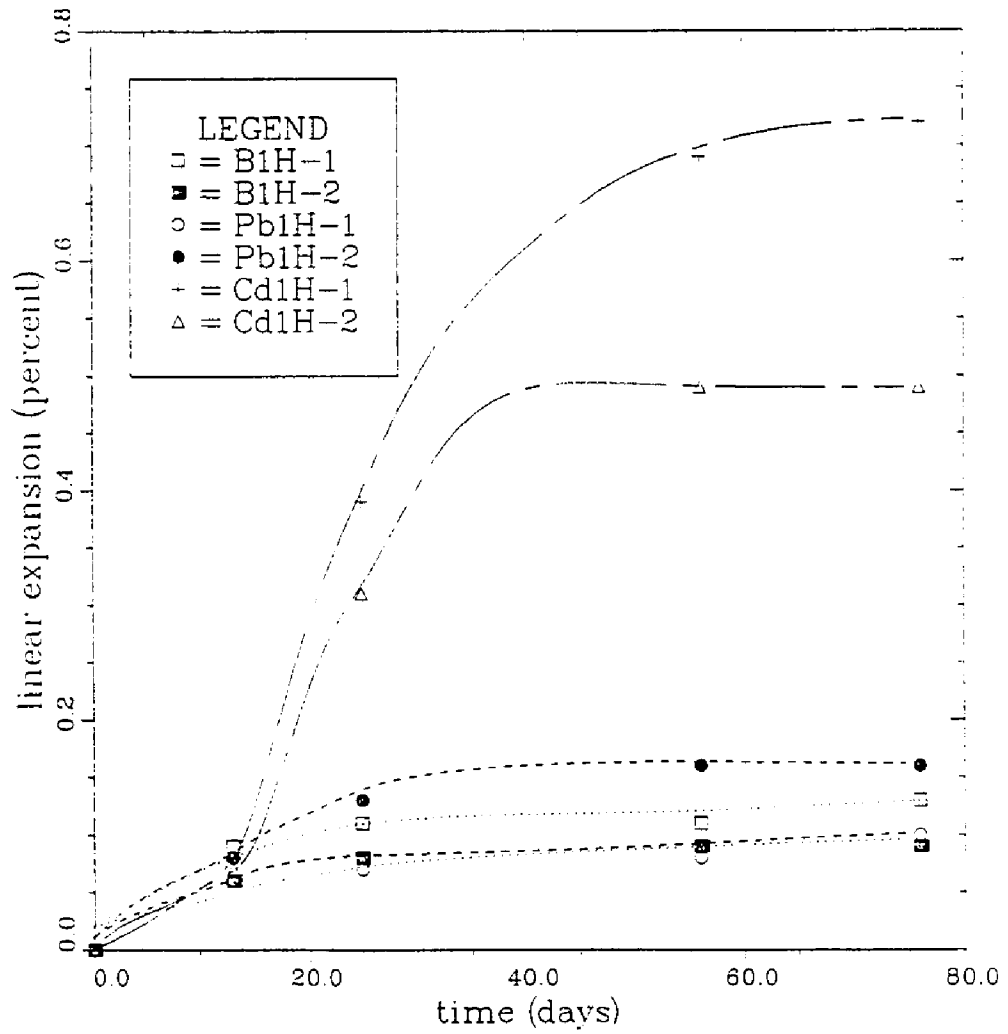


Figure 6.2 - Linear expansion of duplicate specimens after seawater storage. Cadmium (Cd1H) specimens show the largest expansion as compared to Lead (Pb1H) and Blank (B1H)

showed initial signs of cracking beginning around day eighteen.

SEM/EDAX - The microstructure of the seawater samples underwent discernable changes. Figure 6.3 shows SEM photomicrographs of the surficial layer observed on all metal waste samples leached in seawater. The surface layer is characterized by calcite and aragonite crystals which are both calcium carbonate crystals of the acicular pyramidal crystal habit as shown in Figure 6.3a and 6.3b. Brucite ( $Mg(OH)_2$ ) crystals are also observed as thin plates among the calcite (Figure 6.3a). Figure 6.3c shows a different crystal habit of aragonite commonly termed urchins (Regourd, 1980). Figure 6.3d shows other aragonite morphologies surrounded by nodular calcite crystals usually observed on the surface of hardened cement paste subject to seawater corrosion.

EDAX detected traces of cadmium in calcite and aragonite microstructures but not in brucite. Lead was not detected in surficial microstructures.

The internal microstructure of the seawater leached cadmium, lead and control waste specimens is shown in Figures 6.4. The control cement paste before and after leaching is shown in Figure 6.4a and b. Figure 6.4c is an SEM photomicrograph of the unleached cadmium waste and Figures 6.4d through f show the internal microstructure of the cadmium waste specimens leached in seawater for more

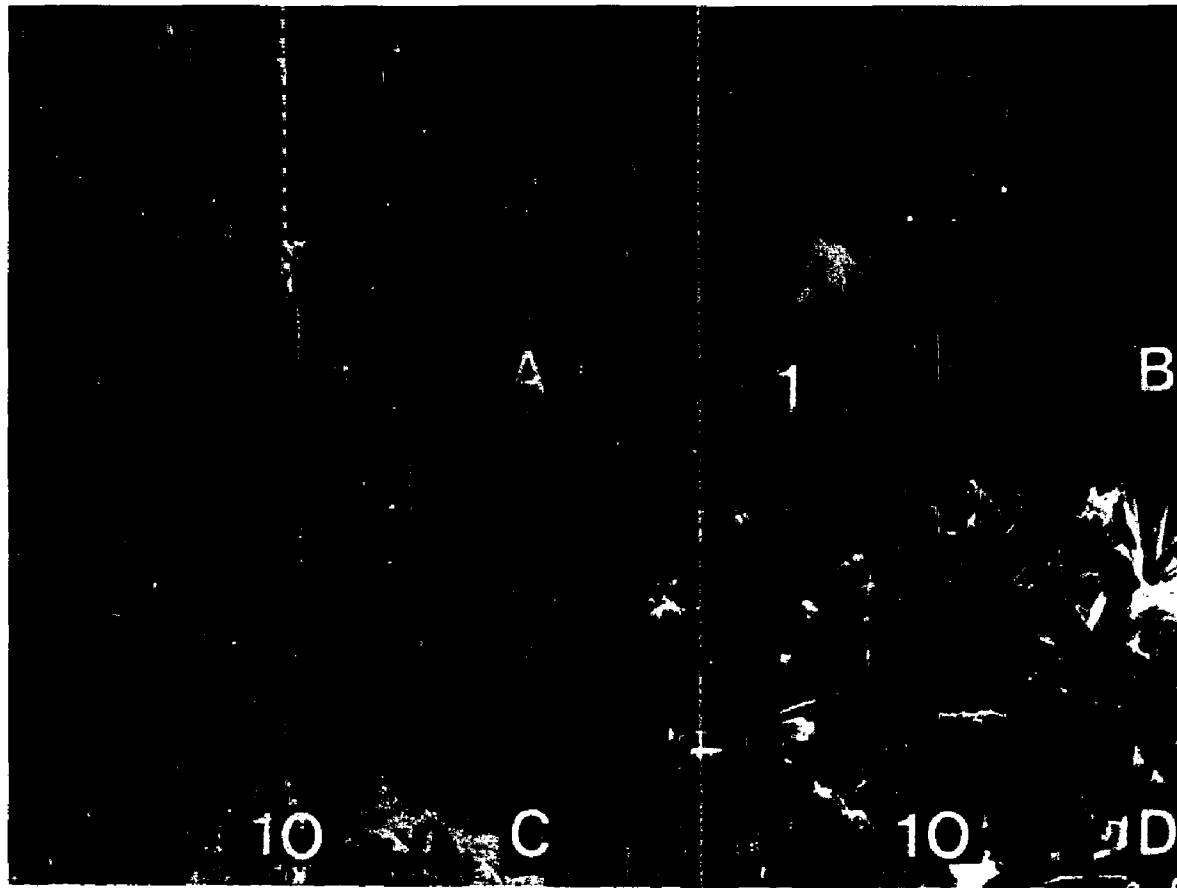


Figure 6.3 - SEM photomicrograph of surface layer of metal waste after seawater corrosion. A) nodular calcite B) pyramidal aragonite C) aragonite urchins D) aragonite crystals. All specimens stored in seawater for over 50 days

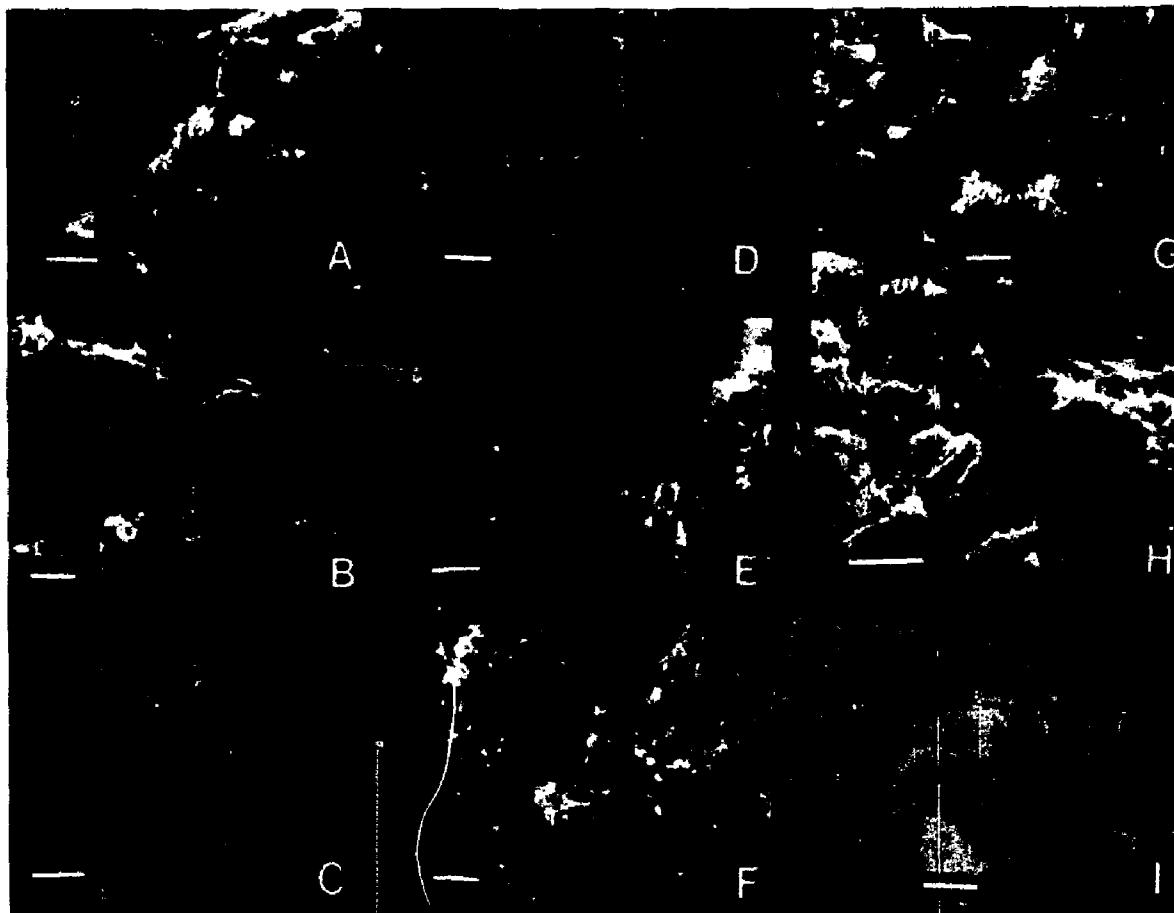


Figure 6.4 - SEM photomicrograph. Blank A) before B) after seawater leaching;  
Cadmium waste C) before D-F) after seawater leaching;  
Lead waste G) before H-I) after seawater leaching

than 50 days. The unleached and seawater leached lead waste is shown in Figure 6.4g, h and i respectively.

The microstructure of the cadmium waste is characterized by CSH gel and ettringite crystals. Most of the calcium hydroxide typically observed as hexagonal plates were not observed after leaching and have probably been dissolved. The "fibrous" CSH Type I and "reticulated" Type III (per Diamond, 1976 classification) were most abundant at this stage of seawater corrosion. Abundant ettringite crystals of varying sizes from less than 1 um to 15um were observed throughout the waste. The larger ettringite crystals were typically deposited in the pores while the smaller crystallites were protruding from the surface of the hydrated cement grains as shown in Figure 6.4d and 6.4e. Figure 6.4e shows the microstructure typically observed in layers under the cracks where ettringite crystals appear short and stubby.

The microstructure of the seawater leached lead waste consists of similar CSH Type II and Type III as shown in Figures 6.4h and i. Ettringite crystals are observed in the lead specimens however they do not appear nearly as abundant as in the cadmium waste. The ettringite crystals observed in the lead waste samples range in size between 3 and 10 um. However, no colloidal size ettringite crystals were observed in lead waste as were observed with cadmium waste.

The microstructure of the seawater leached control

paste appears more dense with fibrous Type II CSH covering cement grains. Ettringite crystals ranging in size from 5 to 10 um are observed in voids as well as deposited on the surfaces.

Cadmium was detected in ettringite crystals and CSH gel after leaching, however lead was not detected in ettringite but was detected in CSH structure. A large amount of sulfate and chloride was detected in all specimens in CSH gel and ettringite crystals.

The expansion potential of ettringite has been associated to its chemical composition. Conjeaud (1980) observed Si-ettringite to be expansive while Kalousek and Benton (1970) found Fe-poor (Al-rich) ettringite to be more expansive than the Fe-rich. It is not sufficiently clear that cadmium-ettringite is responsible for expansion of cadmium waste subject to seawater corrosion. Further studies are needed on this mater before definitive conclusions may be drawn.

X-ray Diffraction Analysis - Phase identification using XRD shows calcium hydroxide, ettringite, calcite from atmospheric carbonation and residual alite and belite from unhydrated cement to be the major crystalline compound in the waste and control specimens. Figure 6.5 shows XRD patterns of the cadmium and lead waste before and after seawater leaching.

Cadmium hydroxide was detected in the hydrated cement

CH - CALCIUM HYDROXIDE  
E - ETTRINGITE  
CdH - CADMIUM HYDROXIDE

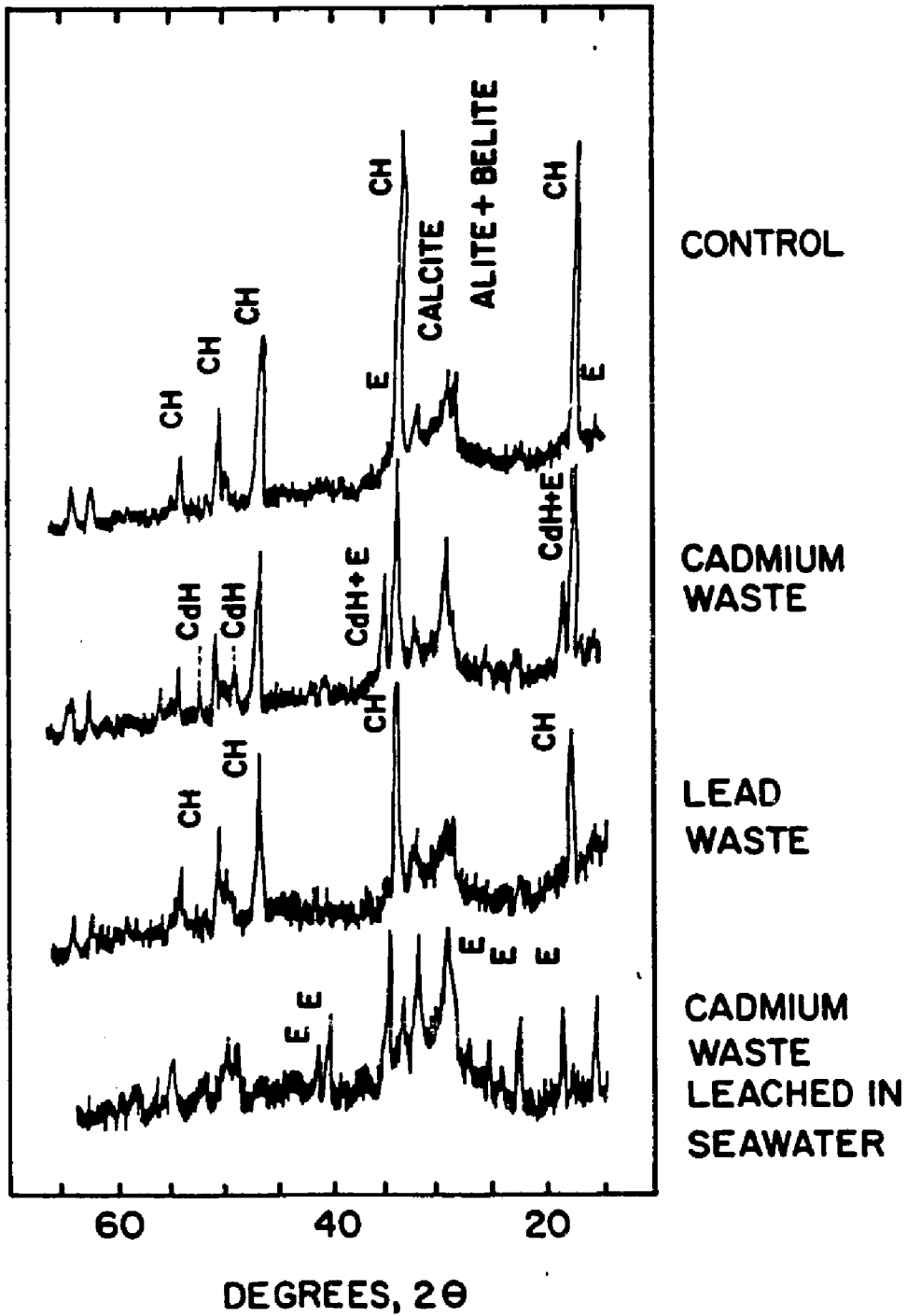


Figure 6.5 - XRD patterns before and after leaching in seawater

waste however lead was not. XRD showed no evidence of lead hydroxide, lead nitrate, lead sulfates or plumbites (as previously discussed in Chapter IV). Calcite, aragonite and brucite crystals were detected on the exterior surface of all leached sample particles. Ettringite was the major crystalline compound detected in the subsurface layer of the waste and control specimens.

Quantitative phase analysis for CH and ettringite was conducted using  $Al_2O_3$  as an internal standard. Table 6.2 shows the relative values of CH and ettringite to  $Al_2O_3$  before and after leaching in seawater. The presented values are an average of four readings and the coefficient of variation varied between 3 and 12 percent. These results support SEM observations indicating a decrease in CH and an increase in ettringite formation after seawater leaching. The cadmium waste shows the highest increase in ettringite while the control and lead specimens show comparable increases. The control specimen retained the largest amount of CH after leaching.

### Discussion

The observed microstructure provides an explanation to the large linear expansion associated with the cadmium waste leached in seawater. The excessive expansions appear to be induced by expansive ettringite formation. Large amounts of ettringite crystals were observed by SEM and quantified



Table 6.2 - Quantitative Phase Analysis  
QXRD - Al<sub>2</sub>O<sub>3</sub> Internal Standard

	<u>Phase</u>	<u>Control</u>	<u>Lead</u>	<u>Cadmium</u>
Before Seawater Leaching	CH	7.47 ± 1.32	6.62 ± 1.92	5.76 ± 1.11
	Aft	0.67 ± 0.12	0.52 ± 0.19	1.14 ± 0.14
After Seawater Leaching	CH	2.10 ± 1.01	1.21 ± 0.48	0.81 ± 0.32
	Aft	1.70 ± 0.55	1.56 ± 0.43	3.36 ± 0.38

-----  
All values are ratios of each phase to Al<sub>2</sub>O<sub>3</sub>

by QXRD analysis in the cadmium waste as opposed to the lead waste and control samples.

The induced cracking coincided with increased rates of cadmium release as determined by metals leaching tests shown in Figure 6.6 and 6.7 (after Melchinger, 1987). Figure 6.6 shows the pH and alkalinity and Figure 6.7 shows the cadmium released in the seawater leachant. Initially, the pH is higher than that of seawater and the alkalinity is much lower, and subsequently levels off with that of seawater. This is attributed to surface interactions that eventually plug the pores and limit further dissolution of calcium hydroxide and lime rich hydrates (Melchinger et al, 1987 and El Korchi et al., 1986).

The increased rate of cadmium release correlates with the physical cracking on the leached waste particles. Microcracks were visually observed only one sampling day after the initial increase in cadmium release, albeit microcracks had probably already developed. No lead was detected in the seawater leachant. The increased rate of metal release would probably be a function of the increased leaching sites and surface area resulting from the induced cracking, if cadmium stabilization is physical in nature and the metal release is kinetically controlled. The metal release also seems to follow adsorption/desorption characteristics (Benjamin et al., 1982).

The leaching studies conducted by Melchinger (1984) is

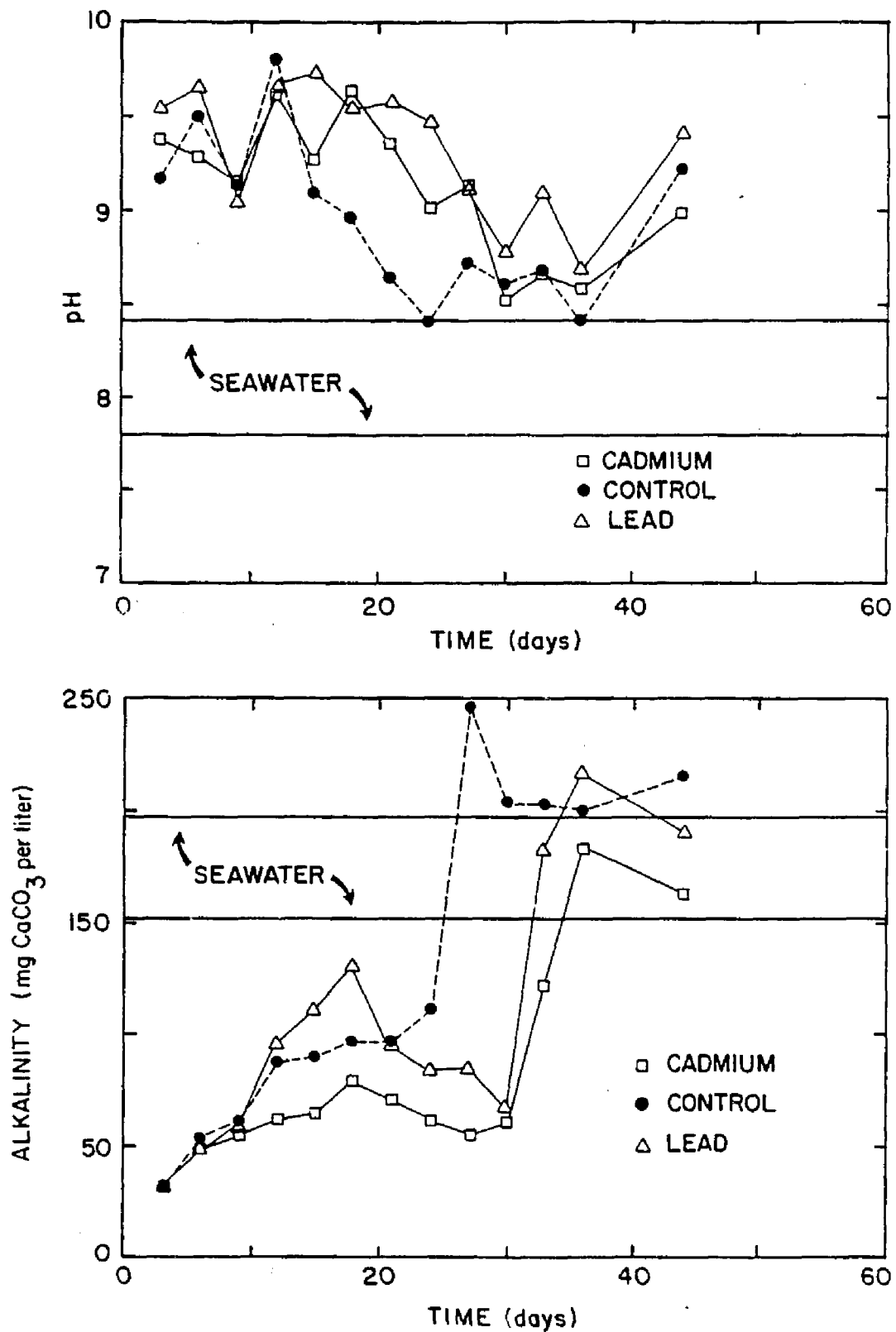


Figure 6.6 - pH and Alkalinity of seawater leachant. Adapted from Melchinger et al (1987)

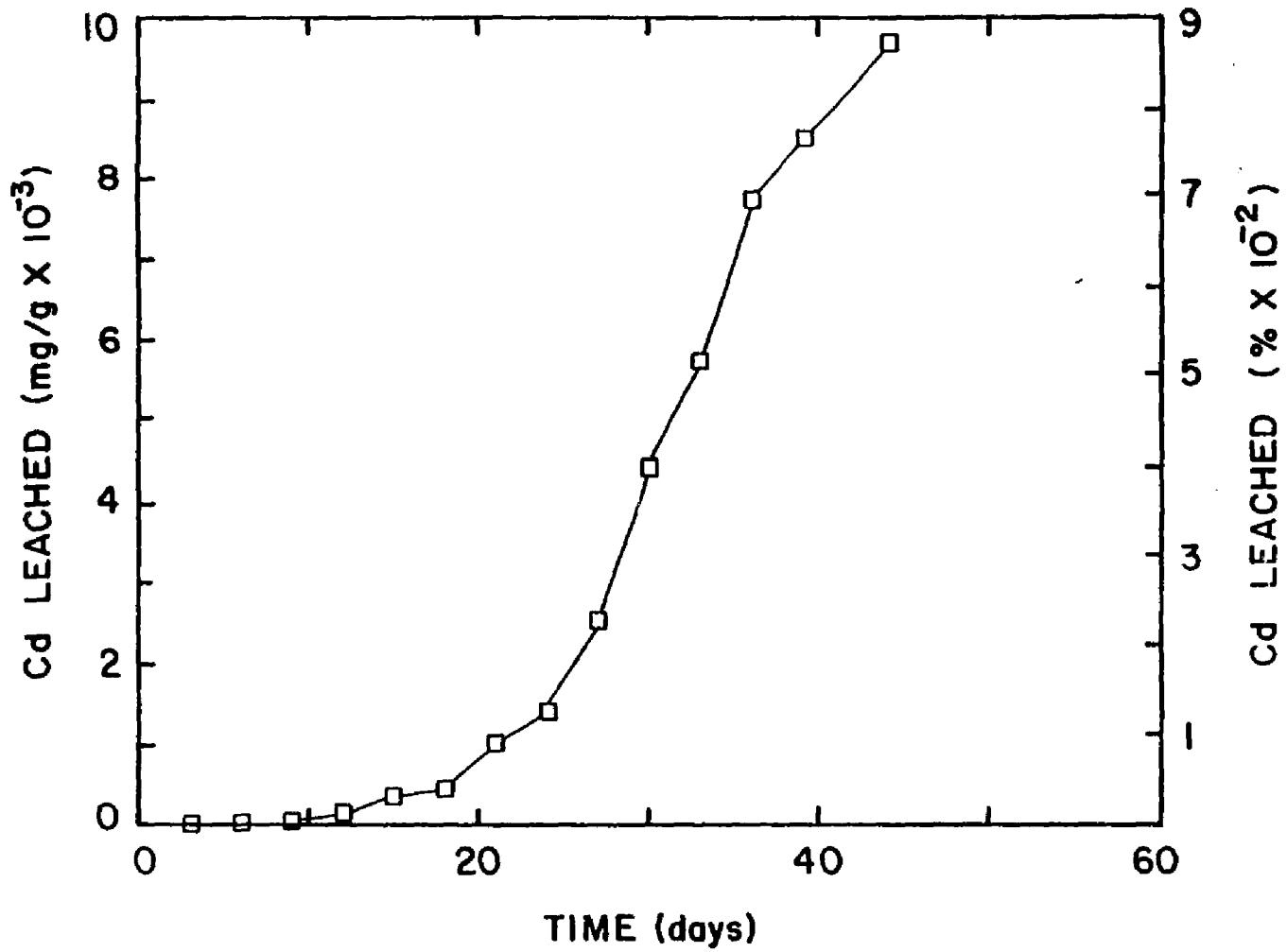


Figure 6.7 - Cadmium release in the seawater leachant.  
Adapted from Melchinger et al (1987)

useful in determining the leaching characteristics of the particular geometrical specimens under investigation, however, modelling long term leaching would be difficult due to the unsteady state physio-chemical characteristics of the surface.

The incorporation of cadmium or cadmium hydroxide has an effect on the formation of expansive ettringite. The formation of cadmium hydroxide in the hydrated cement paste creates an environment conducive for expansive ettringite. The ettringite formed in the cadmium waste leached in seawater ranged in size between less than 1  $\mu\text{m}$  and 15  $\mu\text{m}$  while the ettringite formed in the lead waste and the control consisted of the larger size ettringite as shown in Figure 6.4.

According to the crystal growth theory and the swelling theory (Cohen, 1983) the size of the crystal and the presence of lime affects expansion. In the presence of excess lime, sulfate and alumina bearing hydrates, ettringite is formed as small crystals which contribute to expansion. Furthermore, in the absence of lime, ettringite is formed as large ettringite crystals and hence do not contribute to expansion. The expansion is either due to the colloidal ettringite formed by through-solution or the larger crystals formed topochemically. The necessary lime is supplied by the calcium hydroxide present in the pore solution or from dissolution of cadmium hydroxide. The

similarity of  $\text{Cd}^{2+}$  and  $\text{Ca}^{2+}$  are well documented where  $\text{Cd}^{2+}$  will enter into cation exchange reactions with  $\text{Ca}^{2+}$ .

Two scenarios detailing the role of cadmium hydroxide in the formation of expansive ettringite are offered. The first scenario relies on the probability that most of the cadmium is precipitated in the cement interstices as cadmium hydroxide during hydration. Cadmium hydroxide has a maximum insolubility at a pH of 13.6 (Stumm and Morgan, 1981). This pH level is approached in the pore solution during cement hydration. In comparison, lead hydroxide has a maximum insolubility at a pH less than 10 (Newkirk et al., 1982) and demonstrates amphoteric behavior at high pHs.

The intrusion of chloride and sulfate ions into the paste matrix would force the dissolution of calcium hydroxide and cadmium hydroxide. The pore solution of the lead waste would not be similar to the pore solution of the cadmium waste as the amphoteric nature of lead hydroxide would force the solidification of lead as ions or complexes. In the presence of sulfate ions supplied by seawater, alumina hydrates supplied by monosulfo-aluminate and unhydrated  $\text{C}_3\text{A}$ , water and excess  $\text{Ca}^{2+}$  and  $\text{Cd}^{2+}$  ions expansive ettringite will form. However a high pH must be maintained since the stability of ettringite is jeopardized if the solution pH drops below the range 10 (Midgely and Illston, 1983) to 11.8 (Bailey and Hampson, 1982).

The second scenario requires a reduced stiffness of a matrix subject to ettringite formation. This relies on the probability that not all of the cadmium is precipitated as cadmium hydroxide in the hardened cement paste prior to leaching. During leaching, cadmium hydroxide formation resulting from free  $\text{Cd}^{2+}$  ions in the pore solution and  $\text{OH}^-$  ions made available by dissolution of calcium hydroxide (after  $\text{Cl}^-$  ions intrusion) would decrease or even deplete the hydroxide ions in the paste which is known to weaken the CSH phase (Mehta, 1983). The formation of cadmium hydroxide at the expense of calcium hydroxide was observed to decrease the strength of the paste markedly as presented previously in Chapter IV. When the necessary ingredients for ettringite formation are present in such a weakened matrix expansion is inevitable. This is based on Mehta's swelling theory (Mehta, 1983). Mehta maintains that a weakened CSH is necessary for expansion due to colloidal ettringite formation. A weakened CSH results when the surrounding pore solution is depleted of hydroxide ions and continually renewed with sulfate ions.

In the case of lead waste, no detrimental expansion nor excessive ettringite formation was observed. The inclusion of lead in the cementitious matrix does not appear to enhance the formation of ettringite during seawater corrosion. Although not experimentally investigated, it is possible that the surface layer in the lead waste was more

efficient in preventing sulfate and chloride intrusion into the bulk sample. This would limit the formation of expansive ettringite.

The scope of work was extended to attempt to further clarify the mechanism of expansion in the cadmium waste specimens subject to seawater corrosion, as described in the following section.

### Chemical Corrosion

Further microstructural investigation was conducted to determine the mechanism of expansion of cadmium in seawater. It is also important to isolate the corrosive ions (for example sulfates and chlorides) associated with this expansion phenomenon. Furthermore it would be beneficial to determine if expansion is associated exclusively with the formation of expansive ettringite or in combination with other crystal salts. For example, does Friedal's salt form during the early stages of corrosion and then redissolve since it is not stable in sulfate solutions. Does cadmium form other complexes at early ages of leaching?

### Experimental

Corrosion studies for cadmium waste were conducted in a sulfate, a chloride and a sulfate-chloride solution. Seawater was used as a control solution. The solutions were prepared from a reagent grade sodium sulfate and sodium



chloride at concentrations of 4.0 g/L sulfate (higher concentration than seawater to accelerated the corrosion process) and 18.7 g/L chloride. A batch-type reactor as described in previous section was also used for this experiment.

### **Results**

The microstructure of the cadmium waste leached in sulfate, chloride and seawater solutions for 12 days is shown in Figure 6.8. The seawater leached samples exhibit a reticulated CSH microstructure with ettringite crystals deposited on the surface of hydration product. Ettringite crystals larger than 1  $\mu\text{m}$  are apparent in the voids and CH dissolution is noted. The CSH of samples leached in chloride solution has a "reticulated" CSH Type III morphology and samples leached in sulfate solutions exhibit an "equant grain" morphology. The paste samples leached in the sulfate-chloride solutions develop ettringite crystals on the surface that are typically less than 1  $\mu\text{m}$ . Calcium hydroxide is observed in all specimens at this age.

The microstructure of the cadmium waste leached for 18 days is shown in Figure 6.9. The microstructure of the waste leached in seawater (Figure 6.9a), chloride (Figure 6.9c) and sulfate-chloride (Figure 6.9d,e) solutions show increasingly reticulated CSH Type III. The sulfate solution leached waste still exhibits similar "equant grain" CSH Type



Figure 6.8 - SEM photomicrograph of camium waste specimens leached for 12 days in A) seawater B) sulfate solution C) sulfate-chloride solution D-F) chloride solution

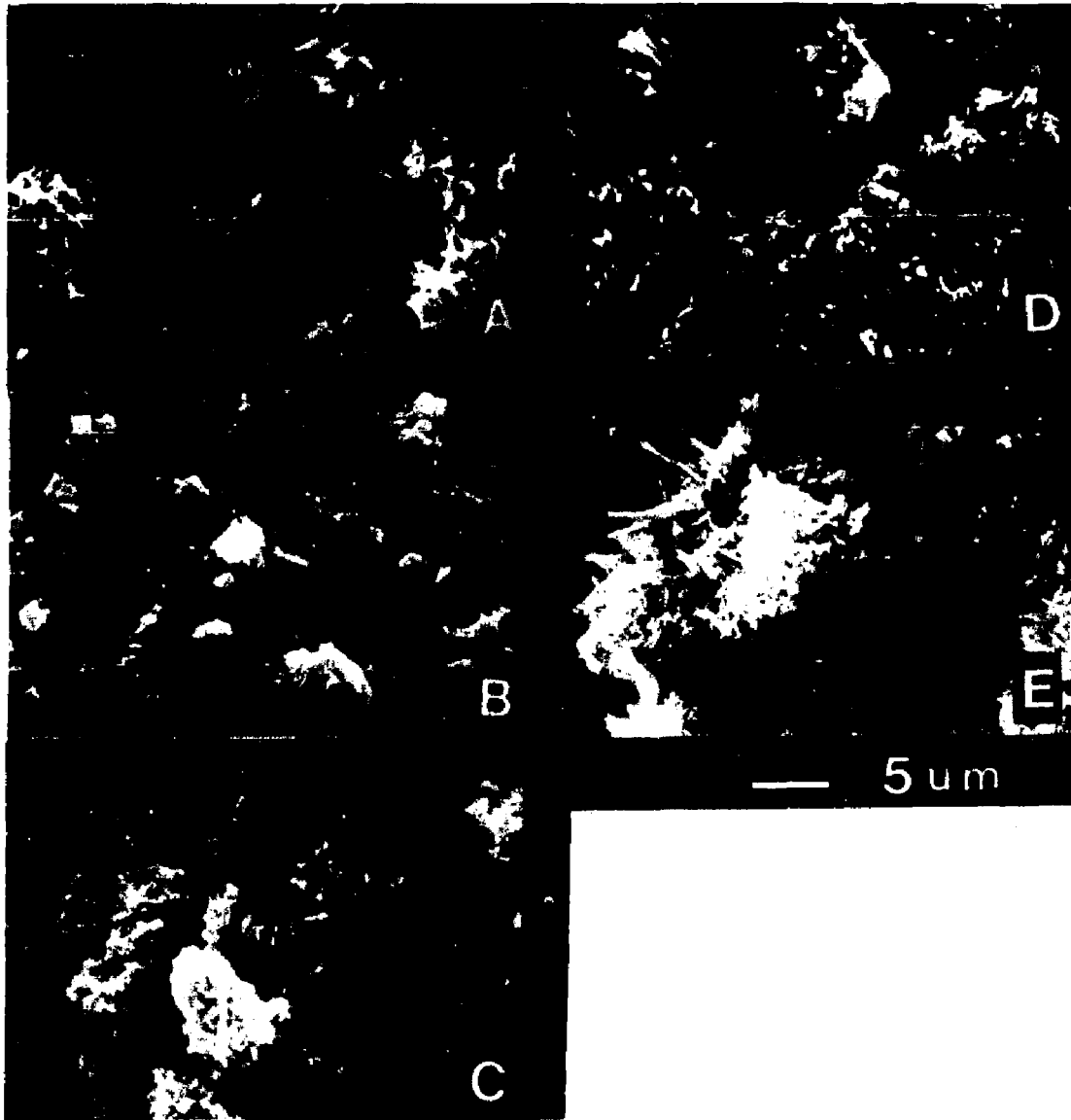


Figure 6.9 - SEM photomicrograph of cadmium waste specimens leached for 18 days in A) seawater B) sulfate solution C) chloride solution D-E) sulfate-chloride solution

II as shown in Figure 6.9b. Micro-cracks are apparent on the surface of the specimen. These cracks are relatively smaller cracks that may be due to gypsum formation (detected by EDAX) or shrinkage cracks incurred during sample preparation.

Ettringite crystals are more abundant in waste samples leached in seawater and sulfate-chloride solutions. The larger ettringite crystals are approximately 5  $\mu\text{m}$  long and are deposited on the surface of the hydration product or in the pores. The smaller crystals are approximately 1  $\mu\text{m}$  long and 0.25  $\mu\text{m}$  across and are shown protruding out of the hydrated surface. Figure 6.9 shows a "micro-crack" across the surface of the specimen. The specimens were visually inspected periodically for hairline cracks under a binocular microscope. Hairline cracks were observed on the surface of the specimens leached in sulfate-chloride and seawater solutions after 18 days. The "micro-crack" observed on the grain surface in Figure 6.9d is attributed to expansion resulting from ettringite formation.

Figure 6.10 shows SEM photomicrographs of cadmium specimens leached for 33 days. Extensive ettringite crystallization is evident in specimens leached in seawater (Figure 6.10a and b) and sulfate-chloride (Figure 6.10g, h and i) solutions. Ettringite crystal formations are observed surrounding individual grains and intermeshed between grains. The ettringite crystals protruding from the

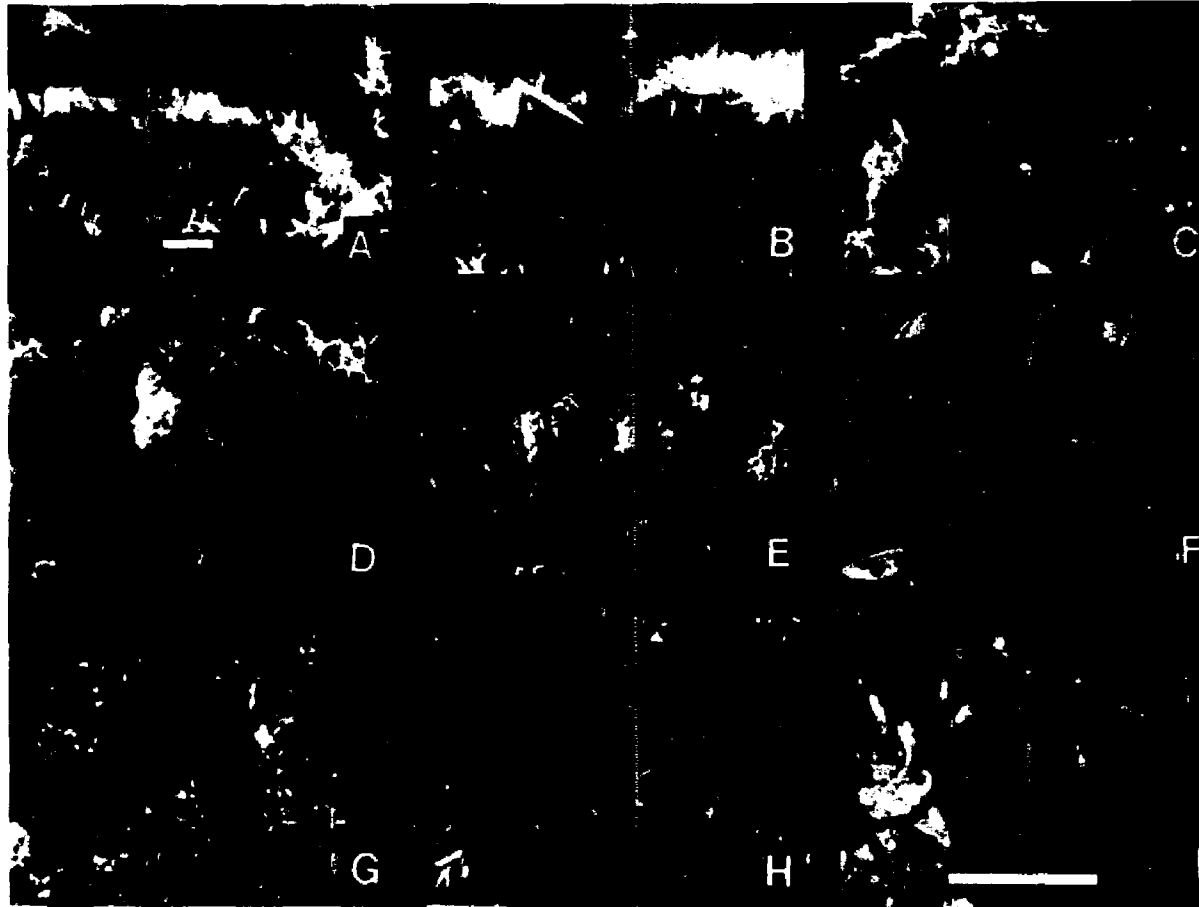


Figure 6.10 - SEM photomicrograph of cadmium waste specimens leached for 33 days in A-B) seawater C-D) sulfate solution E-F) chloride solution G-I) sulfate and chloride solution

surface of the particle grains are typically less than 1  $\mu\text{m}$  as shown in Figure 6.10i. Gypsum crystals are occasionally observed in seawater leached specimens as shown in Figure 6.10b indicating supersaturation with respect to calcium sulfate.

Gypsum crystallization is more prominent in samples leached in sulfate solution as shown in Figure 6.10c and d. The CSH Type II "equant grain" morphology persists. However, the larger interparticle voids observed with all chloride containing solutions have been filled with newly formed hydration material or gypsum formation. The chloride leached specimens (Figure 6.10e and f) exhibit a highly reticulated microstructure with CH dissolution and interparticle voids being more evident.

X-ray diffraction analysis conducted after 18 and 33 days of leaching showed gypsum to be the main crystalline phase present in sulfate leached specimens with a trace of ettringite and sodium sulfate. Calcium hydroxide is a dominant peak in the chloride leached specimens with weak ettringite peaks and traces of calcium chloro-aluminate (Friedals salt) although none were observed with SEM. XRD patterns for specimens leached in sulfate-chloride solutions exhibit weak CH and ettringite peaks. All leached specimens show strong cadmium hydroxide peaks.

Figure 6.11 shows SEM photomicrographs of the cadmium waste leached in seawater for more than 70 days. The

microstructure observed is similar to that described at 33 days. Ettringite crystals are still abundant with the larger ones in solution and smaller crystals on the surface of hydrated grains. The CSH structure is extremely reticulated as shown in Figure 6.11b.

The microstructure of cadmium waste leached in excess of 200 days is shown in Figure 6.12. Seawater leached specimens are shown in Figure 6.12a. The microstructure appears to be globules of amorphous silicate hydrate and gypsum crystallization. Extensive ettringite growth as observed earlier does not exist probably because of the unstable environment that has been created after leaching of lime-rich hydrates. The pore solution has probably dropped below the stable pH as determined by Hampson and Bailey(1983). Physical characterization of the waste at this time appeared weak and friable and the color of the surface was a pale orange probably due to the residual iron.

The sulfate leached specimens shown in Figure 6.12b,c still maintain their "equant grain" morphology with extensive gypsum crystallization. Inter-granular cracks are still evident and even surface cracking is observed by this time. Well defined ettringite crystals are not observed. This indicates that expansion and cracking in this case is probably due to a combination of gypsum crystallization and ettringite swelling.

Specimens leached in chloride and sulfate-chloride

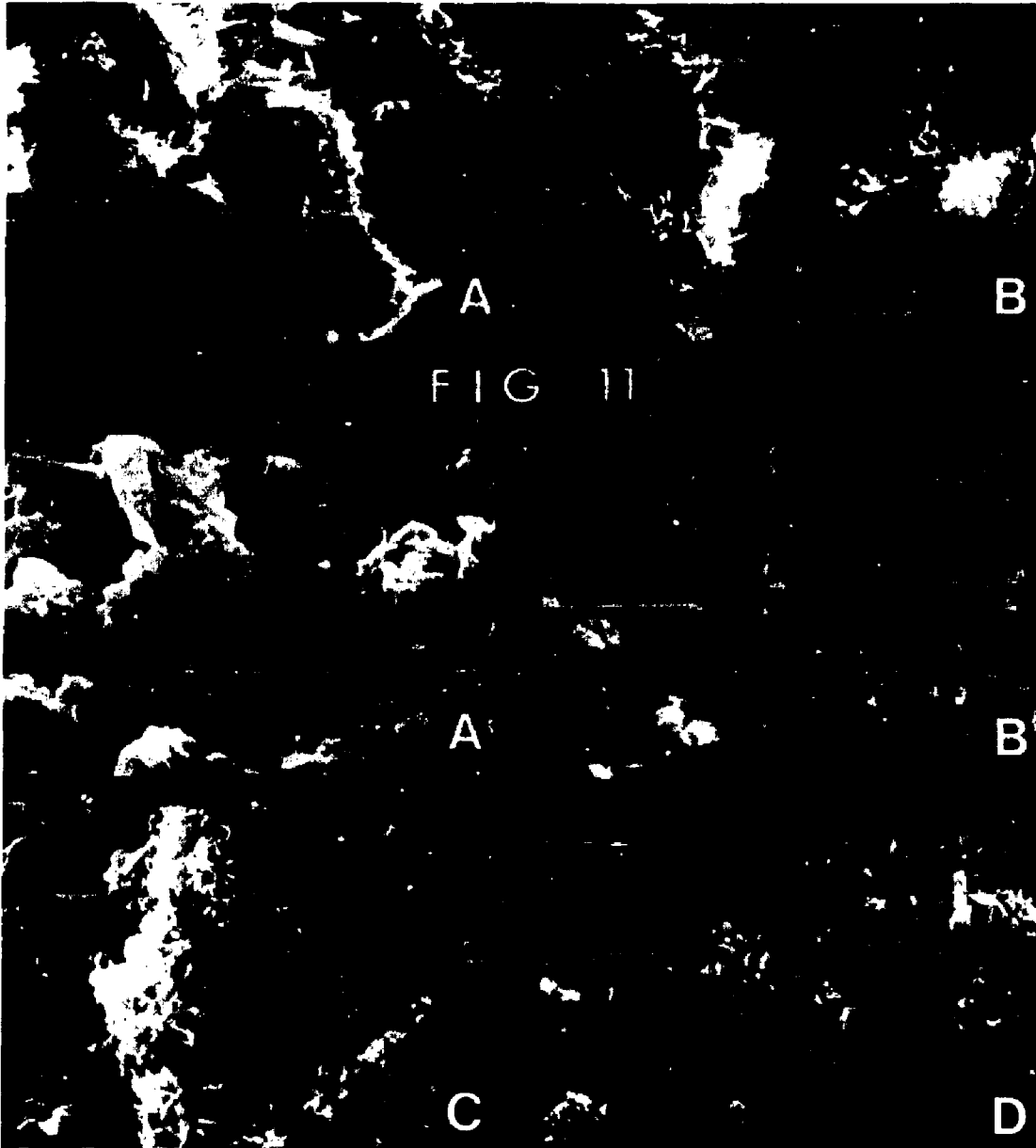


Figure 6.11 - SEM photomicrograph of cadmium waste leached for over 70 days

Figure 6.12 - SEM photomicrograph of cadmium waste leached for over 200 days in A) seawater B) sulfate solution C) chloride solution and D) sulfate-chloride solution



solutions (Figure 6.1d and e) still retain their reticulated microstructure with ettringite crystals deposited on the surface. The stability of these ettringite crystals is apparently still maintained as compared to the seawater leached specimens.

The surface layer of cadmium waste leached in seawater shows typical calcite, aragonite and brucite microstructures as shown in Figure 6.13. Calcite crystals observed at early ages (Figure 6.13a taken at 12 days) are relatively large ranging in size from 10 to 15  $\mu\text{m}$ . The crystals do not show any dissolution of their triangular center. However, the samples leached for 50 to 70 days (Figure 6.13b) show partial dissolution of their center and still maintain the pyramidal morphology. After this corrosion period, the crystal size has decreased to approximately 5  $\mu\text{m}$ . The hollow center does not appear to be a result of fracturing during sample preparation. After 200 days in seawater (Figure 6.13c), these crystals lose their center totally and their rigid pyramidal structure and conversion to brucite becomes more prominent.

These temporal transformations are very important in passifying the surface layer of the waste. It is important to determine if the conversion from calcite to brucite increases or decreases the apparent permeability of these wastes. These observations are consistent with those of Conjeaud (1980) and the literature she cited. Aragonite was

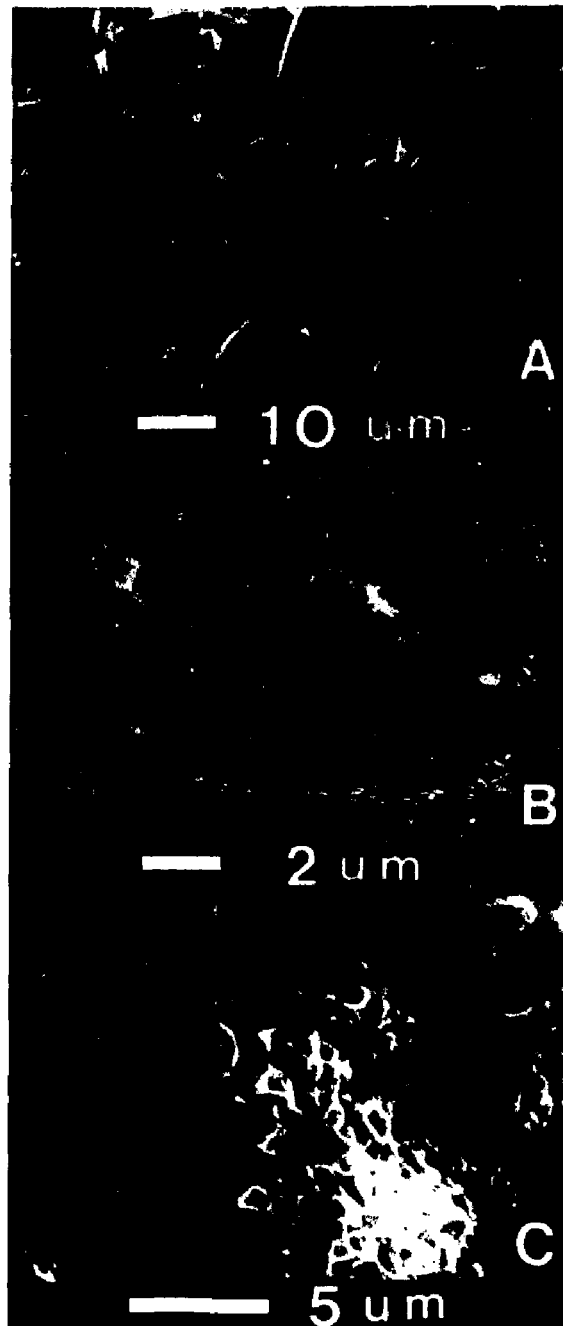


Figure 6.13 - SEI photomicrograph of surface layer of cadmium waste leached in seawater for A) 12 days B) 50 days and C) 200 days

not observed as urchins in the early days of corrosion.

### Discussion

Expansion is still due to ettringite formation as observed by SEM and XRD analysis. However, ettringite is only weakly detected by XRD in cadmium waste specimens leached in sulfate-chloride solutions. This may be attributed to the small size of the crystal and/or to the quasi-amorphous nature of this particular phase (gel as described by Mehta, 1973).

The higher rate of expansion appears to be associated with sulfate and chloride interaction as observed in seawater and sulfate-chloride leached specimens. The ettringite responsible for expansion is colloidal in size and forms topochemically. The larger crystals in the 5 to 15  $\mu\text{m}$  length are generally observed in interparticle voids or induced cracks caused by expansion indicating a through-solution formation. The reticulated nature of the CSH phase is due to the chloride ion in solution. Similar observations on this reticulated microstructure have been made by others (Conjeaud, 1980; Regourd, 1980; Chattarji, 1978)

Gypsum formation was predominant in samples leached in sulfate solutions and is responsible for the less porous matrix as observed in early days of leaching. However, the micro-cracks observed under the SEM and under the binocular

microscope at later ages are probably attributed to this gypsum crystallization in combination with ettringite formation which is only weakly detected by XRD at early ages. It is evident that ettringite formation in a cadmium waste matrix requires the essential sulfate-chloride combination.

In general, the corrosion process for these S/S wastes is initiated by  $\text{Cl}^-$  ion intrusion and dissolution of calcium rich hydrates. This would create an even more porous matrix for  $\text{SO}_4^{2-}$  ion penetration. When sulfate ions combine with alumina bearing hydrates in a highly alkaline environment and in a cadmium-hydroxide weakened matrix expansive ettringite is formed. Supersaturation of pore solution with sulfate ions will in turn lead to the formation of secondary gypsum.

Seawater corrosion studies were also conducted on other cadmium waste samples. Linear expansion tests were conducted on 3 year old cadmium waste specimens having a water-cement ratio of 0.5 and 14 day unconfined compressive strength over 2900 psi. No significant linear expansion was observed in these specimens.

In another seawater expansion test, cadmium waste samples prepared by Ransom (1983) did not show any significant expansion either. These samples had a water-cement ratio of 1.0 and cadmium concentrations in the sludges used for mixing were 25,000 and 50,000 ppm.

However, the sludges were synthesized using cadmium chloride in comparison to cadmium nitrate used in this study. The compressive strength of these samples was greater than 1500 psi at 14 days. No microstructural or seawater leaching studies were conducted on these wastes previously.

These linear expansion studies suggest that not all cadmium waste subject to seawater corrosion would lose dimensional stability. However, it is cautioned that in the presence of high sulfate and chloride solutions, a weak cadmium waste matrix may suffer dimensional instability.

#### Conclusion

- o Detrimental expansion was observed in the cadmium waste leached in seawater. Expansion is attributed to ettringite formation.
- o Expansive ettringite crystals appear to be colloidal in size and formed topochemically.
- o Sulfate and chloride ions are most aggressive in the corrosion processes.
- o Not all cadmium waste undergoes sulfate-chloride attack, however, it is cautioned that cadmium waste could behave in a detrimental fashion when subject to seawater or sulfate-chloride corrosion.
- o Lead waste did not exhibit detrimental expansion when subject to seawater corrosion.

#### Proposed Future Work

- o Determine the critical conditions where cadmium waste behaves detrimentally when subject to sulfate-chloride and seawater attack. The important parameters would include cadmium concentration, curing period, water-cement ratio which will govern initial porosity, and the passivating nature of calcite, aragonite and brucite.

o Investigate the feasibility of cadmium substitution for calcium in ettringite.

o Effect of sample size on long term leaching in seawater.

o The effect of other metals and sulfate resistant portland cements.

## CHAPTER VII

### ASSESSING THE FREEZE THAW RESISTANCE OF SOLIDIFIED STABILIZED WASTE

#### Introduction

The objective of S/S processes is to solidify liquid wastes and minimize their mobility to the surrounding environment. This is achieved through the desirable selection of additives that react with the contaminants and reduce their solubility and through the construction of a solid monolith which decreases the apparent surface area and accessibility of leachants to leaching sites. Any physical disintegration of the solid monolith will increase the apparent permeability and expose of more leaching sites. Such physical disintegration could be caused by adverse climatic conditions such as freezing and thawing and wetting and drying.

These S/S wastes are designed to be enclosed under an earth cap of very low permeability to reduce water infiltration. Freeze thaw damage must be given consideration for those situations which allow the S/S waste to freeze in a saturated state. At disposal sites where freezing and thawing occur, it is necessary to assess the freeze-thaw durability and resistance as an integral part of

S/S process evaluation.

Currently, there are no specifications for evaluating the freeze-thaw durability of S/S wastes. Bartos and Palermo (1977) however have used ASTM D560-57 "Freezing and Thawing Tests for Compacted Soil-Cement Mixtures". In their work this method was applied to four treated wastes with different physical characteristics. The specimens were low-strength concrete, a rubber-like solid, plastic-encased blocks and a soil-like material. All samples disintegrated after 12 freeze-thaw cycles except for the plastic encased specimen. The failed samples consisted of 62 percent failure after only 2 cycles of freezing and thawing. Only limited information is presently available on the freeze-thaw durability of S/S wastes. Information is, however, available in the literature relative to the freeze-thaw durability of portland cement paste, mortar, and concrete, bricks, rocks soils and porous glass and will partially be reviewed herein.

**Postulated Distress Mechanisms During Frost Action in Porous Materials and Portland Cement Concrete**

**Hydraulic Pressure Theory**

In severe cold climates, damage to concrete structures can be caused by frost action or cycles of freezing and thawing. The degree of freeze-thaw deterioration is a complex phenomenon and depends on the microstructure of the particular material as well as environmental conditions.



According to Powers (1958) the mechanism of frost action is attributed to the hydraulic pressure generated by the 9% volume increase when water freezes in a cavity. The magnitude of this hydraulic pressure is dependent on the rate of ice formation, the size of the pores and the permeability of the host material which Powers terms the distance to an "escape boundry". These "escape boundries" have been successfully created within the paste phase of a concrete matrix with the proper use of air-entraining agents.

Concrete destruction appears only when concrete is critically saturated. Typically, if capillary pores contain freezable water in excess of 91.7 percent by volume, expansion may not be accommodated (Powers, 1945). Even the highest strength concrete cannot withstand the stresses exerted by freezing of water which may be in excess of 30,000 psi (Philleo, 1987). The hydraulic pressure theory was related to the saturation level by Fagerlund (1975).

#### Osmotic Pressure Theory

In addition to hydraulic pressure resulting from the action of freezing water, Powers (1958) proposed that osmotic pressure generated by partial freezing of pore solutions could also be another source of deterioration. It is known that the capillary pore solution is not pure water, but contains soluble alkalies, chlorides, and calcium

hydroxide. The higher the salt concentration in a solution the lower the temperature of freezing (Litvan, 1972). The source of osmotic pressure is attributed to differences in local salt concentration gradients between contiguous capillaries.

Yamato et al. (1987) restates that when the water in capillary cavities begins to freeze, the solution concentration increases. Hence a higher solution concentration will result in the capillary pores than in the surrounding gel pores. Osmotic pressure gradients develop in the direction toward the capillary cavities opposite the flow of water. The pressure required to force capillary water into the gel cavities is a combination of hydraulic and osmotic pressure.

Yamato et al. (1987) observed a decrease in freeze-thaw resistance with increasing chloride content in both water and seawater freezing mediums. Air-entrained concrete with 0.3% NaCl showed a better freeze-thaw resistance while concrete containing more than 0.5% NaCl did not perform satisfactorily. Osmotic pressure is proposed to be the cause of deterioration in the high chloride concentration samples due to the higher salt content.

#### **Capillary Effect Theory**

Osmotic pressure and hydraulic pressure are not the only proposed causes of expansion during frost action.

Beaudoin and McInnis (1974) observed expansion in paste samples even when benzene, which contracts on freezing, was used as the pore fluid. Capillary effects as proposed by Meier and Harnik (1978) involving large-scale migration of water from small to large pores is suggested to be the primary cause of freeze-thaw damage in porous bodies.

Capillary effects are based on the theory proposed by Litvan (1972) which basically states that the more tightly bound the water the lower the mobility of these molecules to rearrange themselves structurally into ice and hence the lower the freezing point. Capillary pore water would be expected to freeze first followed by adsorbed water in the gel pores and finally interlayer water in the CSH structure. It is estimated that water in gel pores does not freeze above  $-78^{\circ}\text{C}$  (Powers 1975, Mehta, 1986). Thermodynamically, a state of disequilibrium between frozen water in capillary pores and super cooled water in the gel pores exists during the initial freezing stage. Due to the positive entropy created, the super cooled water is forced to migrate to the large cavities where it can freeze. This process is identical to shrinkage however in this case water movement is due to the loss of thermodynamic balance when the capillary water freezes and thus increases the surplus of free water energy in the gel pores. The extent of deterioration is a function of the internal stresses that are developed and the resulting expansion. Moisture

transport from the CSH phase will contribute to the contraction phenomenon as observed in some air-entrained pastes (Powers, 1958).

**The Effect of Salt and Air-Entrainment on the Freeze Thaw Durability of Portland Cement Concrete**

**Effect of Dissolved Salts**

Litvan (1976) states that the effect of dissolved salts in a pure liquid such as water lowers the vapor pressure of a solvent. The undesirable consequence of this physiochemical occurrence is an higher degree of saturation a porous body attains at a given relative humidity if it contains soluble salts. A second significant consequence of the decreased vapor pressure is the reduction in freezing point which may be viewed as positive effect. However Litvan (1972) warns that the outside pores could be blocked by formation of crystals of pure liquid that migrate to the outer surface and impede flow of the liquid. Crystallization of salt in super saturated solutions may also cause internal stresses and deterioration as suggested by Bjegovic et al. (1987).

**Effect of Air-Entrainment**

The frost resistance of hardened paste is controlled by the simultaneous interaction of several factors namely the pore structure, continuity of pores and their pore size

distribution, distance to escape boundaries, degree of saturation, rate of cooling and tensile strength of the hardened matrix. Proper air entrainment that creates air void spacing in the order of 100 to 200  $\mu\text{m}$  has been shown to adequately protect against frost damage.

ACI Committee 201 (1980) recommends that the air void spacing factor not exceed 200  $\mu\text{m}$ , as concretes with such values of air void spacing factor satisfactorily resist rapid freezing and thawing tests. However, Pigeon and Lachance (1981) determined a spacing factor of 680  $\mu\text{m}$  for w/c ratio of 0.5 and 570 for a w/c ratio of 0.6 at a freezing rate of  $2^\circ\text{C/hr}$  as compared to  $11^\circ\text{C/hr}$  used by Powers and ACI Committee 201. In another experiment Pigeon et al. (1985) investigated the freezing rate on freeze-thaw durability. For their particular experimental condition for a 0.5 w/c ratio the critical air-void spacing factor was determined to be 630  $\mu\text{m}$  for a freezing rate of  $4^\circ\text{C/hr}$  and 450  $\mu\text{m}$  for  $6^\circ\text{C/hr}$ .

The review just presented indicates the mechanism of frost action in portland cement concretes and porous bodies to be a complex phenomenon that depends on the physio-chemical properties of the porous body and environmental conditions. These factors include the pore structure, saturation level of pores, salt concentration of the pore fluid, rate of cooling, rate and level of hydraulic pressure

developped, and tensile strength of the local skeletal walls.

### **OBJECTIVE**

The objective of this study was to develop a non-destructive testing method to assess freeze-thaw durability of S/S wastes. The sonic method was adopted and modified to yield information relating to changes in the internal structure of the material. Weight measurements as previously used (Bartos and Palermo, 1977; Hannak, 1986) are not always in direct agreement with the condition of the internal structure which contributes to the apparent permeability and leaching potential. In addition to development of the sonic method the following points were evaluated:

- a) effect of heavy metal addition (Cd, As, Cr )
- b) effect of curing (100 percent humidity, seawater)
- c) effect of air entrainment
- d) effect of high water-cement ratio and pozzolanic binders

### **Derivation of Acoustic Parameters**

The objective of the acoustic-stress wave testing effort was to develop a non destructive technique to evaluate the freeze-thaw durability of S/S waste in an effort to study the relationship between the sample microstructure and freeze-thaw durability. The dynamic modulus ( $E_{dynamic}$ ) and quality factor ( $Q$ ) were chosen

as the study parameters. The factor (Q) was adopted since it can be more sensitive to changes within the internal structure even if changes of natural frequency are not observed.

The natural frequency is routinely determined in concrete testing for calculating E dynamic using the standard ASTM "Test for Fundamental Transverse, Longitudinal, and Torsional Frequencies of Concrete Specimens "(C215-60; reapproved 1985). For this particular study, E dynamic is calculated for a prismatic specimen subject to axial vibration by equation (7-1) after (Pickett, 1945; Spinner and Tefft, 1961).

$$E \text{ dynamic} = D W (fn)^2 \quad (7-1)$$

Where:

$$D = \frac{.01035 L}{b t} ; \text{ s}^2 / \text{ in}^2$$

$fn^2$  = longitudinal resonant frequency;  $s^{-1}$   
W = weight; lbs  
L = length; in  
b = base width; in  
t = thickness; in

Assuming no change in weight and geometric properties, E dynamic is proportional to the square of the natural frequency  $(fn)^2$  of the specimen beams. Relative dynamic modulus is proportional to the square of the normalized

natural frequency (NNF) and used for evaluating concrete durability to freezing and thawing. NNF is determined before and after each freeze-thaw cycle as shown in equation (7-2). The NNF parameter is related to durability factor calculated using ASTM "Test for Resistance of Concrete to Rapid Freezing and Thawing" (C666-71; reapproved 1984), typically reported as an indicator of freeze-thaw durability for concrete.

$$\text{NNF} = \frac{[fn(i)]^2}{[fn(0)]^2} \times 100 \quad (7-2)$$

where:

- NNF = square of normalized natural frequency
- fn(0) = natural frequency at zero cycles
- fn(i) = natural frequency at the ith cycle

The quality factor is a frequency domain measurement of the width of the spectral peak. The amplitude of the response is expressed in decibals (db) as shown in equation (7-3). A decrease in Q will indicate an increase in structural disintegrity and in our particular case, increased freeze-thaw deterioration.

$$\text{spectrum level (db)} = 10 \log \frac{[V_{rms} (f_i)]}{[V_{rms} (f_n)]} \quad (7-3)$$



where:

$V_{rms} (f_i)$  = rms voltage at the  $i$  th frequency

$V_{rms} (f_n)$  = rms voltage at natural frequency

The spectrum level is plotted as a function of frequency as shown in Figure 7.1. The spectral peak width is defined by the - 3db frequencies ( $f_1$ ,  $f_2$ ) located on either side of resonance frequency. These frequencies correspond to the half power frequencies as normalized at natural frequency. The quality factor,  $Q$ , is defined by equation (7-4) as:

$$Q = \frac{f_n}{f_2 - f_1} \quad (7-4)$$

The  $Q$  factor (which is also a measure of the sharpness of resonance) is related to the log decrement and in materials with low damping the relationship is defined by equation (7-5) (Thomson, 1981).

$$Q = \frac{\pi}{d} \quad (7-5)$$

where:

$d$  = log decrement

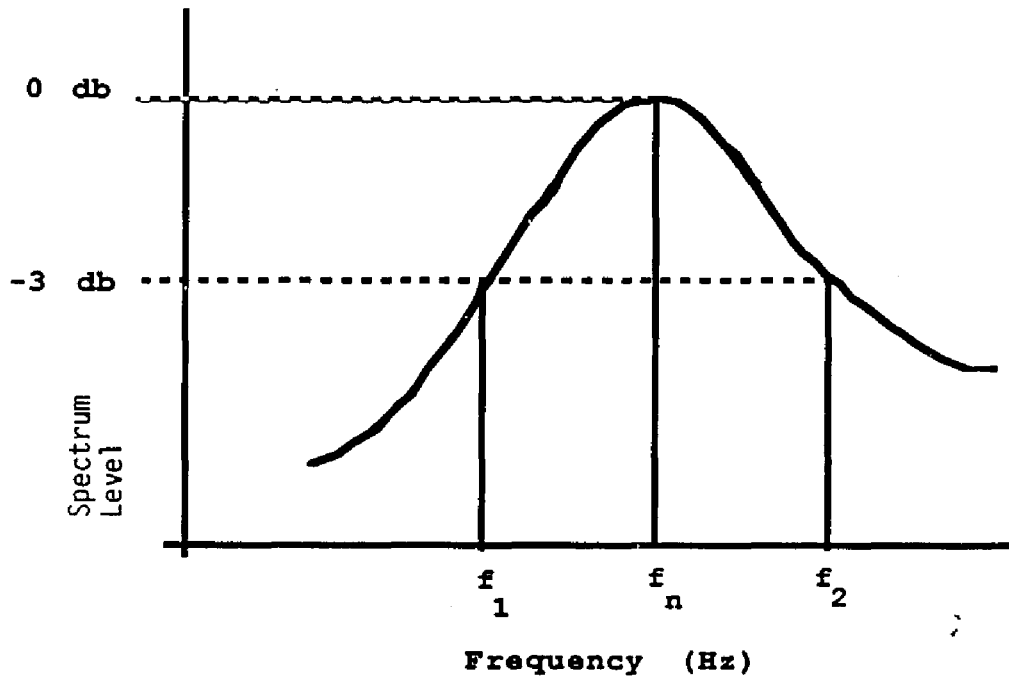


Figure 7.1 - Generic spectrum level vs. frequency plot indicating the parameters necessary for determining Q factor, the sharpness of the resonance peak.

## Experimental

### Sample Preparation

The sample beams used to evaluate freeze-thaw durability were prismatic and measured 1 by 1 by 5.5 inches. The beams were cast with mounting studs on the free ends. The stud used for attachment to the driving coil of an electro-mechanical shaker table was a cut threaded rod 1/4 inch in diameter with 20 threads per inch (1/4-20). The mounting stud for the transducer was a 10-32 steel rod cut 3/4 inches long and one end rounded to have an exact fit to the base. The studs were degreased and screwed in the mold at the specified intrusion.

The heavy metal sludges as described in Chapter IV corrected for solid content were used as mix water and were added to type II portland cement at a w/c of 0.5 and 1.0. Mixing was conducted in accordance with ASTM "Standard Method for Mechanical Mixing of Hydraulic Cement pastes and Mortars of Plastic Consistency" (C305-65 reapproved 1975). Air entrainment was added at the end of the sequence and mixing was continued for an additional two minutes. The beams were cast in a well greased mold and subjected to vigorous tamping and screeding to evacuate the entrapped air. Great caution was exercised not to disturb the preset studs. The mold was placed in the humidity room after two hours to prevent undesirable shrinkage during hardening of

the samples. The samples were subsequently demolded after 24 hours and cured for 28 days in approximately 100 percent relative humidity or in synthetic seawater at 20 °C.

### **Freeze-Thaw Cycling**

Both freezing and thawing cycles were carried out in water. Four beams were placed per container and submerged under two inches of water. The specimen beams were randomly placed in containers that were also randomly placed in the temperature cycling compartment of the freeze-thaw machine. The specimens were temperature cycled from 40 ± 5 °F to 0 ± 5 °F at a cooling rate of 9 °F/h to 40 ± 5 °F at a heating rate of 11 °F/h. Thermocouples were cast in companion sample beams which were placed in the center and along the edge to monitor the temperature variation across the freeze-thaw compartment and to ensure that all samples had reached the desired temperatures. This procedure, as adopted from ASTM C-666 procedure A, is more vigorous than procedure B which specifies freezing in saturated air and thawing in water.

The freeze-thaw apparatus used was a standard Soiltest<sup>R</sup> freeze-thaw machine used for concrete freeze-thaw testing in accordance to ASTM C-666. The apparatus is calibrated to monitor the temperature by a 1200 ohms resistor cast into an air entrained mortar sample and placed in the center of the freeze-thaw compartment.

ASTM recommendations were adopted for sample storage

when it was necessary for freeze-thaw cycling to be interrupted. Samples were stored in a freezer set at  $0 \pm 2$  °F and measures were taken to prevent moisture loss.

### Acoustic Testing

The continuous wave technique involves exciting the specimen beams on one end and receiving on the other end. To begin this technique, the specimen beams are directly mounted to the electro-mechanical shaker table by way of the cast-in studs. The beams were torqued at 10 inch-pounds to the shaker table using a modified torque wrench that grips the specimen beams at the base.

The shaker table is driven by a sine wave generator and amplifier which provide the excitation to the specimen beams. The wave propagation is monitored on the free-end with a Bruel & Kjaer 4374 accelerometer. The accelerometer output passes through a Bruel & Kjaer 2626 charge amplifier. Both the charge amplifier output and the sine wave generator are monitored on a Nicolet 320 digital oscilloscope. Maintaining a constant drive voltage, the sine wave frequency is varied and changes in received signal amplitude are recorded. The shaker table and the accelerometer both have flat frequency responses in the frequency band of interest. Figure 7.2 is a schematic drawing of the measurement system and test set up.

The test procedure begins by sweeping the frequency

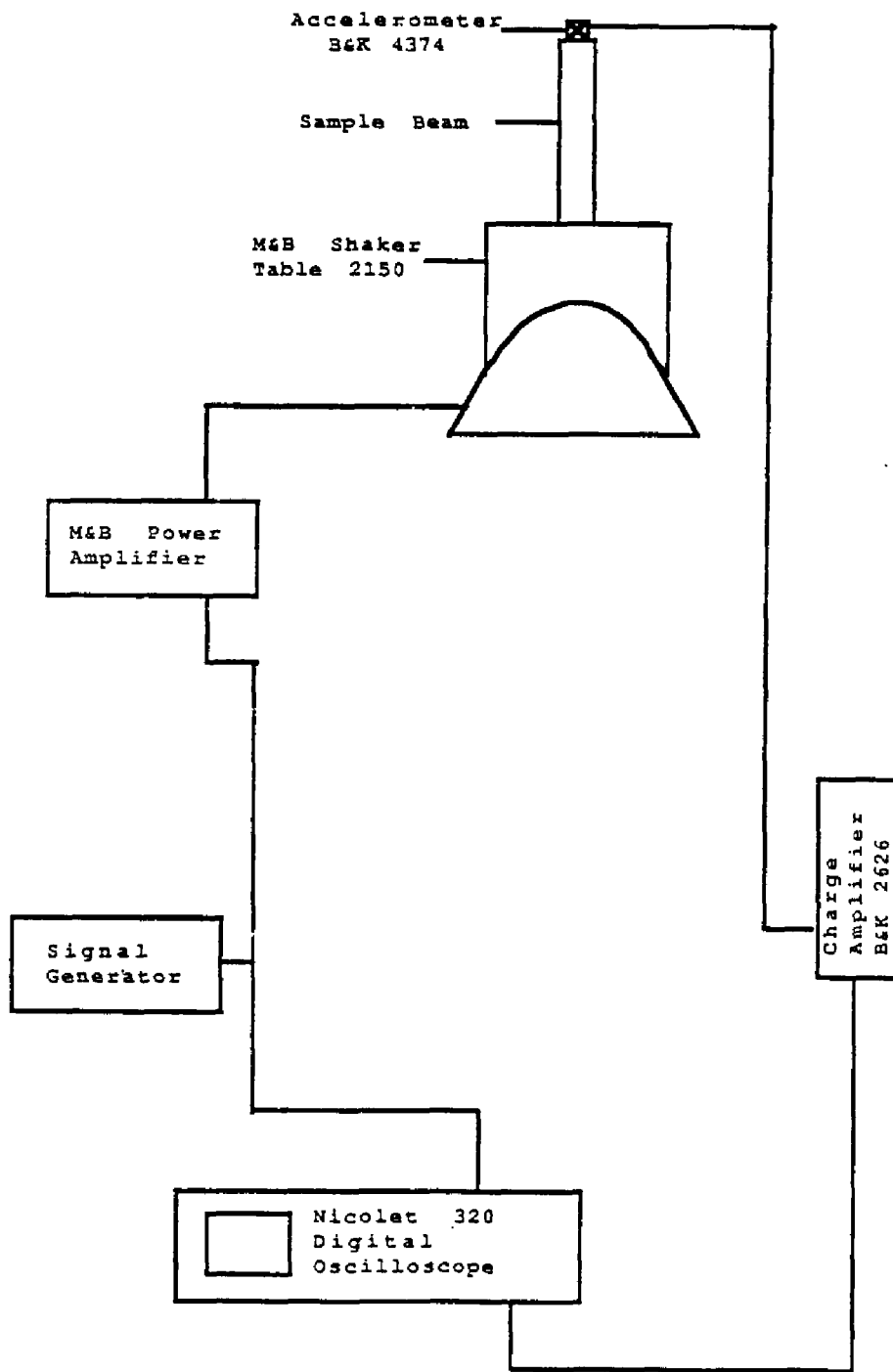


Figure 7.2 - Measurement system schematic indicating the arrangement of equipment necessary to obtain the spectrum level-frequency data

range between 2 and 5 kHz to determine  $f_n$ . Continuing with a constant drive voltage, the frequency was sampled contingent upon  $f_n$  and the observed rate of amplitude decay with frequency during the experiment. Effectively, a conditional sampling scheme is manifested in the neighborhood of the resonant frequency. A plot of relative amplitude (db) versus frequency (Hz) is then constructed with the data curve fitted to enable the determination of the -3db frequencies,  $f_1$  and  $f_2$ , required for the Q parameter calculations.

#### Results - First Run

The objective of the first test run is to assess the freeze-thaw resistance of different solidified heavy metal wastes and to investigate the effect of curing and air-entrainment on freeze-thaw durability.

The distribution and identification of specimen beams is shown in Table 7.1. Freeze-thaw results for the first run are presented in Table A-1 (Appendix A) in the form of band width and natural frequencies and test parameters NNF and Q. Table A-2 summarizes the number of cycles to failure as defined by 60 percent of the original NNF. Analysis of Variance (ANOVA) was performed on this set of data. Results indicate that air-entrainment produces a more durable material to freezing and thawing. No significant difference was observed between different non-air-entrained

mixes. No significant difference was observed between seawater and humidity curing. It is interesting to note that Q parameter values for this particular criteria results in higher Q values for the heavy metal samples as compared to the control.

The control samples with sludge to cement ratios of 1.0 did not survive the second cycle. This led to the decision not to further test the heavy metal samples at the high sludge to cement ratio.

Table 7.1 - Specimen Identification and Number of Samples Tested in the First Run

	Blank	Cadmium	Arsenic	Chromium
<u>Humidity</u>				
No Air	B5H 3	Cd5H 3	As5H 2	Cr5H 2
Air	B5HA 2	Cd5HA 2	As5HA 2	Cr5HA 2
<u>Seawater</u>				
No Air	B5S 2	Cd5S 3	Cd5S 3	Cr5S 3
Air	B5SA 2	Cd5SA 2	Cd5SA 2	Cr5SA 2

B = Blank; Cd = cadmium; 5 = w/c = 0.5; H = humidity cure;  
As = arsenic; Cr = chromium; S = seawater cure



### Discussion - First Run

As anticipated air-entrainment improves the resistance to repeated cycles of freezing and thawing as shown by the high value of  $Q$  and lower rate of decrease of  $Q$  and NNF. The control specimens do not appear to be improved by air-entrainment; however this is due to lack of sufficient air-entrainment generated within these samples. All metal samples have higher  $Q$  values as compared to the control. This lower value of  $Q$  for the control specimens is not clear at this point and can only be explained as an artifact of testing as will be shown in the second run. The control specimens were tested first during the early stages of experimentation while system improvements were being continually implemented.

A decrease in  $Q$  is observed in all non air-entrained specimens after storage while testing was interrupted. Samples were stored in a freezer set at  $0 \pm 2^\circ\text{F}$  for six months. This interruption occurred between the fourth and fifth cycle in cadmium and arsenic samples and between the second and third cycles in chromium samples. The test parameter is unaffected or increases for air entrained specimens subject to freezer storage.

### Results - Second Run

Acoustic system modifications were implemented during this run and it was decided not to store the beams in the

freezing cycle for more than 24 hours due to possible osmotic or capillary effects as seen in the first run. The freeze-thaw cycle was also changed to alternate between 0 and 68 °F for convenience with the same cooling and heating rates as indicated in the first run. Table 7.2 shows the sample beam identification and quantity of samples tested during this run. Results of this 2nd run are presented in Table A-3 in the form of natural frequency, band width at -3 db, NNF and Q factor.

Table 7.2. Number of Specimens Tested During Second Run

Blank		Cadmium	
<u>Humidity</u>	<u>Seawater</u>	<u>Humidity</u>	<u>Seawater</u>
Blank	Blank/Sea	Cadmium	Cadmium/Sea
3*	4	4	4

\* one specimen beam broke after first cycle.

The average values for Q and NNF parameter as a function of freeze-thaw cycles are shown in Figures 7.3 and 7.4 respectively. The data points are connected by an n-order polynomial using the least square method as presented in Appendix B. The cadmium waste specimens show better freeze-thaw resistance as compared to the control.

# Freeze Thaw Durability Q Factor Vs Cycles

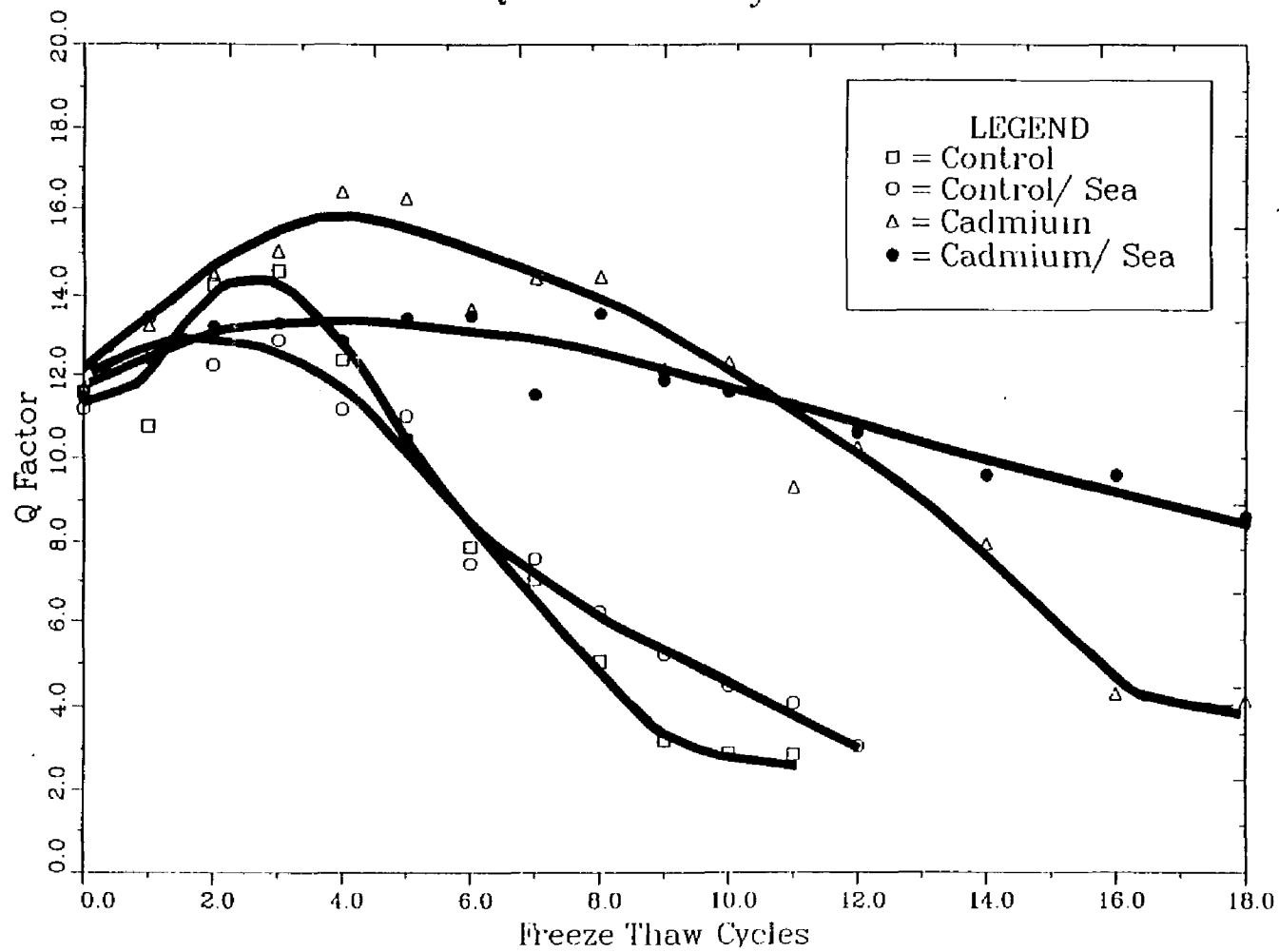


Figure 7.3 Freeze-thaw durability as monitored by Q factor.

# FREEZE THAW DURABILITY

## Normalized Natural Frequency vs Cycles

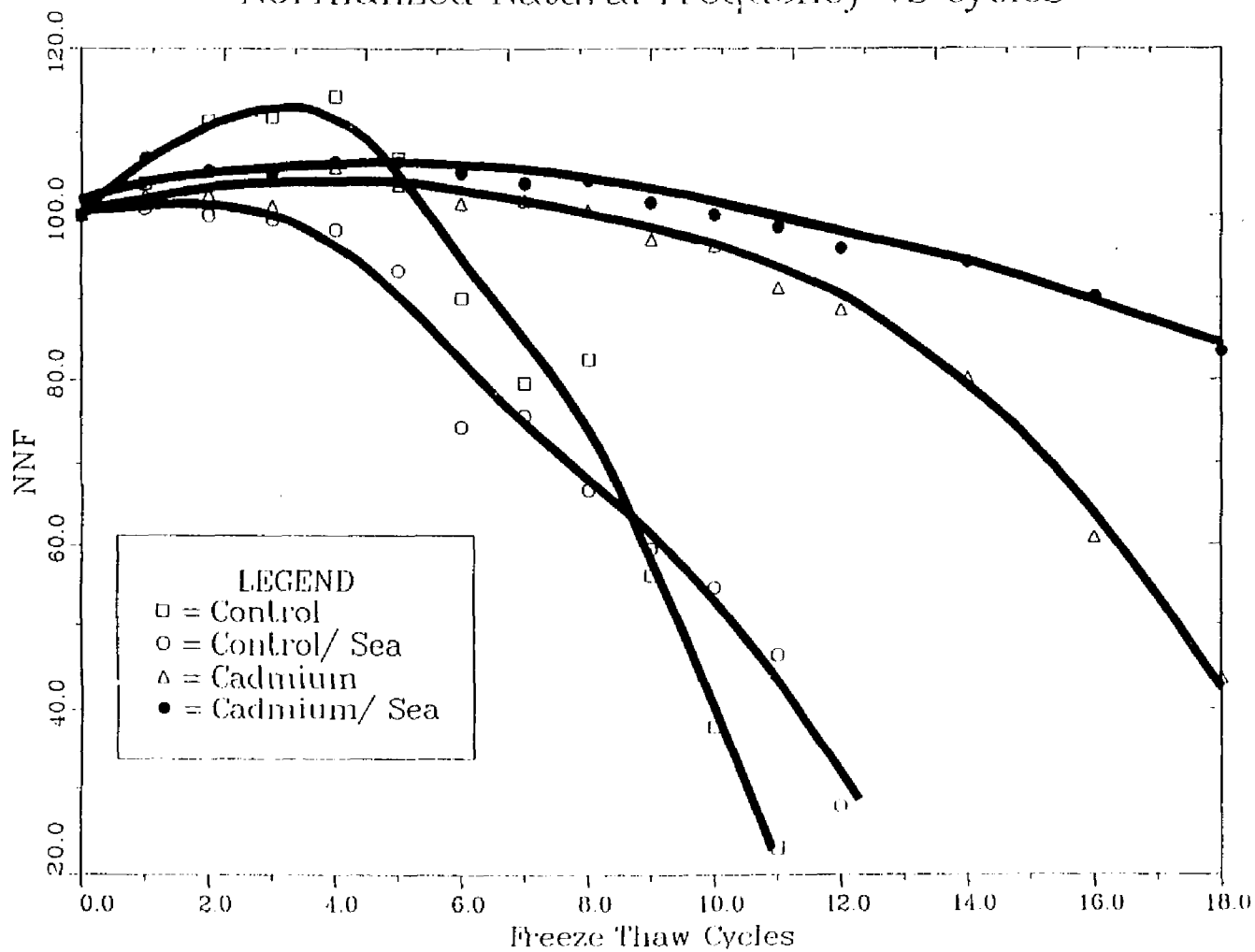


Figure 7.4. Freeze-thaw durability as monitored by NNF values.

Seawater curing changes the steepness of the slopes of the curves indicating a decreased rate of freeze-thaw deterioration hence an improved performance.

The Q factor plots in Figure 7.3 peak between the second and fourth cycle in both mixtures and both treatments. The control and cadmium specimens cured in 100 % RH exhibit a higher initial peak followed by a steeper slope indicating a more pronounced change in internal structure as compared to the specimens cured in seawater. This suggests that seawater curing produces a more desirable result especially with the cadmium waste.

Least squares statistical analysis was conducted on this set of data as shown in Table A-4. The statistical analysis is based on selecting an arbitrary failure cycle (i.e.  $C_f = C_o$  when  $Q < 7$  or  $NNF < 70\%$ ). Results varied depending on the criteria used for hypothesis testing, however, most results support the improved resistance of cadmium cured in 100 percent relative humidity and cadmium cured in seawater. There was not enough evidence to support the hypothesis that seawater curing influences the freeze-thaw resistance of the control mix.

A microstructural investigation using SEM, was conducted on companion samples prior to freeze-thaw cycling. The microstructure as observed by SEM of the cadmium waste specimen cured in 100% RH appears different than the control. The control specimen consists of calcium hydroxide

plates and a dense CSH gel while the cadmium waste specimen appears more porous with a highly fibrous CSH. Seawater curing appears to reduce the larger voids in the cadmium specimen which retains a highly reticulated CSH. The control specimen cured in seawater creates a more fibrous CSH and increased ettringite formation without deleterious expansion. The seawater cured specimens exhibit a varying microstructure from the surface to the bulk matrix. The visual porosity at the surface appears more dense than the bulk matrix due to CH dissolution and  $\text{CaCO}_3$  and brucite formation. This difference in the visually observed microstructure (coupled with porosity measurements on seawater cured specimens presented in Chapter V) could be related to the difference in freeze-thaw resistance observed.

The specimens tested in this run endured more freeze-thaw cycles to failure. This is due to the difference in storage treatment and to a lesser extent the temperature cycle. These specimens were not allowed to stay in water or stored in the freezer for extended periods causing possible critical saturation to be attained sooner.

#### **Discussion - Second Run**

Cadmium addition increases the resistance to freezing and thawing as compared to the control. This improved characteristic could be related to changes in porosity and

pore size distribution as discussed in Chapter V. Cadmium increases the total porosity and changes the derivative pore distribution to the larger sizes. This change in porosity could be analogous to air-entrainment if the pores do not become critically saturated as a result of the increased permeability.

The difference in microstructure and visual porosity in the seawater cured specimens would indicate possible differences in apparent permeability. I therefore suggest that the permeability of the bulk matrix could be large enough to diffuse the generated hydraulic pressure as proposed by Powers (1958). The permeability of the surface layer would be low enough to delay attainment of critical saturation.

The observed increase in  $Q$  value after initial freeze-thaw cycling is attributed to the proposed mechanism. The increase in  $Q$  value is attributed to a decrease in internal friction caused by a decrease in void space. All specimens appear to be initially improved by the freeze-thaw cycles. One way to increase the value of  $Q$  is through the creation of a more dense material through increased and/or continued hydration of the anhydrous particles. Actually, apparent density will not increase providing no external water enters the pores. Continued hydration will more likely decrease larger void space since the hydration material produced has a lower density than anhydrous particles. This behavior

could be explained at the micro level.

As mentioned earlier, not all of the water freezes in the pores during the freezing stage of the test due to the small size of the pore. During the freezing process some of the pore solution is pushed into unsaturated voids by hydraulic pressure and some particle re-orientation would be expected. Unhydrated cement particles would then be exposed to pore solution and hydration can occur or continue at an increased rate. An increase in hydration product could decrease existing void space and in turn internal friction. This would minimize the energy loss associated with the transfer of p-waves and a larger Q parameter value may result.

The initial increase in Q factor and the steepness of the slope of the curve in the seawater cured specimens is less dramatic than specimens cured in 100 % RH. This behavior is also related to the microstructure of the solidified waste. The seawater curing increases total porosity and changes the pore size distribution. Visual observations under SEM exhibit a different but uniform porosity as demonstrated by the reticular morphology. For these specimens, initial freeze-thaw cycling does not alter the microstructure significantly such as to increase the value of Q as presented in Figure 7.3. The improved freeze-thaw resistance of these specimens is due to an altered microstructure and a possible freezing point depression by



the increased salt concentration in the pore fluid.

### Results - Third Run

The objective of this run was to evaluate the freeze-thaw resistance of samples with very high water-cement ratio. The mix proportions used for these specimens are typical of true S/S processes used in practice. The sample composition is shown in Table 7.3. All sample beams were cured in 100 percent relative humidity for two months to allow for pozzolonic activity to take place.

The results for Q and NNF are presented in Table 7.4. All samples failed (lost structural integrity preventing further acoustic measurements) before completion of the third cycle. There was no discernable difference in freeze-thaw resistance between the two mixtures.

### Discussion - Third Run

The low freeze-thaw resistance of these samples is not surprising. The high water-cement ratio of these samples will result in a highly porous matrix with excessive permeability. Critical saturation in these specimens is probably attained much sooner than the samples tested during the first and second run at a much lower water-cement ratios. Also, the higher the water-cement ratio the higher the amount of freezable water in the pores (Powers, 1958). The addition of heavy metals to such a cementitious matrix

Table 7.3 - Freeze-Thaw Sample Composition  
Third Run

---

	<u>Sample A</u>	<u>Sample B</u>
Cement	12.7 %	4.0 %
fly ash*	59.2	54.4
lime	0.0	12.7
water	28.1	29.6

---

\* Sundance classified fly ash supplied by Alberta Environmental Centre Vegreville, Alberta.

\*\* All samples cured in 100% relative humidity for 2 months prior to freeze-thaw testing.

Table 7.4 - Test Parameters for Freeze-Thaw Cycling  
Third Run

<u>Beam No.</u>	<u>A1</u>		<u>A2</u>		<u>A3</u>		<u>A4</u>		<u>A5</u>	
<u>Cycle</u>	<u>Q</u>	<u>NNF</u>	<u>Q</u>	<u>NNF</u>	<u>Q</u>	<u>NNF</u>	<u>Q</u>	<u>NNF</u>	<u>Q</u>	<u>NNF</u>
0	13.07	100.0	12.44	100.0	9.88	100.0	12.23	100.0	7.30	100.0
1	8.42	93.5	7.76	95.0	7.91	100.0	8.66	91.9	7.33	108.9
2	8.27	78.6	----	failure----	----	failure----	----	failure----	----	failure----
3	----	failure----	----	failure----	----	failure----	----	failure----	----	failure----

<u>Beam No.</u>	<u>B1</u>		<u>B2</u>		<u>B3</u>		<u>B4</u>		<u>B5</u>	
0	11.93	100.0	12.41	100.0	9.49	100.0	9.97	100.0	10.29	100.0
1	8.66	90.4	8.65	92.4	----	failure----	9.18	92.5	9.51	96.2
2	----	failure----	7.80	75.1	----	failure----	8.02	89.7	----	failure----
3	----	failure----	----	failure----	----	failure----	----	failure----	----	failure----

\* failure indicates total structural breakdown or sufficient scaling to prevent application of the necessary torque

will probably not increase its freeze-thaw resistance as seen in the previous runs. However, it would be interesting to determine if air-entrainment would improve freeze-thaw resistance at such a high water-cement ratio.

### Conclusion

o The sonic method was successfully adopted to assess the freeze-thaw durability of S/S wastes.

o As expected, air entrainment improves the resistance to freeze-thaw durability of S/S wastes.

o Unexpectedly metal addition and seawater curing improves freeze-thaw resistance due to the creation of an altered porosity and pore size distribution for the low water-cement ratio used here.

o Freezing and Thawing could be detrimental to S/S wastes made of very high water-cement ratios if measures to prevent critical saturation are not undertaken.

### Proposed Future Work

o Evaluate possibility of applying the stress wave technique to cored samples without mounting studs or any other permanent coupling aid.

o Evaluate the freeze-thaw durability of S/S wastes using a more representative temperature cycle and saturation level. Our present technique could be too vigorous.

o Refine the method to be able to sweep through the frequencies automatically and not manually as done here.

## SUMMARY

Cement based materials are effective binders for stabilizing select heavy metal wastes. The final characteristics of the solidified waste depends on the metal type, additives used, binder matrix, water to cementitious ratio and curing regime. The leaching of metals depend on the physio-chemical characteristics of the matrix and the corrosive nature of the leaching medium. The stability of solidified waste in seawater is waste specific as observed in this study.

The microstructure of the cement solidified waste was analyzed by SEM/EDAX and XRD. Cadmium hydroxide was identified as the only crystalline metal phase, however, lead, chromium and arsenic did not exhibit similar crystalline behavior. It is postulated that the metals have been incorporated within the hydrated cement phases or have formed an amorphous complex. The microstructure is distinctly affected by the addition of heavy metal sludges which affects the binding characteristics of the solidified waste. Detection of all heavy metals was made possible by EDAX. All the heavy metals ( Cd, Pb, As, Cr) were detected in the CSH structure; Cr, Cd and As were detected in the CSH structure and Cd was detected in CH.

The addition of heavy metal sludge increases the total

porosity and shifts the pore-size distribution to the larger pores within the cementitious matrix. The porosity does not appear to be the only parameter affecting the compressive strength and leaching behavior of the waste specimens. Hence, the chemical composition of the binding material formed must contribute to the strength properties and metal release behavior. Cadmium and lead specimens with similar porosities showed different leaching characteristics.

The solidified cadmium and lead specimens were leached in seawater. The seawater leachability appears to be related to the metal complex formed and the microstructural changes that occur during seawater corrosion. The formation of calcite aragonite and brucite has a major effect on the sulfate corrosion and expansion process and metal release behavior.

Excessive expansion of the cadmium waste leached in seawater is attributed to a combination of expansive ettringite formation and matrix weakening induced by softening of the CSH phase and gypsum formation. The rate of expansion and subsequent deterioration is caused by the amount and combination of sulfate and chloride ions that penetrate the surficial layer.

Cement solidified wastes are not durable to repeated cycles of freezing and thawing as expected, due to a lack of air-entrainment. This physical deterioration will

affect its chemical stability and leaching behavior in an aggressive environment. However, it is not known what effect air-entrainment will have on chemical stability and leaching behavior of the solidified waste.

The sonic method was successful as a nondestructive technique for evaluating the freeze-thaw durability of cement solidified heavy metal waste.

### LIST OF REFERENCES

ACI Committee 201, "Guide to Durable Concrete" (ACI 201.2R-77), American Concrete Institute, Detroit, 37 pp., 1977.

Alford N., Rahman A. and Salih N., "The Effect of Lead Nitrate on the Physical Properties of Cement Paste", Cement and Concrete Research, Vol. 11, pp. 235-245, 1981.

American National Standard/American Society of Testing Materials, Standard C305-65, Standard Method for "Mechanical Mixing of Hydraulic Cement Pastes and Mortars of Plastic Consistency," reapproved 1975.

ASTM, Standard C39-84, Standard Test Method for "Compressive Strength of Cylindrical Concrete Specimens", reapproved 1984.

ASTM, Standard C617-85, Standard Practice for "Capping Cylindrical Concrete Specimens", reapproved 1985.

ASTM, Standard C215-60, Standard Test Method for "Fundamental Transverse, Longitudinal, and Torsional Frequencies of Concrete Specimens", reapproved 1985.

ASTM, Standard C666-71, Standard Test Method for "Resistance of Concrete to Rapid Freezing and Thawing", approved 1984.

ASTM, Standard D560-57, Standard Test Method for "Freezing and Thawing Compacted Soil Cement Mixtures", reapproved 1982.

Arliguie G., Ollivier J.P. and Grandet J., "Etude de L'Effet Retardateur du Zinc Sur L'Hydratation de la Pate de Ciment Portland", Cement and Concrete Research, Vol. 12, pp. 79-86, 1982.

Arliguie G. and Grandet J., "Etude Par Calorimetrie de L'Hydratation du ciment Portland en Presence de Zinc", Cement and Concrete Research, Vol. 15, pp. 825-832, 1985.

Bartos M.J. and Palermo M.R., "Physical and Engineering Properties of Hazardous Industrial Wastes and Sludges", US-EPA-600/2-77-139, Cincinnati, Ohio, 1979.



Batchelor B. and McDevitt M., "An Innovative Method for Treating Recycled Cooling Water", Journal WPCF, Vol. 56, pp. 1110-1117, 1984.

Beaudoin J. and MaInnis C., Cement and Concrete Research, Vol. 4, pp.139-148, 1974.

Benjamin M.M. and Leckie T.O., "Multiple-Site Adsorption of Cd, Cu, Zn, and Pb on Amorphous iron Oxyhydroxide", J. of Colloid and Interface Sci., Vol. 79, No.1, PP. 209-221, 1979.

Benson R. E., Chandler H. W. and Chacey K. A., "Hazardous Waste Disposal as Concrete Admixture", J. of Environmental Engineering, Vol. 111, No. 4, pp. 441-447, 1985.

Bensted J. and Varma S.P., "Studies of Ettringite and Its Derivatives: Part I", Cement Technology, Vol. 2, No. 3, pp. 73-76, 1971.

Bensted J. and Varma S.P., "Studies of Ettringite and Its Derivatives: Part II. Chromate Substitution", Silicate Industriels, Vol. 37, No. 12, pp. 315-318, 1972.

Bensted J. and Varma S.P., "Studies of Ettringite and Its Derivatives: Part III. Investigation of Strontium and Barium Substitution in Ettringite", Cement Technology, Vol. 3, No. 5, pp. 185-187, 1972.

Bensted J. and Varma S.P., "Studies of Ettringite and Its Derivatives: Part IV. The Low-Sulphate Form of Calcium Sulphoaluminate (monasulphate)", Cement Technology, Vol. 4, No. 3, 112-116, 1973.

Bensted J. and Prakash V., "A Discussion of the Paper: 'Thaumasite Formation: A Cause of Deterioration of Portland Cement and Related Substances in The presence of Sulphates' by J.H.P. Van Aardt and S. Visser", Cement and Concrete Research, Vol 6, pp. 321-322, 1976.

Bensted J., "A Discussion of the Paper: 'The Effects of Several Heavy Metal Oxides on the Formation of Ettringite and the Microstructure of Hardened Ettringite' by C. Tashiro, J. Oba and K. Akama", Cement and Concrete Research, Vol. 10, pp. 119-120, 1980.

Ben-Yair M., "The Effect of Chlorides on Concrete in Hot and Arid Regions", Cement and Concrete Research, Vol. 4, pp. 405-416, 1974.

Berntsson L. and Chandra S., "Damage of Concrete Sleepers by Calcium Chloride", Cement and Concrete Research, Vol. 12, pp. 87-92, 1982.

Bhatty M.Y., "Mechanism of Pozzolanic Reactions and Control of Alkali-Aggregate Expansion", Cement, Concrete and Aggregates, Vol. 7, No. 2, pp. 69-77, Winter 1985.

Birchall J.D., Howard A.J. and Double D.D., "Some General Considerations of a Membrane/Osmosis Model for Portland Cement Hydration", Cement and Concrete Research, Vol. 10, pp.145-155, 1980.

Birchall J.D., "Evidence as to the Formation and Nature of CSH from the Chemistry of Sucrose in OPC Paste", Presented at the Materials Research Society, Symposium M, Boston, Ma., Dec. 1986.

Bishop P.L., Gress D.L. and Olofsson J.A., "Cement Stabilization of Heavy Metals: Leaching Rate Assessment", Industrial Waste -Proceedings of the Fourteenth Mid Atlantic Conference, edited by J.E. Alleman and J.T. Kavanaugh, Ann Arbor Science, Ann Arbor, Mi, pp. 459-467, 1982.

Bishop P.L. and Gress D.L. Sea Grant Proposal, 1983.

Bishop P. and Gress D., "Evaluation for Marine Disposal of Stabilized/Solidified Inorganic Hazardous Waste" Report Submitted to National Oceanic and Atmospheric Administration, Office of Sea Grant, R/PMR-86, 1986.

Bjegovic D. et al. "Theoretical Aspect and Methods of Testing Concrete Resistance to Freezing and Deicing Salts", SP-100, ACI, Concrete Durability, pp. 947-971, 1987.

Blachere J.R. and Young, "Freezing and Thawing Tests and Theories of Frost Damage", J. of Testing and Evaluation, Vol. 3, No. 4, pp. 273-277, July 1975.

Brown Todd, Masters Thesis, University of New Hampshire, Durham, N.H., December, 1984.

Brown L.S., Discussion of the Paper by Kalousek and Benton on the "Mechanism of Seawater Attack on Cement Pastes", ACI Journal, pp. 646-648, August, 1970.

Buil M., "Thermodynamic and Experimental Study of the Crystallization Pressure of Water-Soluble Salts." International Colloquium on Materials Science and Restoration, Esslingen 6-8 Sept. 1983, Ed. F.H. Wittmann, pp. 373-378.

Buenfeld N.R. and Mewman, "The Permeability of Concrete in a Marine Environment" Magazine of Concrete Research, Vol. 36, No. 127, pp. 67-80, June, 1986.

Chatterji S., "Mechanism of the CaCl<sub>2</sub> Attack on Portland Cement Concrete", Cement and Concrete Research, Vol. 8, pp. 461-468, 1978.

Chen S. and Mehta P.K., "Zeta Potential and Surface Area Measurements on Ettringite", Cement and Concrete Research, Vol. 12, pp. 257-259, 1982.

Cohen M.D. and Richards C. W., "Effects of the Particle Sizes of Expansive Clinker on Strength-Expansion Characteristics of Type k Expansive Cements", Cement and Concrete Research, Vol. 12, pp. 717-725, 1982.

Cohen M.D., "Modeling of Expansive Cements", Cement and Concrete Research, Vol. 13, pp. 519-528, 1983.

Cohen M.D., "Theories of Expansion in Sulfoaluminate - Type Expansive Cements: Schools of Thought", Cement and Concrete Research, Vol. 13, pp. 809-818, 1983.

Cohen M.D., "A Reply to a Discussion by B. Mather of the Paper: 'Theories of Expansive Cements: Schools of Thought'", Cement and Concrete Research, Vol. 14, pp. 610-612, 1984.

Conjeaud M., "Mechanism of Seawater Attack on Cement Mortar", in Performance of Concrete in Marine Environment, edited by V.M. Malhotra, ACI Sp-65, pp. 39-61, American Concrete Institute, Detroit, MI, 1980.

Cote P.L., Doctoral Dissertation, McMaster University, Alberta, Canada, February 1986.

Crammond N.J., "Thaumasite in Failed Cement Mortars and Renders From Exposed Brickwork", Cement and Concrete Research, Vol 15, pp. 1039-1050, 1985.

Diamond S., in Hydraulic Cement Pastes: their structure and properties, Cement and Concrete Association, Slough, England, p.2, 1976.

Diamond S., "Chloride Concentrations in Concrete Pore Solutions Resulting from Calcium and Sodium Chloride Admixtures", Cement, Concrete and Aggregates, Vol. 8, No. 2, pp. 97-102, Winter 1986.

Double D.D., Hellawell A. and Perry S.J., "The Hydration of Portland Cement", Proc. Royal Soc. London, Vol. A359, pp. 435-451, 1978.

Efes Y., "Porengrossenverteilung Von Morteln Nach Lagerung Im Wasser Und In Einer Chloridlosung", Cement and Concrete Research, Vol. 10, pp. 231-242, 1980. (Abstract Available).

El Korchi T., Masters Thesis, University of New Hampshire, Durham, N.H., 1982.

El Korchi T., Melchinger K., Gress D. and Bishop P., "Evaluating the Potential for Stabilizing Two Heavy Metals in Portland Cement Paste", presented at the AICHe National Summer Meeting, Boston, MA, 1986.

Fagerlund G., "The Significance of Critical Degrees of Saturation at Freezing of Porous and Brittle Materials", in Durability of Concrete, ACI SP-47, pp. 13-65, 1975.

Falcone J.S., Jr, Spencer R.W., Reifsnnyder R.H. and Katsanis E.P.L., "Chemical Interactions of Soluble Silicates in the Management of Hazardous Wastes", Hazardous and Industrial Waste Management and Testing: Third Symposium, ASTM STP 851, pp. 213-229, Larry P. Jackson, Alan R. Rohlik, and Richard A. Conwys, Eds., American Society for Testing and Materials, Philadelphia, 1984.

Ftikos Ch. and Parissakis G., "The Combined Action of  $Mg^{2+}$  and  $Cl^{-}$  Ions in Cement Pastes", Cement and Concrete Research, Vol. 15, pp. 593-599, 1985.

Ghosh M. and Johannesmeyer H., "Fixation of Chromium and Cadmium From Electroplating Waste Sludges", Proc. of the Environmental Eng. Div. Spec. Conf., ASCE, pp 381-391, 1985.

Gjorv O.E. and Vennesland O., Cement and Concrete Research, Vol. 9, pp. 229-238, 1979.

Goto S. and Roy D., "Diffusion of Ions Through Hardened Cement Pastes", Cement and Concrete Research, Vol. 11, pp. 751-757, 1981.

Hampson C.J. and Bailey J.E., "On the Structure of Some Precipitated Calcium Aluminmo-Sulphate Hydrates", Journal of Materials Science, Vol. 17, pp. 3341-3346, 1982.

Hampston C.J. and Bailey J.E., "The Microstructure of the Hydration Products of Tri-Calcium Aluminate in the Presence of Gypsum", J. of Materials Science, Vol. 18, pp. 402-410, 1983.

Hoffmann D. W., "Changes in Structure and Chemistry of Cement Mortars Stressed by a Sodium Chloride Solution", Cement and Concrete Research, Vol. 14, pp. 49-56, 1984.

Hughes D. C., "Sulphate resistance of OPC, OPC/Fly Ash and SRPC Pastes: Pore Structure and Permeability", Cement and Concrete Research, Vol. 15, pp. 1003-1012, 1985.

Jawed I., Skalny J. and Young in Structure and Performance of Cements, P. Barnes Ed., Applied Science Publishers, 1983.

Kalousek G. L. and Benton E. J., "Mechanism of Seawater Attack on Cement pastes", ACI Journal, pp. 187-192, 1970.

Kantro D.L., "Tricalcium Silicate Hydration in the Presence of Various Salts", J. of Testing and Evaluation, Vol. 3, No. 4, pp. 312-321, July 1975.

Komarneni S. and Roy D.M., "Mechanisms of Immobilization of Nuclear Waste Elements by Cement Minerals, Cement and Mortar", Cement and Concrete Research, Vol. 11, pp. 789-794, 1981.

Kondo R., Daimon M., Sakai E. and Ushiyama H., "Influence of Inorganic Salts on the Hydration of Tricalcium Silicate", J. Appl. Chem. Biotechnol., Vol. 27, pp. 191-197, 1977.

Kurdowski W. and Thiel A., "On the Role of Free Calcium Oxide in Expansive Cements", Cement and Concrete Research, Vol. 11, pp. 29-40, 1981.

Landreth R. E., "Guide to the Disposal of Chemically Stabilized and Solidified Waste", EPA SW-872, Cincinnati, Ohio, 1986.

Lieber W., "The Influence of Lead and Zinc Compounds on the Hydration of Portland Cement" 5th International Symposium on the Chemistry of Cement, Vol. 2, pp. 444-454, 1968.

Lin C.H., Walker R.D. and Payne W.W., "Effect of Cooling Rates on the Durability of Concrete", Transportation Research Board, Vol.

Litvan G.G., "Phase transition of Adsorbates: IV, Mechanism of Frost Action in Hardened Cement Paste", J. American Ceramic Society, Vol. 55, No. 1, pp. 38-42, 1972.

Litvan G.G., "Frost Action in Cement in the Presence of De-Icers" Cement and Concrete Research, Vol. 6, pp. 351-356, 1976.

Lubowitz H.R., Telles R.W., Zilash B.M. and Unger S.L., "Land Disposal of Hazardous Wastes", Proc. of 10th Annual Res. Symp., EPA-600/ 9-84-007, 205-210, 1984.

Lukas W., Cement and Concrete Research, Vol. 6, No. 2, pp. 225-233, 1976.

Malone P.G. and Larson R.J., "Scientific Basis of Hazardous Waste Immobilization", Hazardous and Industrial Solid Waste Testing: Second Symposium, ASTM STP 805, Philadelphia, Pa., pp. 168-, 1983.

Marchese B., "Chemical Resistance of Cement Pastes: Patinal Alterations", Cement and Concrete Research, Vol. 8, pp. 501-508, 1978.

Mascolo G., "Hydrotalcite Observed In Mortars Exposed to Sulfate Solutions - A Discussion", Cement and Concrete Research, Vol. 16, pp. 610-612, 1986.

Mather B., "A Discussion of the Paper: 'Mechanisms of the CaCl<sub>2</sub> Attack on Portland Cement Concrete,' by S. Chatterji", Cement and Concrete Research, Vol. 9, pp. 135-136, 1979.

Mather B., "A Discussion of the Paper: 'Theories of Expansion in Sulfoaluminate-Type Expansive Cements: Schools of Thought' by M.D. Cohen" Cement and Concrete Research, Vol. 14., pp. 603-609, 1984.

Mehta P. K., "Mechanism of Expansion Associated With Ettringite Formation", Cement and Concrete Research, Vol. 3, pp. 1-6, 1973.

Mehta P. K., "Scanning Electron Microscope Studies of Ettringite Formation", Cement and Concrete Research, Vol. 6, pp. 169-182, 1976.

Mehta P.K. and Manmohan D., Proc. of the Seventh Int. Congr. on Chemistry of Cements, Paris, 1980.

Mehta P. K. and Wang S., "Expansion of Ettringite By Water Adsorption", Cement and Concrete Research, Vol. 12, pp. 121-122, 1982.

Mehta P. K., "Mechanism of Sulfate Attack on Portland Cement Concrete - Another Look", Cement and Concrete Research, Vol. 13, pp. 401-406, 1983.

Mehta P.k., "Discussion of the Paper 'Expansion Properties of the Mixture C4ASH12-CS and A Hypothesis on the Expansion Mechanism' by V. A. Rossetti et al.", Cement and Concrete Research, Vol. 13, pp. 591-592, 1983.

Mehta P.K., Concrete: its Structure, Properties and Materiels, Prentice-Hall, Inc., Englewood Cliffs, NJ, 1986.

Meier U. and Harnik A.B., Cement and Concrete Research, Vol. 8, pp. 545-551, 1978.

Melchinger K., El-Korchi T. Gress D. and Bishop P., "Stabilization of Cadmium and Lead in Portland Cement Paste Using a Synthetic Seawater Leachant", Environmental Progress, Vol. 6, No. 2, pp. 99-103, May, 1987.

Melchinger K., Masters Thesis, University of New Hampshire, Durham, N.H., 1987.

Midgley H.G. and Illston J.M., "The Penetration of Chlorides into Hardened Cement Pastes", Cement and Concrete Research, Vol. 14, pp. 546-558, 1984.

Mikhail R. Sh., Abo-El-Enein S.A. and Hanafi S., "Ettringite Formation in Compressed Expansive Cement Pastes", Cement and Concrete Research, Vol. 11, pp. 665-673, 1981.

Mindess S. and Young J.F., Concrete, Prentice Hall, Englewood cliffs, NJ, 1981.

Nakamura T., Sudoh G. and Akaiwa S., "Mineralogical Composition of Expansive Cement Clinker Rich in SiO<sub>2</sub> and Its Expansibility", 5th International Symposium on the Chemistry of Cement, Tokyo, Vol. 4, pp. 351-364, 1968.

Negro A. and Bachiorrini A., "Expansion Association with Ettringite Formation at Different Temperatures", Cement and Concrete Research, Vol. 12, pp. 677-684, 1982.

Nevill A.M., Properties of Concrete, Halsted Press, Division of Wiley and Sons, New York, NY, 1983.

Newkirk D.D., Warner M. G. and Barros S., "Treatability Studies on Heavy Metal Removal in Selected Inorganic Chemical Industries", Proc. of the 36th Purdue Industrial Waste Conference, Ann Arbor, Mi, p. 579, 1982.

Odler Il., "A Discussion of the Paper: 'Mechanism of Sulfate Attack on Portland Cement Concrete - Another Look' by P.K. Mehta", Cement and Concrete Research, Vol. 14, pp. 147-148, 1984.

Ogawa K. and Roy D.M., "C4A3S Hydration, Ettringite Formation, and Its Expansion Mechanism: II. Microstructural Observation of Expansion", Cement Concrete Research, Vol. 12, pp. 101-109, 1982.

Orr C. Jr., "Application of Mercury Penetration to Materials Analysis", Powder Technology, Vol. 3, pp. 117-123, 1969.

Page C.L., short N.R. and El Tarras A., "Diffusion of Chloride Ions in Hardened Cement Pastes", Cement and Concrete Research, Vol. 11, pp. 395-406, 1981.

Philleo R., "Frost Susceptibility of High Strength Concrete", ACI SP 100-46, Concrete Durability, pp. 819-842, 1987.

Pickett G., "Equations for Computing Elastic Constants from Flexural and Torsional Resonant Frequencies of Vibration of Prisms and Cylinders." ASTM Proc. Vol. 45, pp. 846-863., 1945,

Pigeon M. and Lachance M., "Critical Air Void Spacing Factors for Concrete Submitted to Slow Freeze-Thaw Cycles", ACI Journal Proceedings, Vol. 78, No. 4, pp. 282-291, July-Aug. 1981.

Pigeon M., Prevost J., and Simard J. "Freeze-Thaw Durability Versus Freezing Rate" ACI Journal, Vol. 82, pp. 684-692, Sept-Oct. 1985.

Pettifer K. and Nixon P.J., "Alkali Metal Sulphate - A Factor Common to Both Alkali Aggregate Reaction and Sulphate Attack on Concrete", Cement and Concrete Research, Vol 10, pp. 173-181, 1980.

Pojasek R. B., "Disposing of Hazardous Chemical Wastes", Env. Sci. and Techn., Vol. 13, No. 7, pp. 810-811, July, 1979.

Poon C.S., Peters C.J. and Perry R., "Use of Stabilization Processes in the Control of Toxic Wastes", Effluent and Water Treatment Journal, Vol. 23, pp. 451-459. 1983.

Poon C.S., Peters C.J., Perry R., Knight C.P.V., "Assessing the Leaching Characteristics of Stabilized Toxic Waste by Use of Thin Layer Chromatography", Environ. Technol. Lett., Vol. 5, pp. 1-6, 1984.

Poon C.S., Clark A.I., Perry R., "Investigation of the Physical Properties of Cement-based Fixation Processes for the Disposal of Toxic Wastes", The Public Health Engineer, Vol. 13, pp. 108-111, 1985a.

Poon C.S., Peters C.J., Perry R., Barnes P., Baker A.P., "Mechanisms of Metal Stabilization of Cement Based Fixation Processes", Sci. Total Environ., Vol. 41, pp. 55-71, 1985b.



Poon C.S., Clark A.I., Peters C.J. Perry R., "Mechanisms of Metal Fixation and Leaching by Cement based Fixation Processes", Waste Management & Research, Vol. 3, pp. 127-142, 1985c.

Poon C.S., Clark A.I., Perry R., Barnes P., Barker A.P., "Permeability Study on the Cement Based Solidification Process for the Disposal of Hazardous Wastes", Cement and Concrete Research, Vol. 16, pp. 161-172, 1986a.

Poon C.S., Clark A.I., and Perry R., "Atomic Structure Analysis of Stabilized toxic Wastes", Environmental Technology Letters, Vol. , pp. ,1986b

Powers T.C., "The Physical Structure and Engineering Properties of Concrete", Bulletin 90, Portland Cement Association, Skokie, Ill., 1958.

Powers T.C., "Freezing Effects in Concrete", in Durability of Concrete, ACI SP-47, pp. 1-12, 1975.

Ransom S., Masters Thesis, University of New Hampshire, Durham, N.H., 1983.

Regourd M., "Physico-chemical studies of Cement Paste, Mortars, and Concretes Exposed to seawater", in Performance of Concrete in Marine Environment, ACI SP-65, 1980.

Regourd Micheline, "Chemical Corrosion of Building Materials", Colloquium on Materials Science and Restoration, Esslingen 6-8 Sept. 1983 Ed. F.H. Wittmann.

Reis B. M.O., "Formation of Expansive calcium Sulphoaluminate by the Action of the Sulphate Ion on Weathered Granites in a Calcium Hydroxide - Saturated Medium", Cement and Concrete Research, Vol. 11, PP. 541-547, 1981.

Rossetti V. A., Chiocchio G. and Paolini A.E., "Expansive Properties of the Mixture  $C_4ASH_{12} - 2CS$ : I. An Hypothesis on the Expansion Mechanism", Cement and Concrete Research, Vol. 12, pp. 577-585, 1982.

Rossetti V.A., Chiocchio G. and Paolini A.E., "Expansive Properties of the Mixture  $C_4ASH_{12} - 2CS$  II. Effects of Lime, Porosity and Liquid/Solid Ratio", Cement and Concrete Research, Vol. 12, pp. 667-676, 1982.

Ogawa K. and Roy D.M., " $C_4A_3S$  Hydration Ettringite Formation, and Its Expansion Mechanism: I. Expansion; Ettringite Stability", Cement and Concrete Research, Vol. 11, pp. 741-750, 1981.

Samanta C. and Chatterjee M.K., "Sulfate Resistance of Portland-Pozzolanic Cements in Relation to Strength", Cement and Concrete Research, Vol. 12, pp. 726-734, 1982.

Shively W., Masters Thesis, University of New Hampshire, Durham, N.H., 1984.

Shively W., Bishop P., Gress D. and Brown T., "Leaching Testes of Heavy Metals Stabilized with Portland Cement", J. WPCF, Vol. 58, No. 3, pp. 234-241, 1986.

Skalny J, Odler I. and Hagymassy J. Jr., "Pore Structure of Hydrated Calcium Silicates: Influence of Calcium Chloride on the Pore Structure of Hydrated Tricalcium Silicate", J of Colloid and Interface Science, Vol. 35, No. 3, pp. 434-440, 1971.

Skalny J. and Maycock J.N., "Mechanisms of Acceleration by Calcium Chloride: A Review", J. of Testing and Evaluation, Vol. 3, No. 4, pp.303-311, 1975.

St. John D. A., "An Unusual Case of Ground Wateer Sulphate Attack on Concrete", Cement and Concrete Research, Vol. 12, pp. 633-639, 1982.

Stepanova I. N., Lukina L. G., Svatovskaya L. B. and Sychev M.M., "Hardening of Cement Pastes in Presence of Chlorides of 3d Elements", (Russian) J. of Appl. Chem. c/c Znhurnal Prikladnoi Khimii, Vol. 54, pp. 885-889, 1982.

Sychev M.M., Svatovskaya L.B., Orleanskaya N.B., Sorochkin M.A., Lysukhin M.K., and Nezhdanov V.M., "Influence of Powdered d Metals on Cement Hardening", (Russian) J. of Appl. Chem. c/c Znhurnal Frikladnoi Khimii, Vol. 57, pp. 507-510.

Tashiro C., Takahashi H., Kanaya M., Hirakida I. and Yoshida R., "Hardening Property of Cement Mortar Adding Heavy Metal Compound and Solubility of Heavy Metal From Hardened Mortar", Cement and Concrete Research, Vol. 7, pp. 283-290, 1977.

Tashiro C. and Oba J., "Effects of  $Cr_2O_3$ ,  $Cu(OH)_2$ ,  $ZnO$  and  $PbO$  on the Compressive Strength and the Hydrates of the Hardened C.A pastes" Cement and Concrete Research, Vol. 9, pp. 253-258, 1979.

Tashiro C., Oba J. and Akama K., "The Effects of Several Heavy Metal Oxides on the Formation of Ettringite and the Microstructure of Hardened Ettringite", Cement and Concrete Research, Vol. 9, pp. 303-308, 1979.

Tashiro C. and Oba J., "The Effects of  $\text{Cu}(\text{OH})_2$  on the Hydration  $\text{C}_3\text{A}$ ", Proc. of the 7th Int. Congr. on Chemistry of Cement, Edition Septima, Paris, 1980, Vol. II, pp.58-63.

Tashiro C. and Ueoka K., "Bond Strength Between  $\text{C}_3$  Paste and Iron, Copper or Zinc Wire and Microstructure of Interface", Cement and Concrete Research, Vol. 11, pp. 619-624, 1981.

Tashiro C. and Tatibana S., "Bond Strength Between  $\text{C}_3\text{S}$  Paste and Iron, Copper or Zinc Wire and Microstructure of Interface", Cement and Concrete Research, Vol. 13, pp. 377-382, 1983.

Taylor A. M. and Kuwairi A., "Effets of Ocean Salts on the Compressive Strength of Concrete", Cement and Concrete Research, Vol. 8, pp. 491-500, 1978.

Tenoutasse N., "The Hydration Mechanism of  $\text{C}_3\text{A}$  and  $\text{C}_3\text{S}$  in the Presence of Calcium Chloride and Calcium Sulphate", 5th International Symposium on the Chemistry of Cement, Vol. 2, pp. 372-378, 1968.

Thomas N.L., Jameson D.A. and Double D.D., "The Effect of Lead Nitrate on the Early Hydration of Portland Cement", Cement and Concrete Research, Vol. 11, pp. 143-153, 1981.

Tipping E., Thompson D.W., Ohnstad M. and Hetherington N.B. "Effects of pH on the Release of Metals From Naturally-Occuring Oxides of Mn and Fe", Techn. Letters, Vol. 7, pp. 109-114, 1986.

Van Aardt J.H.P. and Visser S., "Influence of Alkali on the Sulphate Resistance of Ordinary Portland Cement Mortars" Cement and Concrete Research, Vol. 15, pp. 485-494, 1985.

Wiles C.C., "A Review of Solidification/Stabilization Technology", Journal of Hazardous Materials, Vol. 14, pp. 5-21, 1987.

**APPENDIX**

Table A-1 Results of Freeze-Thaw Testing - First Run

BEAM NO.	TEST DATE	CYCLE NO.	f1	f <sub>n</sub>	f2	Δf	Q	NNF
B5H1	09/17/85	0	4120	4450	5010	890	5.00	100
	09/18/85	1	4160	4470	5130	970	4.61	101
	09/19/85	2	4170	4450	5015	845	5.27	100
	09/21/85	4	3300	3600	4150	850	4.24	65
	09/23/85	5	2690	3020	3450	760	3.97	46
B5H2	09/17/85	0	3840	4290	4770	880	4.88	100
	09/18/85	1	4000	4330	4740	740	5.85	102
	09/19/85	2	4190	4460	4860	670	6.66	108
	09/21/85	4	3720	3980	4470	750	5.31	86
	09/23/85	5	2980	3320	3700	720	4.61	60
	09/25/85	6	2680	3080	3590	910	3.38	52
B5H3	09/17/85	0	4190	4390	4660	470	9.34	100
	09/18/85	1	4010	4290	4610	600	7.15	95
	09/19/85	2	4260	4500	4860	600	7.50	105
	09/21/85	4	4200	4480	4900	700	6.40	104
	09/23/85	5	4130	4400	4860	730	6.03	100
	09/25/85	6	3860	4200	4820	960	4.38	92
	10/01/85	7	2140	2540	3270	1130	2.25	33
B5H5A	09/17/85	0	3910	4250	4850	940	4.52	100
	09/18/85	1	4170	4450	4850	680	6.54	110
	09/19/85	2	4280	4590	4860	580	7.91	117
	09/21/85	4	3910	4130	4630	720	5.74	94
	09/23/85	5	3940	4170	4470	530	7.87	96
	09/25/85	6	3400	3720	4180	780	4.77	77
	10/01/85	7	2820	3290	3700	880	3.74	60
B5H6A	09/17/85	0	3960	4250	4730	770	5.52	100
	09/18/85	1	4070	4350	4830	760	5.72	105
	09/19/85	2	4100	4380	4770	670	6.54	106
	09/21/85	4	3490	3720	4450	960	3.88	77
	09/23/85	5	3000	3470	3860	860	4.03	67
	09/25/85	6	2770	3070	3510	740	4.15	52

Table A-1 (cont.)

BEAM NO.	TEST DATE	CYCLE NO.	f1	fn	f2	$\Delta f$	Q	NNF
B5S1	09/17/85	0	4060	4290	4575	515	8.33	100
	09/18/85	1	4020	4250	4600	580	7.33	98
	09/19/85	2	3880	4220	4700	820	5.15	97
	09/21/85	4	3915	4250	4770	855	4.97	98
	09/23/85	5	3790	4000	4395	605	6.61	87
	09/25/85	6	3280	3550	4230	950	3.74	68
	10/01/85	7	3195	3180	4185	990	3.21	55
B5S3	09/17/85	0	4045	4410	4850	805	5.48	100
	09/18/85	1	4010	4255	4550	540	7.88	93
	09/19/85	2	4160	4370	4870	710	6.15	98
	09/21/85	4	3785	4150	4580	795	5.22	89
	09/23/85	5	3905	4200	4560	655	6.41	91
	09/25/85	6	3755	4140	4725	970	4.27	88
	10/01/85	7	2840	3140	3830	990	3.17	51
	10/09/85	8	2350	2700	3240	890	3.03	37
B5S5A	09/17/85	0	4000	4230	4500	500	8.46	100
	09/18/85	1	3750	4040	4410	660	6.12	91
	09/19/85	2	4050	4240	4820	770	5.51	100
	09/21/85	4	3940	4190	4760	820	5.11	98
	09/23/85	5	3740	4040	4460	720	5.61	91
	09/25/85	6	3470	3820	4260	790	4.84	82
	10/01/85	7	2740	3250	3660	920	3.53	59
B5S6A	09/17/85	0	3840	4170	4780	940	4.44	100
	09/18/85	1	3920	4220	4720	800	5.28	102
	09/19/85	2	3770	4120	4650	880	4.68	98
	09/21/85	4	3530	3960	4370	840	4.71	90
	09/23/85	5	3590	3890	4290	700	5.56	87
	09/25/85	6	3020	3410	4040	1020	3.34	67
	10/01/85	7	2450	3090	3610	1160	2.66	55
C5H1	10/09/85	0	4385	4560	4735	350	13.03	100
	10/10/85	1	4060	4235	4430	370	11.45	86
	10/12/85	2	4250	4400	4600	350	12.57	93
	10/21/85	4	3725	3910	4195	470	8.32	74
	04/17/86	5	3080	3250	3550	470	6.91	51
	05/05/86	6	2050	2310	2720	670	3.45	26

Table A-1 (cont.)

BEAM NO.	TEST DATE	CYCLE NO.	f1	fn	f2	$\Delta f$	Q	NNF
C5H2	10/09/85	0	4360	4480	4680	320	14.00	100
	10/10/85	1	4020	4195	4455	435	9.64	88
	10/12/85	2	4015	4165	4445	430	9.69	86
	10/21/85	4	4045	4155	4390	345	12.04	86
	04/27/86	5	2760	2900	3100	340	8.53	42
	05/09/86	6	930	1100	1800	870	1.26	6
C5H3	10/09/85	0	4380	4535	4745	365	12.42	100
	10/10/85	1	4270	4400	4610	340	12.94	94
	10/12/85	2	4270	4400	4615	345	12.75	94
	10/23/85	4	4135	4285	4530	395	10.85	89
	04/21/86	5	2850	3110	3515	665	4.68	47
C5H5A	10/09/85	0	3995	4135	4290	295	14.02	100
	10/10/85	1	3995	4130	4295	300	13.77	100
	10/11/85	2	3920	4060	4245	325	12.49	96
	10/21/85	4	3960	4085	4255	295	13.85	98
	04/17/85	5	3960	4120	4255	295	13.97	99
	05/05/85	6	3885	4035	4180	295	13.68	95
C5H6A	10/09/85	0	4110	4260	4390	280	15.21	100
	10/10/85	1	4105	4200	4400	295	14.24	97
	10/11/85	2	4080	4140	4375	295	14.03	94
	10/22/85	4	4040	4170	4320	280	14.89	96
	04/17/86	5	4035	4160	4305	270	15.41	95
	04/27/86	6	4030	4170	4330	300	13.90	96
	05/07/86	7	4000	4120	4305	305	13.51	94
	05/16/86	8	4005	4130	4310	305	13.54	94
C5S1	10/09/85	0	4355	4465	4655	300	14.88	100
	10/10/85	1	4165	4270	4490	325	13.14	91
	10/11/85	2	4055	4210	4455	400	10.53	89
	10/22/85	4	3710	3865	4105	395	9.78	75
	04/17/86	5	3190	3340	3610	420	7.95	56
	04/27/86	6	2910	3130	3480	570	5.49	49
	05/07/86	7	2800	2880	3270	470	6.13	42
	05/16/86	8	1890	2200	2775	885	2.49	24

BEAM NO.	TEST DATE	CYCLE NO.	f1	fn	f2	^f	Q	NNF
C5S2	10/09/85	0	4520	4660	4840	320	14.56	100
	10/10/85	1	4235	4400	4640	405	10.86	89
	10/11/85	2	4240	4400	4635	395	11.14	89
	10/22/85	4	3920	4070	4320	400	10.18	76
	04/17/86	5	3390	3580	3915	525	6.82	59
	04/27/86	6	3520	3690	3985	465	7.94	63
	05/07/86	7	3270	3510	3820	550	6.38	57
	05/16/86	8	2845	3170	3515	670	4.73	46
C5S3	10/09/85	0	4280	4385	4580	300	14.62	100
	10/10/85	1	3920	4045	4255	335	12.07	85
	10/11/85	2	4040	4190	4385	345	12.14	91
	10/21/85	4	3835	4000	4190	355	11.27	83
	10/29/85	5	3780	4015	4350	570	7.04	84
	04/25/86	6	3420	3550	3875	455	7.80	66
	05/07/86	7	3245	3440	3750	505	6.81	62
	05/16/86	8	2860	2930	3370	510	5.75	45
C5S5A	10/09/85	0	4105	4240	4405	300	14.13	100
	10/10/85	1	4010	4130	4295	285	14.49	95
	10/11/85	2	4010	4140	4355	345	12.00	95
	10/22/85	4	4020	4160	4325	305	13.64	96
	04/17/86	5	4025	4130	4300	275	15.02	95
	04/27/86	6	3985	4110	4320	335	12.27	94
	05/07/86	7	4005	4140	4300	295	14.03	95
	05/16/86	8	4010	4140	4315	305	13.57	95
C5S6A	10/09/85	0	4105	4220	4400	295	14.31	100
	10/10/85	1	3950	4105	4310	360	11.40	95
	10/11/85	2	3950	4085	4270	320	12.77	94
	10/22/85	4	4000	4170	4345	345	12.09	98
	04/17/86	5	4015	4120	4315	300	13.73	95
	04/27/86	6	4020	4140	4300	280	14.79	96
	05/07/86	7	4025	4120	4300	275	14.98	95
	05/16/86	8	4010	4100	4295	285	14.39	94
A5H1	10/07/85	0	4695	4850	5035	340	14.26	100
	10/09/85	1	4480	4635	4900	420	11.04	91
	10/11/85	2	4290	4470	4795	505	8.85	85
	10/22/85	4	4025	4205	4530	505	8.33	75
	04/02/86	5	3880	4160	4350	470	8.85	74
	05/09/86	6	3700	3845	4105	405	9.49	63
	05/16/86	7	3215	3490	3740	525	6.65	52

Table A-1 ( continued)



BEAM NO.	TEST DATE	CYCLE NO.	f1	f <sub>n</sub>	f2	Δf	Q	NNF
A5H3	10/07/85	0	4560	4705	4885	325	14.48	100
	10/09/85	1	4430	4565	4770	340	13.43	94
	10/11/85	2	4300	4470	4700	400	11.18	90
	10/22/85	4	3725	3850	4190	465	8.28	67
	04/17/86	5	3380	3520	3780	400	8.80	56
A5H5A	10/07/85	0	4395	4490	4640	245	18.33	100
	10/09/85	1	4230	4350	4535	305	14.26	94
	10/11/85	2	4290	4410	4590	300	14.70	96
	10/21/85	4	4140	4230	4450	310	13.65	89
	04/02/86	5	4085	4190	4335	250	16.76	87
	05/09/86	6	4230	4310	4480	250	17.24	92
A5H6A	10/07/85	0	4240	4320	4490	250	17.28	100
	10/09/85	1	4110	4195	4395	285	14.72	94
	10/11/85	2	4100	4260	4355	255	16.71	97
	10/21/85	4	4050	4195	4320	270	15.54	94
	04/02/86	5	4020	4150	4295	275	15.09	92
	04/17/86	6	3895	4070	4205	310	13.13	89
	05/09/86	7	3860	4050	4140	280	14.46	88
A5S1	10/07/85	0	4540	4645	4810	270	17.20	100
	10/09/85	1	4410	4525	4760	350	12.93	95
	10/11/85	2	4435	4565	4750	315	14.49	97
	10/21/85	4	4055	4225	4535	480	8.80	83
	04/17/86	5	3620	3730	4000	380	9.82	64
	05/05/86	6	3620	3780	4030	410	9.22	66
	05/09/86	7	3535	3605	3985	450	8.01	60
A5S2	10/07/85	0	4505	4685	4840	335	13.99	100
	10/09/85	1	4360	4485	4710	350	12.81	92
	10/11/85	2	4350	4490	4735	385	11.66	92
	10/21/85	4	4130	4235	4515	385	11.00	82
	10/28/85	5	4050	4245	4510	460	9.23	82
	04/21/86	6	3390	3560	3840	450	7.91	58
	05/09/86	7	2030	2240	2500	470	4.77	23
A5S3	10/07/85	0	4565	4670	4875	310	15.06	100
	10/09/85	1	4310	4480	4690	380	11.79	92
	10/11/85	2	4245	4380	4620	375	11.68	88
	10/21/85	4	4010	4175	4480	470	8.88	80
	04/21/86	5	3530	3740	4060	530	7.06	64
	05/09/86	6	3370	3570	3875	505	7.07	58

Table A-1 (continued)

BEAM NO.	TEST DATE	CYCLE NO.	f1	f <sub>n</sub>	f2	Δf	Q	NNF
A5S5A	10/07/85	0	4255	4385	4520	265	16.55	100
	10/09/85	1	4040	4225	4400	360	11.74	93
	10/11/85	2	4105	4230	4420	315	13.43	93
	10/21/85	4	3900	4035	4270	370	10.91	85
	04/02/86	5	4015	4135	4315	300	13.78	89
	05/09/86	6	4040	4140	4335	295	14.03	89
A5S6A	10/07/85	0	4160	4305	4485	325	13.25	100
	10/09/85	1	4085	4230	4410	325	13.02	97
	10/11/85	2	4085	4220	4395	310	13.61	96
	10/21/85	4	3970	4090	4370	400	10.22	90
	04/02/86	5	4080	4180	4430	350	11.94	94
	05/09/86	6	4025	4150	4350	325	12.77	93
K5H2	10/18/85	0	4455	4605	4760	305	15.10	100
	10/23/85	1	4350	4490	4670	320	14.03	95
	10/29/85	2	4345	4415	4645	300	14.72	92
	04/21/86	3	4025	4150	4360	335	12.39	81
	05/09/86	4	3955	4060	4320	365	11.12	78
	05/16/86	6	3365	3595	3760	395	9.10	61
K5H3	10/18/85	0	4605	4750	4935	330	14.39	100
	10/23/85	1	4510	4640	4830	320	14.50	95
	10/24/85	2	4355	4425	4640	285	15.53	87
	04/21/86	3	4100	4240	4480	380	11.16	80
	04/27/86	4	4060	4195	4415	355	11.82	78
	05/07/86	5	3965	4135	4375	410	10.09	76
	05/09/86	6	3815	3980	4250	435	9.15	70
05/16/86	7	3250	3520	3730	435	8.09	55	
K5H5A	10/18/85	0	3840	4005	4165	325	12.32	100
	10/23/85	1	3770	3890	4100	330	11.79	94
	10/28/85	2	3750	3870	4035	285	13.58	93
	04/21/86	3	2995	3110	3315	320	9.72	60
	05/09/86	4	2085	2340	2540	455	5.14	34
K5H6A	10/18/85	0	3720	3840	4035	315	12.19	100
	10/22/85	1	3715	3820	4010	295	12.95	99
	10/29/85	2	3735	3840	4010	275	13.96	100
	04/21/86	3	3720	3850	4000	280	13.75	101
	04/27/86	4	3740	3845	3985	245	15.69	100
	05/07/86	5	3655	3780	3915	260	14.54	97
05/16/86	6	3650	3760	3930	280	13.42	96	

Table A-1 (cont.)

BEAM NO.	TEST DATE	CYCLE NO.	f1	f <sub>n</sub>	f2	Δf	Q	NNE
K5S1	10/18/85	0	4480	4595	4810	330	13.92	100
	10/23/85	1	4305	4450	4650	345	12.90	94
	10/29/85	2	4310	4435	4620	310	14.31	93
	04/21/86	3	3965	4150	4400	435	9.54	82
	05/05/86	4	3840	3995	4420	580	6.89	76
	05/09/86	5	3555	3760	4160	605	6.21	67
	05/16/86	6	3150	3495	3820	670	5.22	58
K5S2	10/18/85	0	4615	4735	4895	280	16.91	100
	10/22/85	1	4355	4530	4725	370	12.24	92
	10/28/85	2	4355	4510	4725	370	12.19	91
	04/25/86	3	4080	4170	4385	305	13.67	78
	05/07/86	4	3900	4080	4330	430	9.49	74
	05/09/86	5	3710	3925	4175	465	8.44	69
	05/16/86	6	3635	3690	4105	470	7.85	61
K5S3	10/18/85	0	4310	4490	4600	290	15.48	100
	10/23/85	1	4270	4380	4585	315	13.90	95
	10/29/85	2	4150	4260	4485	335	12.72	90
	04/21/86	3	3825	3935	4190	365	10.78	77
	05/09/86	4	3460	3630	3930	470	7.72	65
	05/16/86	6	3215	3330	3725	510	6.53	55
K5S5A	10/18/85	0	3700	3805	3960	260	14.63	100
	10/23/85	1	3550	3650	3860	310	11.77	92
	10/29/85	2	3450	3610	3795	345	10.46	90
	04/21/86	3	3575	3705	3855	280	13.23	95
	04/27/86	4	3540	3680	3850	310	11.87	94
	05/07/86	5	3520	3635	3800	280	12.98	91
	05/16/86	6	3545	3660	3820	275	13.31	93
K5S6A	10/18/85	0	3645	3745	3890	245	15.29	100
	10/23/85	1	2455	2600	2700	245	10.61	48
	10/29/85	2	2570	2680	2880	310	8.65	51
	04/25/86	3	2255	2435	2560	305	7.98	42
	05/07/86	4	2350	2475	2590	240	10.31	44
	05/16/86	5	2340	2470	2575	235	10.51	44

Table A-1 (cont.)

Table A-2 Results of Freeze-Thaw Testing - Second Run

BEAM NO.	TEST DATE	CYCLE NO.	f <sub>n</sub>	f <sub>f</sub>	Q	NNF
BLANK 1	01/30/87	0	4620	360	12.83	100
	01/31/87	1	4590	375	12.24	99
	02/01/87	2	4570	320	14.28	98
	02/02/87	3	4590	325	14.12	99
	02/03/87	4	4680	390	12.00	103
	02/04/87	5	4475	480	9.32	94
	02/05/87	6	3675	680	5.40	63
	02/05/87	7	3240	1050	3.09	49
BLANK 2	01/30/87	0	4700	395	11.90	100
	01/31/87	1	4825	390	12.37	105
	02/01/87	2	4840	340	14.24	106
	02/02/87	3	4830	315	15.33	106
	02/03/87	4	4785	360	13.29	104
	02/04/87	5	4750	390	12.18	102
	02/05/87	6	4575	570	8.03	95
	02/05/87	7	4260	500	8.52	82
	02/06/87	8	4010	880	4.56	73
	02/07/87	9	3520	1060	3.32	56
	02/08/87	10	2960	1150	2.57	40
02/09/87	11	2250	790	2.85	23	
BLANK 3	01/30/87	0	4010	400	10.03	100
	01/31/87	1	4160	390	10.67	108
	02/01/87	2	4575	320	14.30	130
	02/02/87	3	4590	320	14.34	131
	02/03/87	4	4680	395	11.85	136
	02/04/87	5	4475	460	9.73	125
	02/05/87	6	4250	420	10.12	112
	02/05/87	7	4160	440	9.45	108
	02/06/87	8	3850	700	5.50	92
	02/07/87	9	3000	975	3.08	56
02/08/87	10	2330	725	3.21	34	
BLANK SEA 1	01/30/87	0	4525	435	10.40	100
	01/31/87	1	4555	395	11.53	101
	02/01/87	2	4570	390	11.72	102
	02/02/87	3	4595	360	12.76	103

Table A-2 (cont.)

BEAM NO.	TEST DATE	CYCLE NO.	fn	^f	Q	NNF
BLANK	02/03/87	4	4560	400	11.40	102
SEA 1	02/04/87	5	4475	410	10.91	98
continue	02/05/87	6	3825	450	8.50	71
	02/05/87	7	3850	520	7.40	72
	02/06/87	8	3680	630	5.84	66
	02/07/87	9	3580	710	5.04	63
	02/09/87	10	3350	765	4.38	55
	02/09/87	11	3060	775	3.95	46
	02/08/87	12	2380	780	3.05	28
BLANK	01/30/87	0	4650	395	11.77	100
SEA 2	01/31/87	1	4680	360	13.00	101
	02/01/87	2	4615	380	12.14	99
	02/02/87	3	4635	370	12.53	99
	02/03/87	4	4550	395	11.52	96
	02/04/87	5	4425	395	11.20	91
	02/05/87	6	4040	540	7.48	75
	02/05/87	7	4150	480	8.65	80
	02/06/87	8	3950	570	6.93	72
	02/07/87	9	3675	650	5.65	62
	02/09/87	10	3420	740	4.62	54
	02/09/87	11	3200	760	4.21	47
BLANK	01/30/87	0	4510	430	10.49	100
SEA 3	01/31/87	1	4410	335	13.16	96
	02/01/87	2	4410	355	12.42	96
	02/02/87	3	4330	320	13.53	92
	02/03/87	4	4380	430	10.19	94
	02/04/87	5	4240	420	10.10	88
	02/05/87	6	3895	570	6.83	75
	02/05/87	7	3835	550	6.97	72
	02/06/87	8	3500	660	5.30	60
	02/07/87	9	3300	670	4.93	54
BLANK	01/30/87	0	4500	375	12.00	100
SEA 4	01/31/87	1	4615	345	13.38	105
	02/01/87	2	4600	360	12.78	104
	02/02/87	3	4585	360	12.74	104
	02/03/87	4	4540	395	11.49	102
	02/04/87	5	4400	375	11.73	96
	02/05/87	6	3915	566	6.92	76
	02/05/87	7	3975	550	7.23	78
	02/06/87	8	3733	550	6.79	69

Table A-2 ( cont. )

BEAM NO.	TEST DATE	CYCLE NO.	$f_n$	$\Delta f$	Q	NNF	
CADMIUM 1	01/30/87	0	4340	400	10.85	100	
	01/31/87	1	4460	390	11.44	106	
	02/01/87	2	4435	340	13.04	104	
	02/02/87	3	4410	300	14.70	103	
	02/03/87	4	4520	260	17.38	108	
	02/04/87	5	4400	280	15.71	103	
	02/05/87	6	4380	340	12.88	102	
	02/05/87	7	4390	320	13.72	102	
	02/06/87	8	4375	310	14.11	102	
	02/07/87	9	4320	350	12.34	99	
	02/08/87	10	4340	360	12.06	100	
	02/09/87	11	4170	400	10.43	92	
	02/09/87	12	4120	375	10.99	90	
	02/10/87	14	3980	440	9.05	84	
	02/11/87	16	3770	535	7.05	75	
	02/12/87	18	3440	660	5.21	63	
	CADMIUM 2	01/30/87	0	4380	370	11.84	100
		01/31/87	1	4490	385	11.66	105
02/01/87		2	4520	310	14.58	106	
02/02/87		3	4535	300	15.12	107	
02/03/87		4	4550	280	16.25	108	
02/04/87		5	4560	275	16.58	108	
02/05/87		6	4490	315	14.25	105	
02/05/87		7	4525	315	14.37	107	
02/06/87		8	4480	290	15.45	105	
02/07/87		9	4380	380	11.53	100	
02/08/87		10	4440	320	13.88	103	
02/09/87		11	4180	510	8.20	91	
02/09/87		12	4140	440	9.41	89	
02/10/87		14	3950	545	7.25	81	
02/11/87		16	3340	840	3.98	58	
02/12/87		18	2630	670	3.93	36	
CADMIUM 3		01/30/87	0	4380	390	11.23	100
		01/31/87	1	4420	360	12.28	102
	02/01/87	2	4460	300	14.87	104	
	02/02/87	3	4465	285	15.67	104	
	02/03/87	4	4500	360	12.50	106	
	02/04/87	5	4500	250	18.00	106	
	02/05/87	6	4445	285	15.60	103	

Table A-2 (cont.)

BEAM NO.	TEST DATE	CYCLE NO.	$f_n$	$\Delta f$	Q	NNF
CADMIUM 3 continue	02/05/87	7	4480	275	16.29	105
	02/06/87	8	4440	310	14.32	103
	02/07/87	9	4420	310	14.26	102
	02/08/87	10	4280	335	12.78	95
	02/09/87	11	4310	420	10.26	97
	02/10/87	14	4000	465	8.60	83
	02/11/87	16	3430	1080	3.18	61
	02/12/87	18	2500	780	3.21	33
	CADMIUM 4	01/30/87	0	4470	300	14.90
01/31/87		1	4410	270	16.33	97
02/01/87		2	4370	280	15.61	96
02/02/87		3	4255	290	14.67	91
02/03/87		4	4495	290	15.50	101
02/04/87		5	4420	300	14.73	98
02/05/87		6	4380	365	12.00	96
02/05/87		7	4325	325	13.31	94
02/06/87		8	4320	310	13.94	93
02/07/87		9	4190	400	10.47	88
02/08/87		10	4180	395	10.56	87
02/09/87		11	4120	490	8.41	85
02/09/87		12	4150	400	10.38	86
02/10/87		14	3785	560	6.76	72
02/11/87		16	3120	1050	2.97	49
CADMIUM SEA 1		01/30/87	0	4010	410	9.78
	01/31/87	1	4315	390	11.06	116
	02/01/87	2	4250	355	11.97	112
	02/02/87	3	4260	350	12.17	113
	02/03/87	4	4315	245	17.61	116
	02/04/87	5	4315	320	13.48	116
	02/05/87	6	4270	330	12.94	113
	02/05/87	7	4250	350	12.14	112
	02/06/87	8	4220	330	12.79	111
	02/07/87	9	4200	335	12.54	110
	02/08/87	10	4180	365	11.45	109
	02/09/87	11	4150	375	11.07	107
	02/09/87	12	3990	460	8.67	99
	02/10/87	14	4045	460	8.79	102
	02/11/87	16	4020	430	9.35	100
	02/12/87	18	3780	430	8.79	89

Table A-2 (cont.)

BEAM NO.	TEST DATE	CYCLE NO.	fn	<sup>^</sup> f	Q	NNF	
CADMIUM SEA 2	01/30/87	0	4360	345	12.64	100	
	01/31/87	1	4410	370	11.92	102	
	02/01/87	2	4350	310	14.03	100	
	02/02/87	3	4345	325	13.37	99	
	02/03/87	4	4310	345	12.49	98	
	02/04/87	5	4390	325	13.51	101	
	02/05/87	6	4340	335	12.96	99	
	02/05/87	7	4320	370	11.68	98	
	02/06/87	8	4360	320	13.63	100	
	02/07/87	9	4300	365	11.78	97	
	02/08/87	10	4280	340	12.59	96	
	02/09/87	11	4245	375	11.32	95	
	02/09/87	12	4245	330	12.86	95	
	02/10/87	14	4150	425	9.76	91	
	02/11/87	16	4000	435	9.20	84	
	02/12/87	18	3780	490	7.71	75	
	CADMIUM SEA 3	01/30/87	0	4355	350	12.44	100
		01/31/87	1	4430	340	13.03	103
02/01/87		2	4380	310	14.13	101	
02/02/87		3	4355	330	13.20	100	
02/03/87		4	4400	340	12.94	102	
02/04/87		5	4380	350	12.51	101	
02/05/87		6	4400	290	15.17	102	
02/05/87		7	4340	340	12.76	99	
02/06/87		8	4370	310	14.10	101	
02/07/87		9	4230	360	11.75	94	
02/08/87		10	4200	380	11.05	93	
02/09/87		11	4140	390	10.62	90	
02/09/87		12	4100	410	10.00	89	
02/10/87		14	4050	410	9.88	86	
02/11/87		16	3870	450	8.60	79	
02/12/87		18	3740	580	6.45	74	
CADMIUM SEA 4		01/30/87	0	4200	385	10.91	100
		01/31/87	1	4320	320	13.50	106
	02/01/87	2	4380	340	12.88	109	
	02/02/87	3	4360	300	14.53	108	
	02/03/87	4	4400	325	13.54	110	
	02/04/87	5	4350	305	14.26	107	



Table A-2 (cont.)

BEAM NO.	TEST DATE	CYCLE NO.	fn	$\Delta f$	Q	NNE
CADMIUM	02/05/87	6	4320	335	12.90	106
SEA 4	02/05/87	7	4320	350	12.34	106
continue	02/06/87	8	4320	315	13.71	106
	02/07/87	9	4300	380	11.32	105
	02/08/87	10	4250	380	11.18	102
	02/09/87	11	4245	355	11.96	102
	02/09/87	12	4240	390	10.87	102
	02/10/87	14	4175	420	9.94	99
	02/11/87	16	4140	370	11.19	97
	02/12/87	18	4110	360	11.42	96

Table A-3 Regression Analysis For Best Fit  
of Freeze-Thaw Data Second Run Using  
Q Parameter and NNF

---

**Q Parameter**

---

**Blank**

---

1<sup>st</sup> order polynomial:  $Y = B_0 + B_1X_1$

s = 2.39       $R^2 = 67.1 \%$        $F = 62.1 > F(1.29, .95)$

2<sup>nd</sup> order polynomial:  $Y = B_0 + B_1X_1 + B_{12}X_1^2$

s = 2.074       $R^2 = 75.2 \%$        $F = 46.5 > F(2, 28, .95)$

3<sup>rd</sup> order polynomial:  $Y = B_0 + B_1X_1 + B_{12}X_1^2 + B_{13}X_1^3$

s = 1.669       $R^2 = 83.9 \%$        $F = 53.15 > F(3, 27, .95)$

---

**Blank-Sea**

---

1<sup>st</sup> order polynomial:  $Y = B_0 + B_1X_1$

s = 1.423       $R^2 = 81.6 \%$        $F = 190.6 > F(1.29, .95)$

2<sup>nd</sup> order polynomial:  $Y = B_0 + B_1X_1 + B_{12}X_1^2$

s = 1.319       $R^2 = 84.2 \%$        $F = 114.9 > F(2, 28, .95)$

3<sup>rd</sup> order polynomial:  $Y = B_0 + B_1X_1 + B_{12}X_1^2 + B_{13}X_1^3$

s = 1.027       $R^2 = 90.4 \%$        $F = 136.6 > F(3, 27, .95)$

4<sup>th</sup> order polynomial:  $Y = B_0 + B_1X_1 + B_{12}X_1^2 + B_{14}X_1^4$

s = 1.061       $R^2 = 89.8$        $F = 126 > F(3, 40, .95)$

---

Table A-3 (Continued)

-----  
**Cadmium**  
-----

1<sup>st</sup> order polynomial:  $Y = B_0 + B_1X_1$

$s = 2.733$        $R^2 = 52.3 \%$        $F = 67.9 > F(1.60, .95)$

2<sup>nd</sup> order polynomial:  $Y = B_0 + B_1X_1 + B_{12}X_1^2$

$s = 2.09$        $R^2 = 52.3 \%$        $F = 79.8 > F(2, 59, .95)$

3<sup>rd</sup> order polynomial:  $Y = B_0 + B_1X_1 + B_{12}X_1^2 + B_{13}X_1^3$

$s = 1.814$        $R^2 = 90.4 \%$        $F = 77.45 > F(3, 58, .95)$

4<sup>th</sup> order polynomial:  $Y = B_0 + B_1X_1 + B_{12}X_1^2 + B_{14}X_1^4$

$s = 1.814$        $R^2 = 80.0 \%$        $F = 77.5 > F(3, 58, .95)$   
-----

-----  
**Cadmium-Sea**  
-----

1<sup>st</sup> order polynomial:  $Y = B_0 + B_1X_1$

$s = 1.475$        $R^2 = 42.7 \%$        $F = 47.9 > F(1.60, .95)$

2<sup>nd</sup> order polynomial:  $Y = B_0 + B_1X_1 + B_{12}X_1^2$

$s = 1.32$        $R^2 = 53.4 \%$        $F = 37.2 > F(2, 59, .95)$

3<sup>rd</sup> order polynomial:  $Y = B_0 + B_1X_1 + B_{12}X_1^2 + B_{13}X_1^3$

$s = 1.219$        $R^2 = 60.4 \%$        $F = 32.9 > F(3, 58, .95)$

4<sup>th</sup> order polynomial:  $Y = B_0 + B_1X_1 + B_{12}X_1^2 + B_{14}X_1^4$

$s = 1.229$        $R^2 = 59.7 \%$        $F = 32.1 > F(3, 58, .95)$

Table A-3 (cont.)

<b>NNE Parameter</b>				
	<u>polynomial order</u>			
<b>Blank</b>	1	2	3	4
s	20.16	14.87	15.06	15.08
R <sup>2</sup> (%)	50.7	73.2	72.5	72.4
F	31.9	41.9	27.3	27.3
<b>Blank-Sea</b>				
s	7.42	5.28	4.99	
R <sup>2</sup> (%)	86.1	93.0	93.7	
F	286.5	286.0	214.2	
<b>Cadmium</b>				
s	10.8	7.0	7.06	
R <sup>2</sup> (%)	58.8	82.7	82.4	
F	87.9	146.6	96.4	
<b>Cadmium-Sea</b>				
s	7.08	6.45	6.46	6.47
R <sup>2</sup> (%)	37.4	48.1	47.9	47.7
F	38.8	30.2	20.3	20.9

Table A-4:No. of Cycles Based on Failure Criteria

<u>Failure Criteria</u>							
Q<8	Q<7	Q<6	NF<60	NF<70	NF<75	NF<80	NF<85
<b>Blank</b>							
8	5	5	6	5	5	5	5
8	7	7	8	8	7	7	6
8	7	7	9	8	8	8	8
<b>Blank-Sea</b>							
7	7	8	9	8	7	6	5
8	7	8	9	8	7	6	5
6	7	8	8	7	6	6	5
6	6	7	9	8	7	6	5
<b>Cadmium</b>							
16	16	17	19	17	16	14	14
14	14	14	16	15	14	14	13
16	14	14	16	15	14	14	13
14	14	14	15	14	13	13	12
<b>Cadmium-Sea</b>							
19	19	20	23	21	20	19	18
18	20	21	22	19	18	17	16
19	21	21	21	19	18	16	15
20	20	22	26	24	23	22	20

\*cycle values above 18 are extrapolated

Table A-5 ANALYSIS OF VARIANCE  
Freeze-Thaw Data (Second Run)

Q Factor < 8

---

SOURCE	DF	SS	MS	F
FACTOR	3	405.9	135.3	130.4
ERROR	11	11.4	1.1	
TOTAL	14	417.3		

LEVEL	N	MEAN	STDEV
Blank	3	7.33	1.155
Blank-Sea	4	6.75	0.957
Cadmium	4	15.00	1.155
Cadmium-Sea	4	19.00	0.816

POOLED STDEV = 1.019

---

Q Factor < 7

---

SOURCE	DF	SS	MS	F
FACTOR	3	486.5	162.2	211.9
ERROR	11	8.4	0.76	
TOTAL	14	494.9		

LEVEL	N	MEAN	STDEV
Blank	3	6.33	1.155
Blank-Sea	4	6.75	0.500
Cadmium	4	14.50	1.000
Cadmium-Sea	4	20.00	0.816

POOLED STDEV = 0.875

---

Q Factor < 6

---

SOURCE	DF	SS	MS	F
FACTOR	3	511.6	170.5	154.2
ERROR	11	12.2	1.11	
TOTAL	14	523.7		

LEVEL	N	MEAN	STDEV
Blank	3	6.33	1.155
Blank-Sea	4	7.75	0.500
Cadmium	4	14.75	1.500
Cadmium-Sea	4	21.00	0.816

POOLED STDEV = 1.052

Table A-5 (cont.)

---

NNF < 60 %

---

SOURCE	DF	SS	MS	F
FACTOR	3	577.2	192.4	74.5
ERROR	11	28.4	2.58	
TOTAL	14	605.6		

LEVEL	N	MEAN	STDEV
Blank	3	7.67	1.528
Blank-Sea	4	8.75	0.500
Cadmium	4	16.5	1.732
Cadmium-Sea	4	23.00	2.160

POOLED STDEV = 1.607

---

NNF < 70 %

---

SOURCE	DF	SS	MS	F
FACTOR	3	478.7	159.6	62.1
ERROR	11	28.3	2.57	
TOTAL	14	506.9		

LEVEL	N	MEAN	STDEV
Blank	3	7.00	1.732
Blank-Sea	4	7.75	0.500
Cadmium	4	15.25	1.258
Cadmium-Sea	4	20.75	2.363

POOLED STDEV = 1.603

---

NNF < 75 %

---

SOURCE	DF	SS	MS	F
FACTOR	3	455.5	151.83	62.0
ERROR	11	26.9	2.45	
TOTAL	14	582.4		

LEVEL	N	MEAN	STDEV
Blank	3	6.67	1.528
Blank-Sea	4	6.75	0.500
Cadmium	4	14.25	1.258
Cadmium-Sea	4	19.75	2.363

POOLED STDEV = 1.564

Table A-5 (cont.)

---

NNE < 80 %

---

SOURCE	DF	SS	MS	F
FACTOR	3	418.57	139.52	56.49
ERROR	11	27.17	2.47	
TOTAL	14	445.73		

LEVEL	N	MEAN	STDEV
Blank	3	6.67	1.528
Blank-Sea	4	5.75	0.500
Cadmium	4	13.75	0.500
Cadmium-Sea	4	18.50	2.646

POOLED STDEV = 1.550